REPORT DOCUMENTATION PAGE

Form Approved
OMB No. 0704-0188

PLEASE DO NOT RETURN YOUR FORM TO THE ABOVE ADDRESS.

1. REPORT DATE *(DD-MM-YYYY)*	2. REPORT TYPE	3. DATES COVERED *(From - To)*
1/Oct/2001	THESIS	

4. TITLE AND SUBTITLE
DESIGN, CONSTRUCTION AND EVALUATION OF THE CSU OPTICAL FOG DETECTOR

5a. CONTRACT NUMBER

5b. GRANT NUMBER

5c. PROGRAM ELEMENT NUMBER

6. AUTHOR(S)
CAPT EMERT SCOTT E

5d. PROJECT NUMBER

5e. TASK NUMBER

5f. WORK UNIT NUMBER

7. PERFORMING ORGANIZATION NAME(S) AND ADDRESS(ES)
COLORADO STATE UNIVERSITY

8. PERFORMING ORGANIZATION REPORT NUMBER
CI01-257

9. SPONSORING/MONITORING AGENCY NAME(S) AND ADDRESS(ES)
THE DEPARTMENT OF THE AIR FORCE
AFIT/CIA, BLDG 125
2950 P STREET
WPAFB OH 45433

10. SPONSOR/MONITOR'S ACRONYM(S)

11. SPONSOR/MONITOR'S REPORT NUMBER(S)

12. DISTRIBUTION/AVAILABILITY STATEMENT
Unlimited distribution
In Accordance With AFI 35-205/AFIT Sup 1

13. SUPPLEMENTARY NOTES

14. ABSTRACT

DISTRIBUTION STATEMENT A
Approved for Public Release
Distribution Unlimited

20011016 184

15. SUBJECT TERMS

16. SECURITY CLASSIFICATION OF:			17. LIMITATION OF ABSTRACT	18. NUMBER OF PAGES	19a. NAME OF RESPONSIBLE PERSON
a. REPORT	b. ABSTRACT	c. THIS PAGE		232	19b. TELEPHONE NUMBER *(Include area code)*

The views expressed in this article are those of the author and do not reflect the official policy or position of the United States Air Force, Department of Defense, or the U.S. Government

THESIS

DESIGN, CONSTRUCTION AND EVALUATION OF THE CSU OPTICAL FOG DETECTOR

Submitted by

Scott E. Emert

Department of Atmospheric Science

In partial fulfillment of the requirements

for the Degree of Master of Science

Colorado State University

Fort Collins, CO

Summer 2001

COLORADO STATE UNIVERSITY

June 12, 2001

WE HEREBY RECOMMEND THAT THE THESIS PREPARED UNDER OUR SUPERVISION BY SCOTT E. EMERT ENTITLED DESIGN, CONSTRUCTION AND EVALUATION OF THE CSU OPTICAL FOG DETECTOR BE ACCEPTED AS FULFILLING IN PART REQUIREMENTS FOR THE DEGREE OF MASTER OF SCIENCE.

Committee on Graduate Work

Sonia M Kreidenweis

Melvin E Andersen

Adviser

Department Head

ABSTRACT OF THESIS

DESIGN, CONSTRUCTION AND EVALUATION OF THE CSU OPTICAL FOG DETECTOR

The goal of this project was to develop an inexpensive cloud/fog detector that could be used to automate sampling equipment at remote (unmanned) cloud/fog research sites. A secondary objective was to test the ability of this sensor to measure/track trends in fog/cloud liquid water content (LWC). This characteristic is important because LWC is a significant indicator of a cloud's ability to process aerosols and gases and changes in LWC often correspond to changes in fog/cloud solute concentration. The following actions were taken to help realize these objectives.

An evaluation of the use of commercially available optical components for fog detection has been performed. The research reinforced the need to have an inexpensive cloud/fog detector that could be used to automate sampling equipment at remote (unmanned) cloud/fog research sites. No such instrument is currently available commercially.

Requirements for components of the CSU Optical Fog Detector (OFD) were defined. Important factors included transmitter wavelength and modulation characteristics, detector sensitivity, and component stability/durability over a range of environmental conditions. Readily available commercial components were utilized to ensure the sensor could be built economically.

Laboratory tests in a glove box filled with artificially generated fog proved that optical components purchased from Banner Engineering were capable of monitoring changes in fog liquid water content (LWC) when operated in a light attenuation mode. After an initial calibration, the signal from the CSU OFD was found to correlate strongly with LWC measured by a Gerber Scientific Particulate Volume Monitor (PVM-100).

Theoretical calculations of attenuation of 880 nm light passing through a population of fog drops were completed. The results indicated extinction decreases as the drops are shifted to larger sizes (with a fixed LWC and lognormal distribution breadth). Accordingly, the response of the CSU OFD is expected to vary with mean fog/cloud drop size.

Numerous fog detector design configurations were tested and the current attenuation design of the CSU optical fog detector was deemed successful in that it provides, at a minimum, an inexpensive switch capable of automating remote fog sensing equipment. It also provides useful information concerning fog LWC.

Two calibrated OFD's were compared to PVM LWC measurements during initial field tests of orographic clouds at Storm Peak Laboratory (SPL) in Steamboat Springs, Colorado. The combined results from both OFD's over all time periods yields a regression equation of $LWC_{OFD} = 0.99 * LWC_{PVM}$ with a correlation coefficient of 0.92.

Tests performed in the absence of fog on top of our laboratory in Fort Collins provided a measure of OFD baseline noise. Analysis of the observed noise yielded a minimum detection limit of 4.4 mg m^{-3} for the OFD and a comparable value (5.6 mg m^{-3}) for the PVM.

The OFD was incorporated in several automated fog sampling systems deployed in California's San Joaquin Valley as part of the California Regional Particulate Air Quality Study (CRPAQS). The OFD performed well as a fog detector and provided some insight into fog LWC. LWC measurements by a PVM and a co-located OFD showed good correlation ($R^2 = 0.91$) and only modest bias ($LWC_{OFD} = 1.16\, LWC_{PVM}$) during an extended radiation fog episode.

Scott E. Emert
Atmospheric Science Department
Colorado State University
Fort Collins, CO 80523
Summer 2001

ACKNOWLEDGMENTS

First and foremost, I would like to thank my advisor, Dr. Jeffrey Collett. His expertise, insight, and direction during this project were invaluable for its successful completion. I would also like to express my gratitude to my committee members, Dr. Sonia Kreidenweis and Dr. Melvin Andersen, for contributing valuable suggestions that helped guide my research work and strengthen my thesis.

I extend my thanks to the members of the atmospheric chemistry research group for providing advice and technical assistance. Special thanks go to Eli Sherman for his significant contribution in identifying components, technical expertise and encouragement. Without his help, this project would not have been possible. In addition, I want to thank Jenny Hand for her invaluable help with the scattering calculations and to Gong-Unn Kang for his work analyzing the Helm data set. I also want to thank Katharine Moore and Pierre Herckes for offering their help and encouragement whenever necessary.

Finally, I would like to thank my family. The support of my wife and children has been an essential part of my graduate work, just as it is in all aspects of my life. I feel fortunate to be able to express my gratitude to them.

This work was supported by the Air Force Institute of Technology (AFIT) with additional financial support for the CRPAQS from the National Science Foundation (ATM-9980540).

Funding was also provided by the San Joaquin Valleywide Air Pollution Study Agency. The statements and conclusions in this report are those of the Contractor and not necessarily those of the California Air Resources Board, the San Joaquin Valleywide Air Pollution Study Agency, or its Policy Committee, their employees or their members. The mention of commercial products, their source, or their use in connection with the material reported herein is not to be construed as actual or implied endorsement of such products.

TABLE OF CONTENTS

LIST OF FIGURES

LIST OF TABLES

1 Introduction

1.1 Background

The goal of this research was to develop an inexpensive, reliable sensor for ground-based detection of fog and clouds. The research was motivated by the need to have an inexpensive cloud/fog detector that could be used to automate sampling equipment at remote (unmanned) cloud/fog research sites. No such instrument is available commercially. A secondary objective was to test the ability of this sensor to measure/track trends in fog/cloud liquid water content (LWC). This characteristic is important because LWC is a significant indicator of a cloud's ability to process aerosols and gases and changes in LWC often correspond to changes in fog/cloud solute concentration.

We begin here with a brief review of some of the instruments previously used for measuring the drop size distribution and/or LWC of ground-based fogs and clouds. We discuss several fog sensors' abilities to measure fog, discuss their general operating principles and their possible uses as a LWC monitor. In subsequent chapters, we outline the strategy for developing a new fog/cloud sensor, describe laboratory and field tests made comparing the new sensor to an existing sensor, and discuss application of the sensor in a radiation fog field experiment.

1.2 Liquid water content (LWC) measurement methods

The liquid water contents of fogs and clouds are currently measured optically, thermally or by direct sampling. According to Arends (1992), most methods are not very reliable, resulting in errors of 50% or more. Accurate LWC measurements are important for the calculation of the mass balance of the compounds between gas and water phases.

The Integrated Particle Volume or LWC [g/m^3] for water droplets is defined as

$$LWC = (4/3)\pi\rho \int n(r) r^3 \, dr \qquad \text{(Eq'n.1.1)}$$

(Gerber, 1993) where ρ is the drop density [g/cm^3], r is the drop radius [cm], and n(r) [$no./m^3$] is the droplet size distribution.

There are numerous LWC measurement sensors. However, there currently is not a continuously sampling sensor that is considered a standard for LWC measurement. The gravimetric filter sampling method (mass of droplets collected on a filter's surface and the volume of air drawn through the filter can be used to calculate LWC) can be considered as an absolute measuring technique for LWC but it does not provide a continuous measure. This method of LWC measurement produces an error below 10 mg/m^3 while continuous LWC measurement sensors can have large errors (greater than 50%) depending on sampling conditions (Arends et al., 1992).

Different sensors employ different methods to measure LWC. The predominant technique for ground-based instruments is to illuminate the fog/cloud droplets with a laser and measure forward scattering. The scattered light is collected by an optical detector and converted to an analog voltage output. Some instruments measure scattering

by a population of drops and relate the intensity of scattered light to the fog/cloud LWC while others measure scattering by individual drops. In the latter design, the scattering intensity is related to the individual drop size. By measuring large numbers of drops, a drop size distribution can be constructed and integrated to determine the LWC.

Another approach to measure LWC is to monitor the energy required to evaporate droplets collected by inertial impaction and interception on a heated cylinder. This hot wire probe technique is most commonly utilized on aircraft where the aircraft flight speed is fast enough to provide efficient drop collection. The system electronics maintain the hot wire sensor at a constant temperature and monitor the power required to regulate the temperature as droplets vaporize (Korolev et al., 1998). This power is directly related to the amount of heat taken away by convection plus the heat of vaporization. The convective heat losses are known empirically and vary with airspeed, temperature and pressure. The liquid water content is calculated from the power loss found from the difference between the total and convective power losses.

1.3 Commercial optical probes for fog/cloud characterization

Two optical instruments have been widely accepted for use in the ground-based characterization of fogs and clouds: the Gerber Scientific Particulate Volume Monitor (PVM-100) and the Particle Measurement Systems Classical Scattering Aerosol Spectrometer Probe (CSASP-100-HV). The PVM provides information about fog/cloud LWC and particle surface areas (PSA) while the CSASP is designed to measure the drop size distribution.

The PVM-100 (see Figure 1.1) is a forward scattering instrument used to measure particle volume and surface area. Light from a 0.780 μm laser diode scattered by droplets or other particles in the forward direction is collected by receiving optics. The laser diode beam has a pathlength of 42 cm with an optical probing volume of 3 cm^3. Scattered light is collected over a small forward angle (0.32°-3.58°) (Arends et al., 1992). A dump spot prevents direct reception of light emitted by the laser diode. The receiving optics (see Figure 1.2) consist of a lens and beam splitter which collect the scattered light and splits it into two beams which are directed toward independent detectors for LWC and PSA. Each detector consists of a circular spatial filter/sensor combination. The two detector filters have variable transmission in their radial direction. One filter weights the scattered light to produce an output of LWC. The second filter weights the forward scattered light to produce an output of PSA. The instrument is calibrated on-site using a manufacturer-supplied, light-diffusing disk. The manufacturer claims the relationship between scattering intensity and LWC is linear for drop diameters from 3-45 μm (Gerber, 1993) and states an instrument accuracy of +/- 10% and a precision of +/- 0.002 g/m^3.

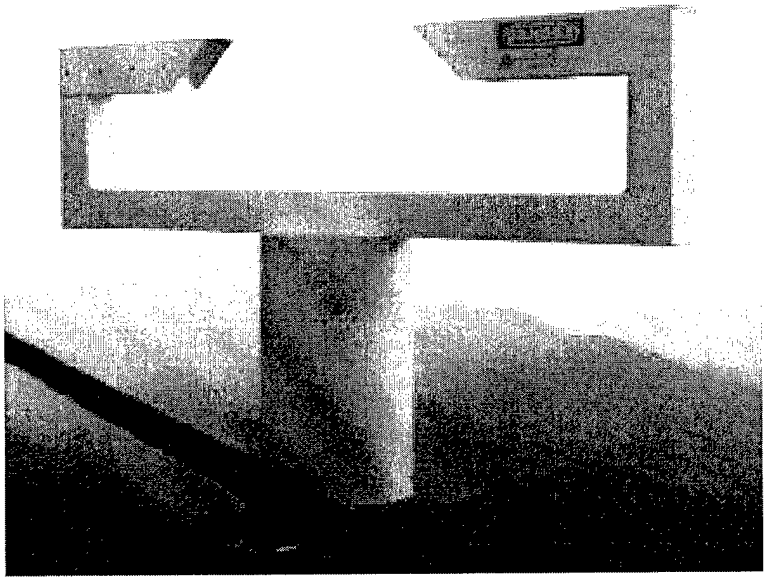

Figure 1.1 Gerber PVM-100.

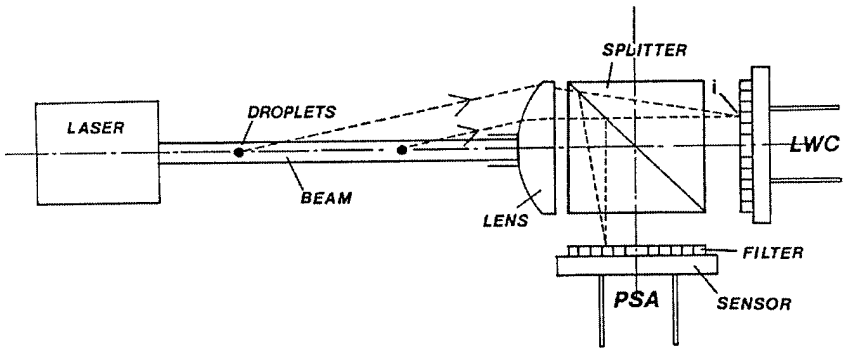

Fig 1.2 Optical configuration for the PVM-100 (Gerber, 1993).

The PMS CSASP-100-HV (see Figure 1.3) is a ground-based water droplet spectrometer used to measure cloud/fog drop size distributions. It is designed to operate under a wide range of environmental conditions. The general principle of the CSASP is

that the light scattered by a particle of known refractive index within a high intensity laser beam (5 mW Helium Neon) is related to its size.

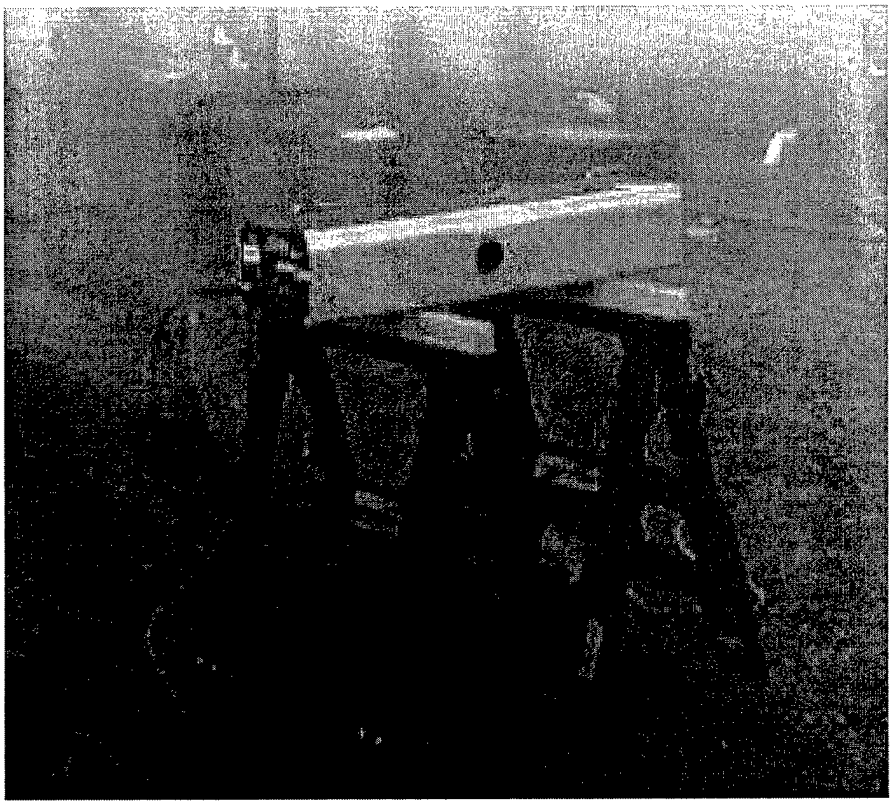

Figure 1.3 CSASP.

The CSASP's laser beam is focused down to a diameter of approximately 250 μm. This is accomplished by the use of a 60 mm focal length condensing lens, which is mounted between the laser source and the sample volume (see Figure 1.4). This laser beam is blocked on the opposite side of the inlet with an optical stop, a "dump spot" to prevent the beam from entering the collection optics (see Figure 1.5). Particles that encounter this beam scatter light in all directions and some of that scattered in the forward direction is directed by a prism though a condensing lens and onto a beam

splitter. The "dump spot" on the prism and aperture of the condensing lens define a collection angle from about 4^{o} - 12^{o}.

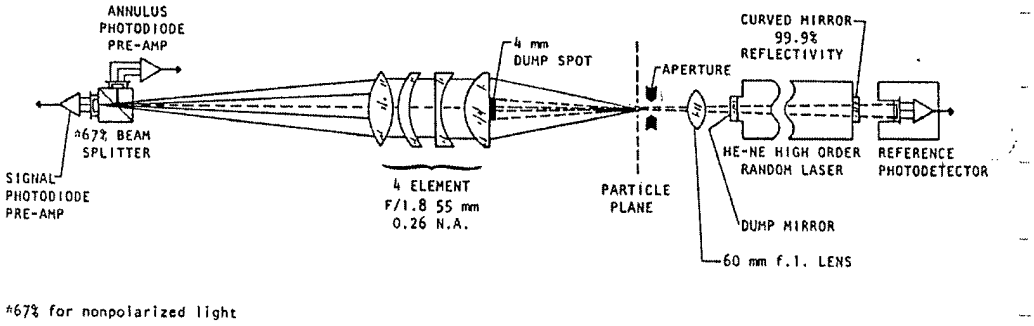

Figure 1.4 CSASP Optics (PMS Tech note, 1989).

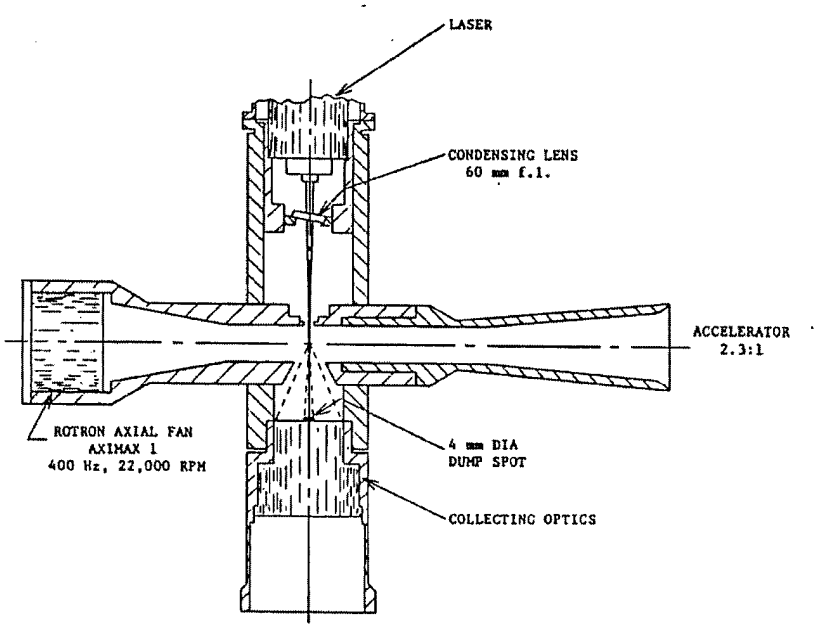

Figure 1.5 CSASP airflow diagram (PMS Tech note, 1989).

The particles passing through the laser beam in the sampling aperture produce pulses of radiant energy that are sensed by the detectors and read into two peak readers. One detector looks at all the energy scattered into its collecting aperture. This detector performs the sizing. The other detector has its center obscured by a mask aperture (1 mm dump spot), thus only collecting the energy outside of this mask. This collector receives its energy from diffuse images that are out of focus and which correspond to particles out of the depth-of-field. By using a high performance, high magnification imaging system and applying differing gain ratios while comparing pulse height measurements, a depth-of-field of small dimensions is defined (PMS Technical Note, 1989). This allows the CSASP-100 a means of resolving and sizing particles in an *in situ* mode. The pulses from the unmasked detector are sized with a pulse height analyzer. The size of the particle is determined by measuring the light scattering intensity and using Mie scattering theory to relate this intensity to the particle size. The size is categorized into one of 16 channels (channel limits are set based upon manufacturer calibration of the instrument) and this information sent to the data system where the number of particles in each channel is accumulated over a pre-selected time period.

1.4 Alternative fog/cloud sensors

Both the PVM and the CSASP are expensive instruments, costing well in excess of $25,000 per unit. This high cost often precludes use of these instruments in large fog/cloud sampling networks. In addition, the commercial availability of these instruments has at times been limited. Over the past two decades a number of approaches have been taken to find or design less expensive instruments suitable for use as fog/cloud

detectors. The main approaches have involved construction of simple optical detectors or testing of the suitability of commercially available visibility sensors. In addition, there has been at least one case where a miniature version of an active cloudwater collector was operated continuously to detect the presence of fogs and intercepted clouds.

1.4.1 Scattering fog sensors

The Caltech fog detector is a backscattering type fog detector. It is comprised of an infrared LED light source, a filtered photodetector, an electronic control module, calibration relay, an air pump and a shielded housing (Collett et al., 1990).

Light is emitted by the LED over a narrow range of wavelengths. The peak spectral emissions occur at 940 nm while the photodetector's peak response occurs at 910 nm. The photodetector's peak spectral response is less than 5% at wavelengths below 750 nm thus reducing the sensitivity to ambient light. To further reduce the ambient light sensitivities, the LED source is modulated at 1 kHz and the photodetector is coupled to the source modulation so only light from the source is detected.

While this helps to minimize the effects of ambient light, it has not been totally eliminated and the sensor has some variation in output due to sunlight. The typical diurnal fluctuation of the detector signal can be seen in Figure 1.6 (Hoffmann et al., 1989).

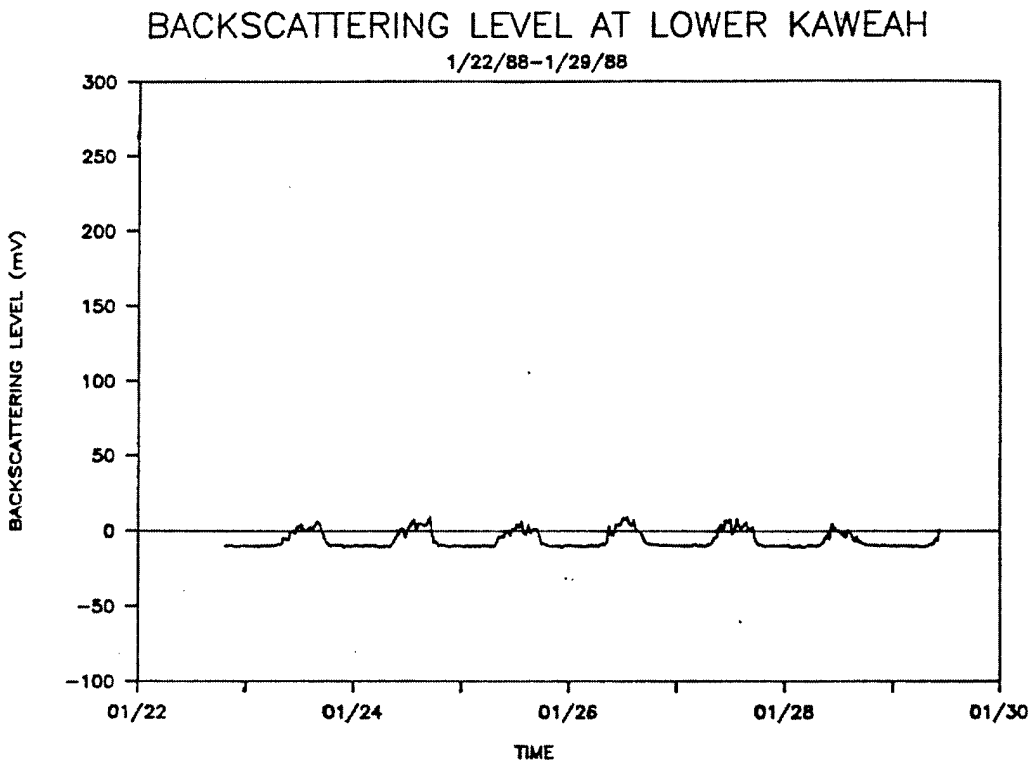

Figure 1.6 Diurnal effects on CALTECH visibility sensor (Hoffmann et al., 1989).

The output from the control module is an analog DC voltage, which ranges from 0.0 to 3.0 volts. Under this setup, as backscattering increases the output voltage increases.

The sight tubes of the housing (see Figure 1.7) contain the source and detector. They are aligned with a 5-degree offset with respect to each other. In this configuration, the detector optical paths intersect about 0.75 m from the sensor. Hoffmann et al. (1989) determined this experimentally yielded the maximum detector output when fog is present.

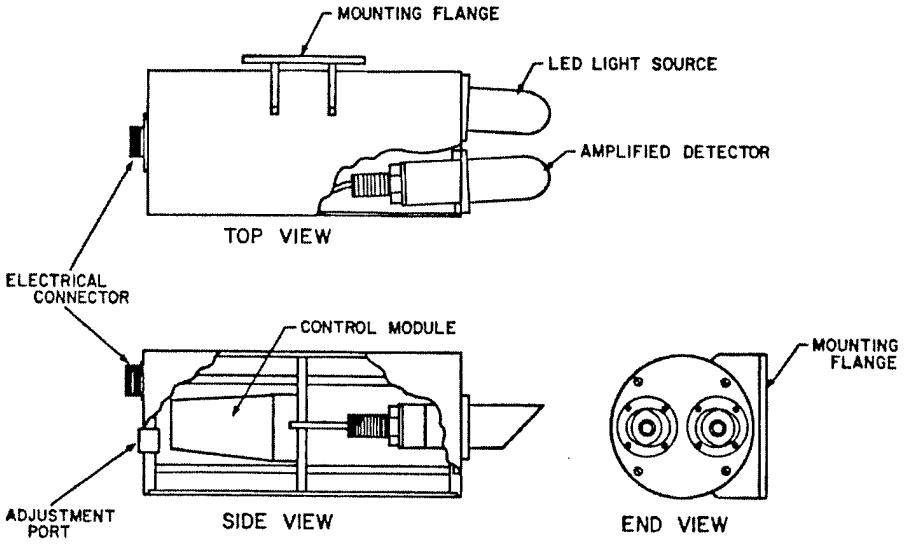

Figure 1.7 Schematic of CALTECH visibility sensor (Hoffmann et al., 1989).

An air pump located in the main housing supplies air to the sight tubes. The airflow is designed to keep the lenses free from condensation and discourages insects from nesting in the tubes.

Hoffmann et al. (1989) state it is evident that the relative backscattering intensity is non-unique, and highly variable, which makes it difficult to determine the true causes of variation in the backscattering output during a fog event. The Caltech sensor works as a presence-of-fog detector but its ability to measure LWC has not been demonstrated.

The Poor man's optical fog detector (see Figure 1.8) is an optical fog detector (OFD) developed at the Netherlands Energy Research Foundation (ECN). The detector, described by Mallant (1990), responds to light that is near-forward-scattered by fog droplets. Mie theory predicts that near infra-red light scattered by fog drops at angles

smaller than 5° will be much more intense than light scattered at larger angles. The ECN OFD's near-forward scattered light configuration was chosen so that the use of highly collimated optics would not be needed.

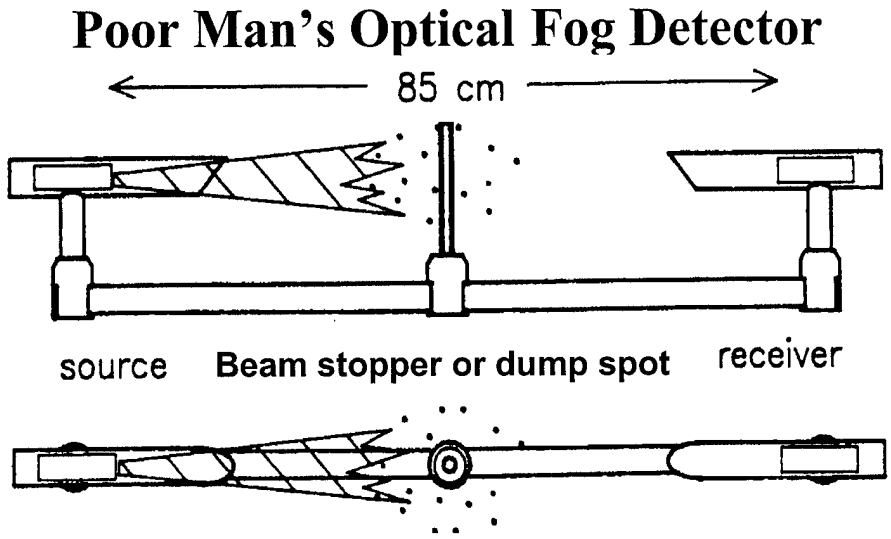

Figure 1.8 ECN's OFD (Mallant, 1990).

The ECN OFD uses a low-cost, commercially available source-receiver combination (manufacturer not identified). A dump spot or beam stopper prevents activation of the detector in the absence of fog because it blocks out the beams source and the sensor is only activated when there is fog present to scatter the light around the dump spot. The sides of the stopper have slots to prevent erroneous signals by particles deposited on the stopper.

The light source is a pulsed IR LED (880 nm). Thus, the receiver's electronics respond to pulsed signals only, limiting the influence of stray light. It was designed to be used as a switching device, with an adjustable threshold and the results were promising, especially for droplets in the 2 –20 μm range. However, Mallant (1990) states the ECN OFD has poor qualities as a LWC indicator.

1.4.2 Commercial visibility sensors

During a number of fog sampling field campaigns the fog chemistry team at CSU deployed visibility sensors to evaluate their suitability as fog/cloud presence detectors. The two sensors evaluated were a Belfort Model 6100 Visibility Sensor and a Jaycor Model 1200-A visibility sensor. A description of the study and results of the tests are described in an unpublished report by Andrews et al. (1997).

The Belfort Model 6100 Visibility Sensor (see Figure 1.9) is designed to monitor visibility conditions over a range of 6.1 m to 16.1 km (Belfort, 2001). The Model 6100 sensor has a digital output signal capable of indicating the present visibility. It also includes alarm outputs which can be adjusted by the user to preset visibility thresholds. That makes it possible to indicate Good/Medium/Poor visibility.

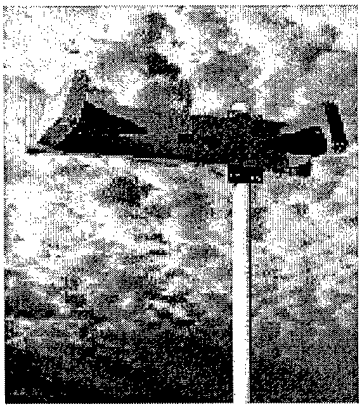

Fig 1.9 Belfort Model 6100 visibility sensor.

The instrument is designed to measure near forward scattering of an infrared source beam. The greater the forward scatter intensity, the worse the atmospheric visibility. A high output infrared (880 nm) LED transmitter projects light into a sample volume. Light scattered in the near forward direction is collected by the receiver. The light source is modulated to permit rejection of background noise and natural variations in background light intensity. The optical path length of the instrument is 64 cm and the sensing volume is estimated as ~ 2500 cm^3. The visibility output from the instrument is estimated to have an uncertainty of 10%.

The Jaycor model 1200A visibility sensor (see Figure 1.10) emits infrared pulses (880 nm) at preprogrammed intervals while the optical detector on the sensor measures the fraction of emitted light, which is scattered back into the sensor field of view (Jaycor, 2001).

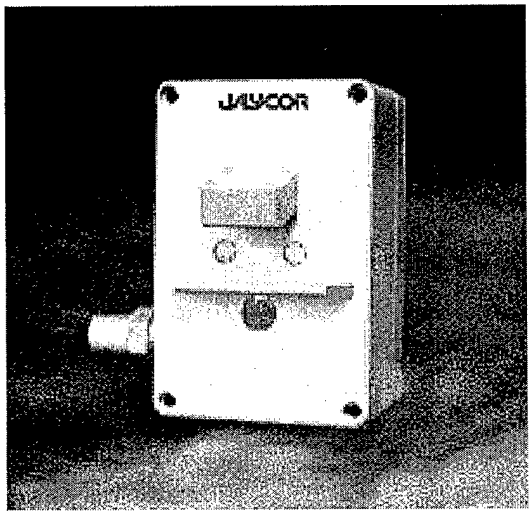

Figure 1.10 Jaycor 1200A visibility sensor.

The backscattered signal is processed by the sensor processor and an alarm is sent when a preset level is detected. The criteria are determined by the number and amplitude threshold of the backscatter pulses, which sets a poor visibility alarm. Both of these

variables are programmable. Once the poor visibility alarm is set, it stays set until visibility improves beyond a programmable threshold and time period. This avoids repetitious or frequent alarms when visibility changes rapidly over time.

The measurement of the backscattered light is related to visibility. The visibility range of the instrument is specified as 23-610 m with an uncertainty of 5%. Poor visibility may be the result of fog, smog, dust, rain, snow, or a combination of these. The volume sampled by the sensor for visibility is in excess of 1.5×10^7 cm^3 while the path length is greater than 360 cm. A one-time calibration procedure in clear air compensates for objects in the field of view after installation. The manufacturer claims the calibration is stable over temperature and power input variations.

Andrews et al. (1997) demonstrated that it is possible to determine the presence of fog or clouds with these two commercially available visibility sensors. They also indicate that the visibility signals can be used to identify trends in LWC. In non-precipitating clouds, Andrews et al. (1997) claim it should be possible to quantify LWC within an uncertainty of approximately 20% if the drop effective radius can be estimated within 10%.

Another interesting sensor worth mentioning is the mini-Caltech Active Strand Cloud Collector (mini-CASCC) (Collett et al., 1990). It is a scaled down version of the CASCC and was used as a fog/cloud presence detector to activate the CASCC. It works on the same principle as the CASCC and when operated in a cloud with a LWC of $0.1 g/m^3$, the calculated collection rate is 0.1 g/min (Collett et al., 1990). The collected water from the strands drains onto an electrical resistance grid. When the grid is bridged by a water droplet, the system is activated.

The system worked fairly well when the ambient temperatures were above 0°C however, it was not functional below that. The main disadvantage occurred due to riming of the collection surfaces when temperatures went below freezing. The inability of this instrument to detect the presence of supercooled fogs and clouds led to the development of the Caltech backscatter sensor.

Due to the cost associated with commercially available optical probes and the limitations of commercial visibility sensors, we decided to design and build our own optical fog detector. This course was necessary because we required a sensor that would allow automation of remote cloud sampling sites and allow us to track trends in LWC.

See Table 1.1 for information concerning sensors discussed in this section.

Sensor Name	Attributes	Light Source	Approximate Cost
Gerber Scientific Particulate Volume Monitor (PVM)-100	Provides information about fog/cloud LWC and particle surface area (PSA).	Forward scattered 0.780 μm laser. Utilizes dump spot	$25,000
Particle Measurement Systems Classical Scattering Aerosol Spectrometer Probe (CSASP-100-HV)	Ground-based water droplet spectrometer used to measure cloud/fog drop size distributions.	Forward scattered 0.780 μm laser. Utilizes dump spot	$25,000
Caltech fog detector	Works as a presence-of-fog detector but its ability to measure LWC has not been demonstrated.	Backscattering infrared LED light source (peak spectral emissions occur at 940 nm)	$1,000
Poor man's optical fog detector (ENC) OFD	Designed to be used as a switching device. Has poor qualities as a LWC indicator.	Near-forward-scattered pulsed IR LED (880 nm). Utilizes dump spot	Unknown
Belfort Model 6100 Visibility Sensor	Indicates present visibility. Includes poor visibility alarm outputs. No direct LWC information.	Near forward scattered infrared (880 nm) LED	$7,200
Jaycor model 1200A visibility sensor	Indicates present visibility. Has a poor visibility alarm. No direct LWC information.	Backscattered infrared (880 nm) LED	$3,000

Table 1.1 Sensor attributes.

2 Design, Construction and Initial Testing

2.1 Requirements

In defining requirements for the components to be used in this sensor, we first looked at various other fog/visibility sensors. Then, component characteristics were identified from those sensors that worked well. We also tried to identify some of the problems encountered with other sensors and eliminated those components that might have contributed to the problem.

We examined what environmental conditions the sensor would be exposed to and came up with our desired requirements. One of the goals was to utilize readily available commercial components. This would allow us to get the components in a timely manner and would help to ensure the sensor could be built economically.

The following sensor requirements were established.

i. Temperature Stable. The sensor had to be able to be used over a wide environmental temperature range (-5°C to 30°C) with very little drift or hysteresis.

ii. The sensor had to be built for outdoor conditions. It had to be National Electrical Manufacturers Association (NEMA) certified since it would have to be operated in all kinds of weather conditions.

iii. The sensor should operate in the infrared range. This would allow us to better be able to detect the cloud droplets as well as provide an eye-safe light source for field application.

iv. Analog output (0-5v preferred). This would allow us to easily incorporate its use with our existing Campbell data loggers.

v. We also were looking for components that had a modulated light source. This would help reject background noise and natural variations in background light intensity.

2.1.1 Component Search

We contacted numerous optics and electronics companies giving them our requirements and describing our preliminary plans to build a fog detector. Many of the industrial engineers at these companies said that they had nothing that would work and they thought it was not realistic for a sensor in the infrared range to detect water droplets.

The components that matched our requirements the best came from the Photoelectric Sensor department at Banner Engineering. We ordered the following components:

i. OASBFX Analog OMNI-BEAM Infrared (880nm) high power sensor (see Figure 2.1). The sensor consists of the infrared light-emitting-diode (LED) modulated light source we required and a photoelectric detector designed to detect light only from the modulated light source (Banner, 2001). It is reported to be temperature stable with a maximum drift equal to $\pm$ 10mV.

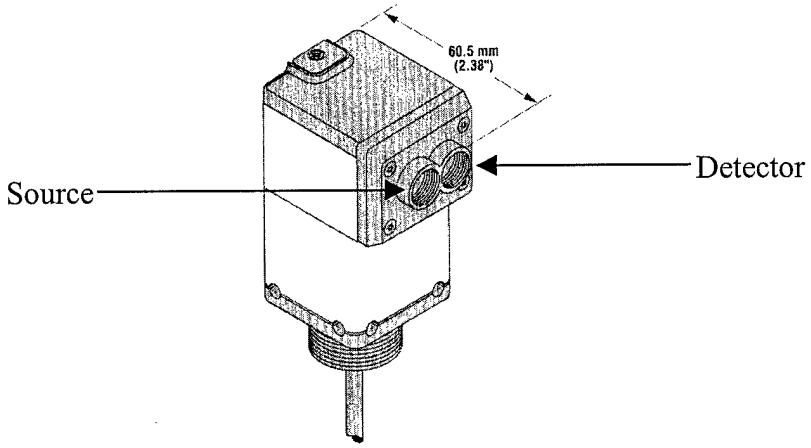

Figure 2.1 Banner OASBFX Analog IR sensor head.

ii. OPBA3 Power block. The power block has a 0 to 10V dc analog output and when properly assembled with the OASBFX sensor, it meets NEMA standards.

iii. Two each IT2.53S, opposed mode glass fiber optic cables.

2.2 Theoretical calculations

The theoretical extinction efficiency (Q_e) versus particle size for spheres can be seen in Figure 2.2. The performance of sensors that depend on light scattering by particles is related to the dimensionless size parameter (α). The size parameter α is related to the particle diameter by the following equation,

$$\alpha = \frac{\pi}{\lambda} d \qquad \text{(Eq'n. 2.1)}$$

where d = diameter of the scattering particle and λ = wavelength of the light source illuminating the particle. In the example figure a wavelength of 0.52 μm has been

chosen. The wavelength for our sensor is 0.88 μm. Figure 2.2 (Hinds, 1999) shows the dependence on particle size becomes less important as the particle becomes larger. Therefore, as α becomes large, Q_e approaches a large particle scattering limit of 2.

In our case, a size parameter value of 20 corresponds to a particle diameter of 5.6 μm. From this, we expect particles with diameters larger than several μm will have an extinction efficiency approximately equal to 2.

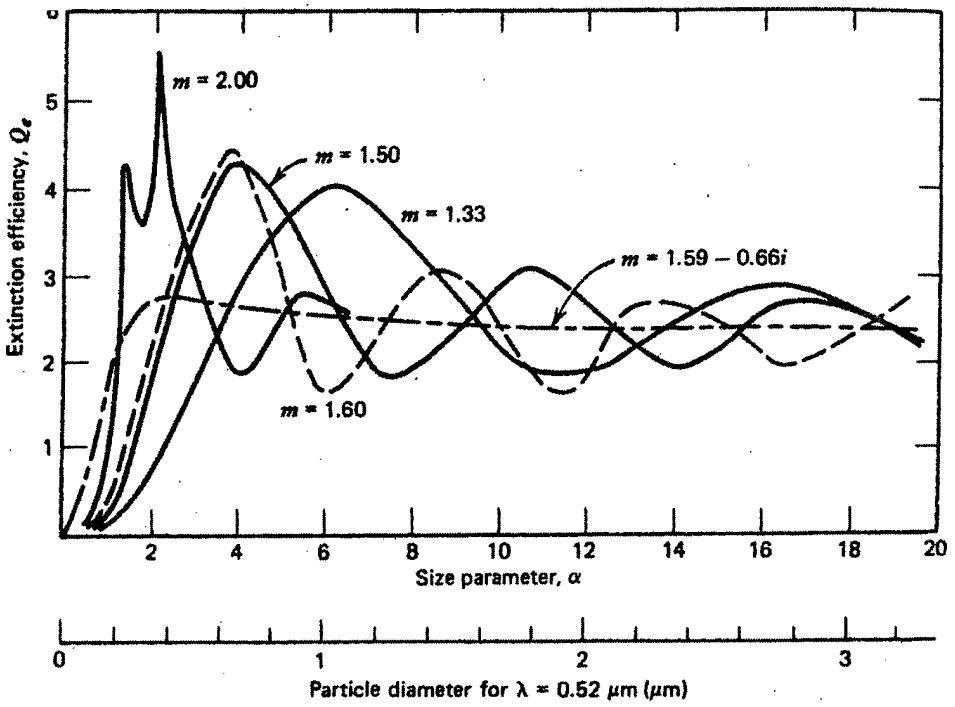

Figure 2.2 Extinction efficiency versus particle size for spheres. (Hinds, 1999)

To understand how our sensor components should theoretically operate in the presence of different fog drop size distributions theoretical scattering calculations were undertaken. The fog extinction coefficient was evaluated while varying drop mean size, LWC (volume) and the breadth of distribution (as expressed by the geometric standard deviation, σ_g). This was done utilizing a Fortran program originally written by Bohren

and Huffman (1983). The modified program we used and the numerical results can be found in appendices A and B respectively. The program calculates the extinction coefficient associated with a log normal distribution of particles with a specified refractive index.

The extinction coefficient (σ_e) is the fractional loss in intensity per unit path length associated with an elemental thickness, dL (Hinds, 1999).

In Figure 2.3, the fog LWC was varied while holding constant the mean size and breadth (σ_g) of the distribution. The extinction coefficient increases when LWC increases or mean drop size decreases.

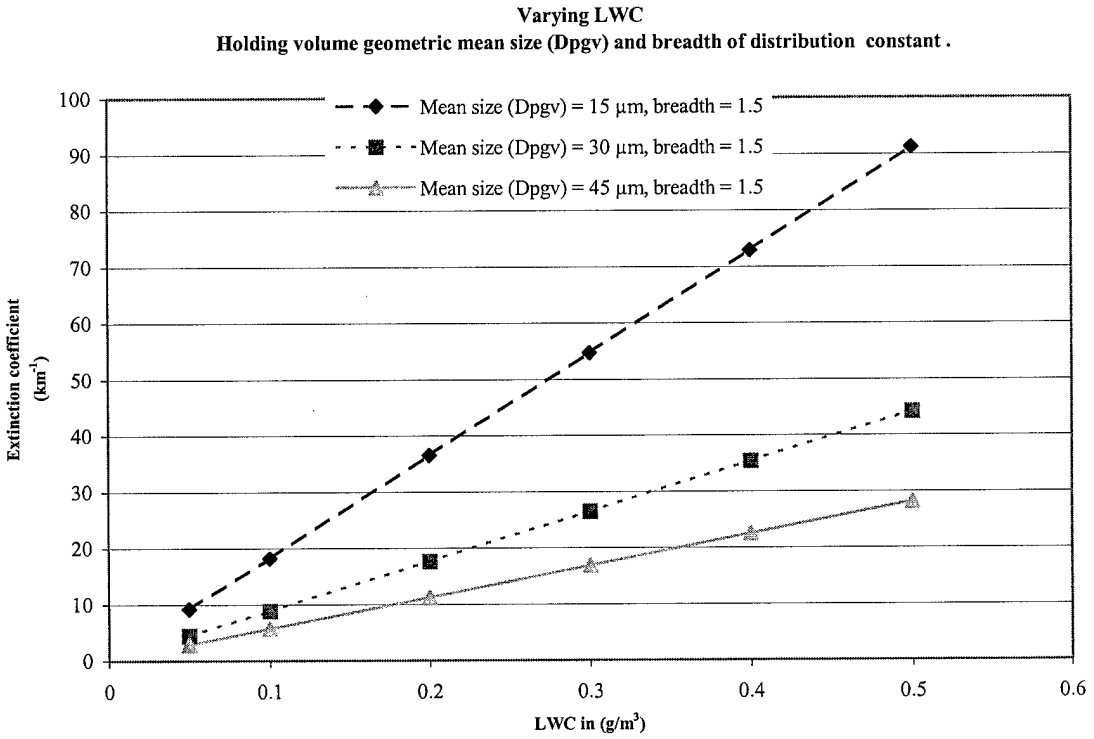

Figure 2.3 Dependence of extinction coefficient on fog LWC and volume geometric mean drop size.

Figure 2.4 shows that as the breadth of the distribution increases the extinction coefficient decreases slightly, if LWC and mean size are held constant.

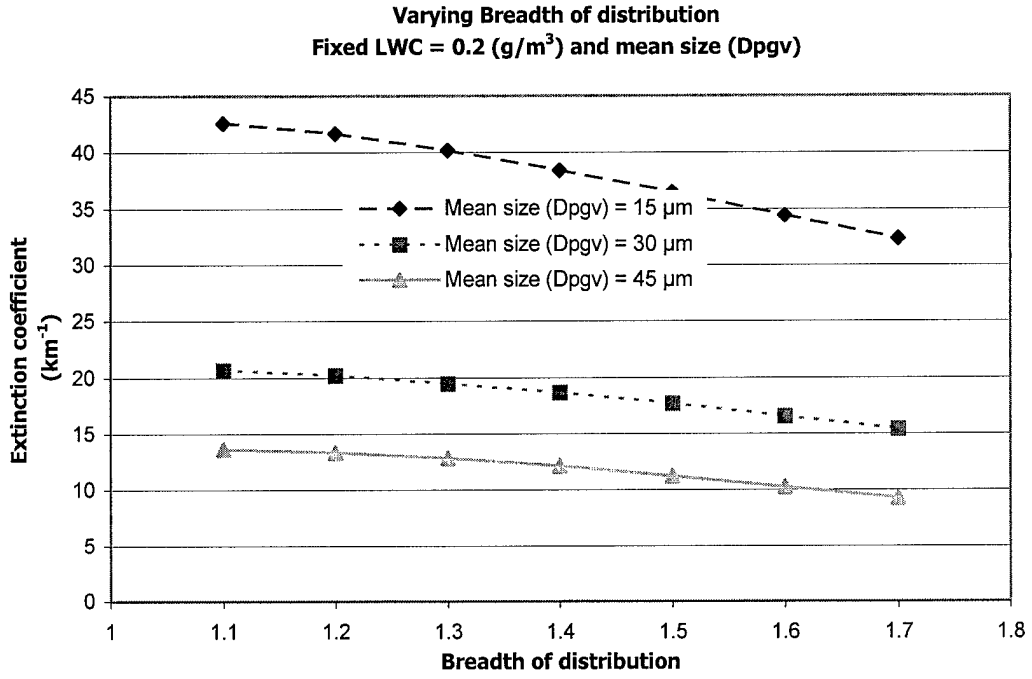

Figure 2.4 Effects of the breadth of distribution on the extinction coefficient when LWC and mean size are fixed.

Next, mean size was varied while holding the LWC and the breadth of distribution constant. As the mean drop size increases the extinction coefficient decreases. This relationship, which is already seen in Figure 2.3, becomes apparent when the relevant equations are considered.

Attenuation ($\frac{I}{I_0}$) is the ratio of light intensity traversing the fog to that incident on the fog (see Figure 2.5) and is described mathematically by the following equation known as Bouguer's law (or the Beer-Lambert Law),

$$\frac{I}{I_0} = e^{-\sigma_e L}, \qquad \text{(Eq'n. 2.2)}$$

where, σ_e = extinction coefficient and L = path length through the fog.

Cross-section of fog sample volume.

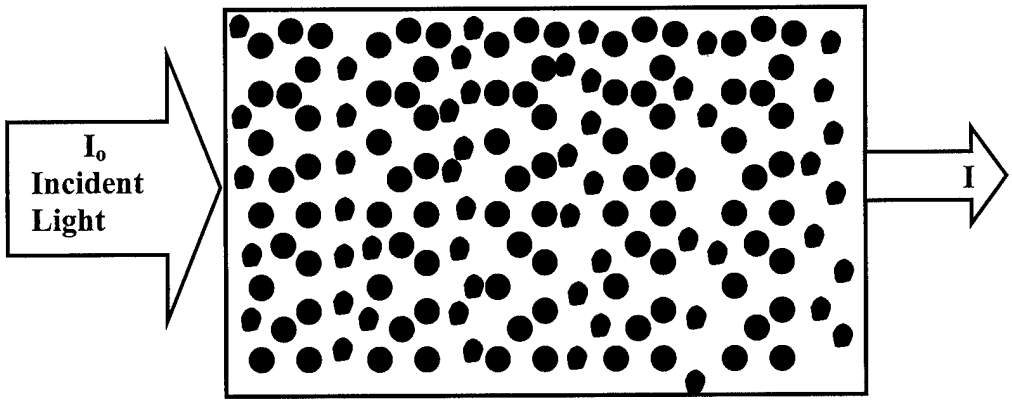

Figure 2.5 Schematic showing light attenuation.

To understand why the extinction decreases as mean particle size increases it is helpful to assume a monodisperse drop distribution. The extinction coefficient for a monodisperse drop distribution containing N particles per unit volume can be written as (Hinds, 1999)

$$\sigma_e = \pi N d^2 \frac{Q_e}{4}, \qquad \text{(Eq'n. 2.3)}$$

where d = drop diameter, N = particles per unit volume and Q_e= drop extinction efficiency (~2 for water drop diameters over 5 μm when $\lambda = .88\mu m$).

It is useful to express the transmission efficiency (given by Eq'n. 2.2) in terms of the mass concentration of a hypothetical monodisperse drop distribution. The mass concentration of drops (or LWC) can be written as

$$C_m = \frac{N\rho_p \pi d^3}{6} \qquad \text{(Eq'n 2.4)}$$

where C_m is the particle mass concentration (LWC), N is the total number concentration and ρ_p is the density of the particle.

Combining equations 2.2, 2.3 and 2.4 we find that

$$\frac{I}{I_0} = \exp(-\sigma_e L) = \exp(-\frac{3C_m Q_e L}{2\rho_p d}) \qquad \text{(Eq'n 2.5).}$$

If we hold the fog liquid water content (C_m) constant and vary the monodisperse fog drop size we can readily see that the extinction coefficient decreases with increasing drop size (as long as Q_e is ~ constant).

Relaxing the assumption that the drop size be monodisperse and using the Bohren and Huffman model to calculate transmission of the IR source beam through fogs with fixed LWC and a lognormal distribution breadth, reveals a similar result: extinction decreases (transmission increases) as the drops are shifted to larger sizes (see Figure 2.6).

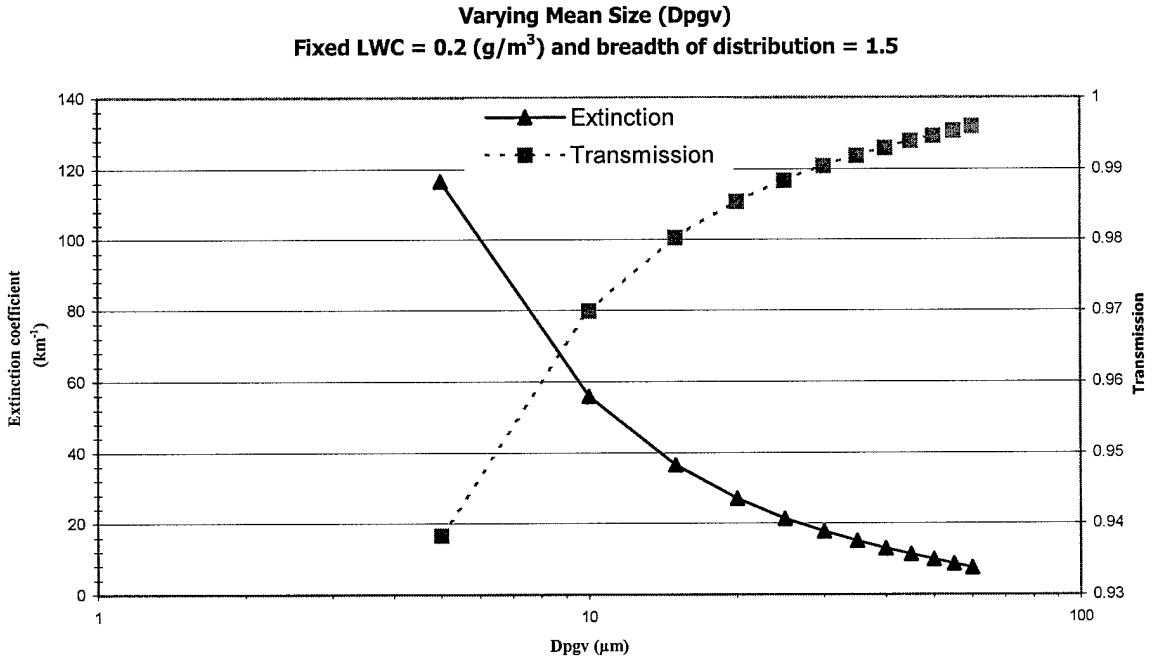

Figure 2.6 Effects of mean size on the extinction coefficient and transmission efficiency when LWC and breadth of distribution are fixed.

Accordingly, it is expected that the response of the CSU OFD will vary with mean fog/cloud drop size.

2.3 Glove box setup and testing

In order to test the sensor components we had to develop a method to create a simulated fog. The first method tried included dropping dry ice into a pan of warm water enclosed by a glove box (see Figure 2.7). This created a shallow, dense fog. The dry ice induced fog was hard to control (e.g., it was difficult to vary LWC). Therefore, it was decided to develop another method to generate fog.

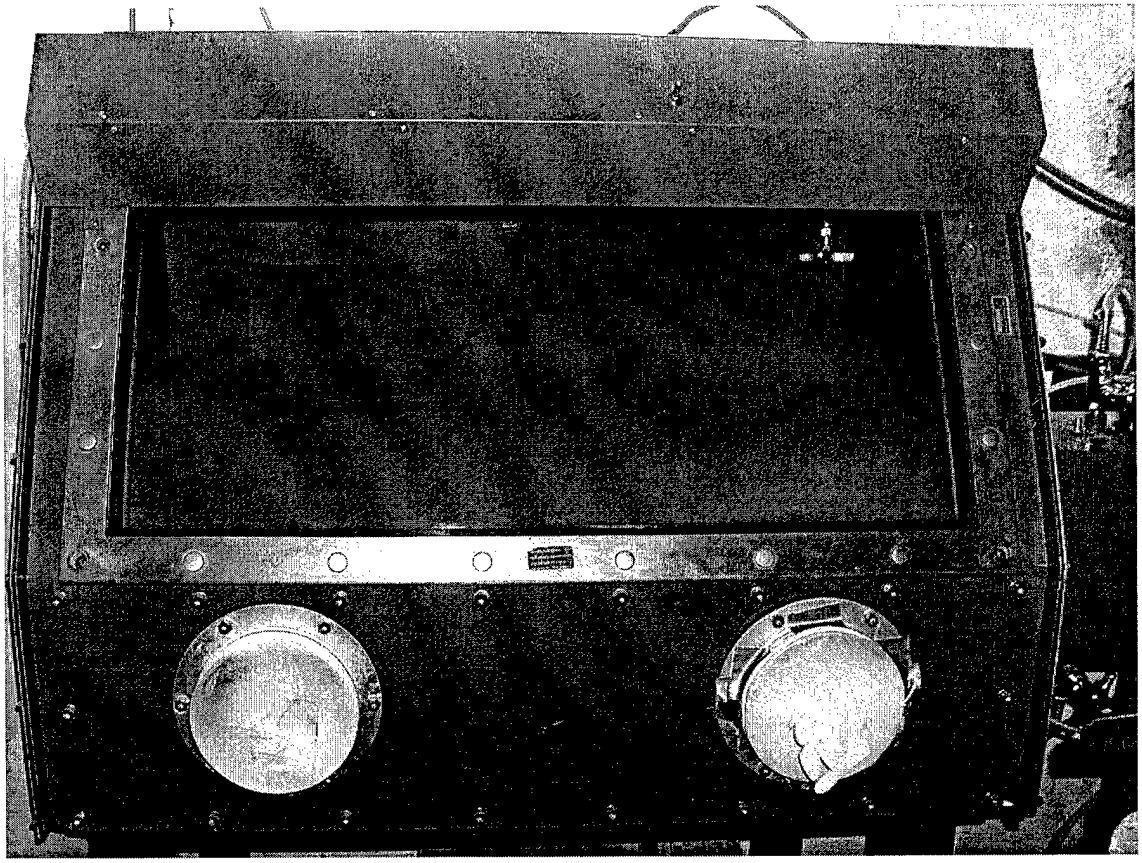

Figure 2.7 Glove box used for fog generation during Sim Lab tests.

For the next attempt at fog generation, an ultrasonic spray-type humidifier was modified to pump its output into the glove box. The humidifier would create fog but it took a long time for the humidifier to raise the LWC above 100 mg/m^3. Therefore, we added a port on the bottom of the humidifier where we could introduce compressed air, thus increasing the generation of fog. This greatly increased our ability to generate fog quickly. However, we were unable to keep the fog at a near constant LWC. Consequently, an additional port for dry compressed air was added. This port allowed us to adjust the flow of dry air into the fog stream to keep the LWC at a more constant rate. See Figure 2.8 for the final fog generation setup.

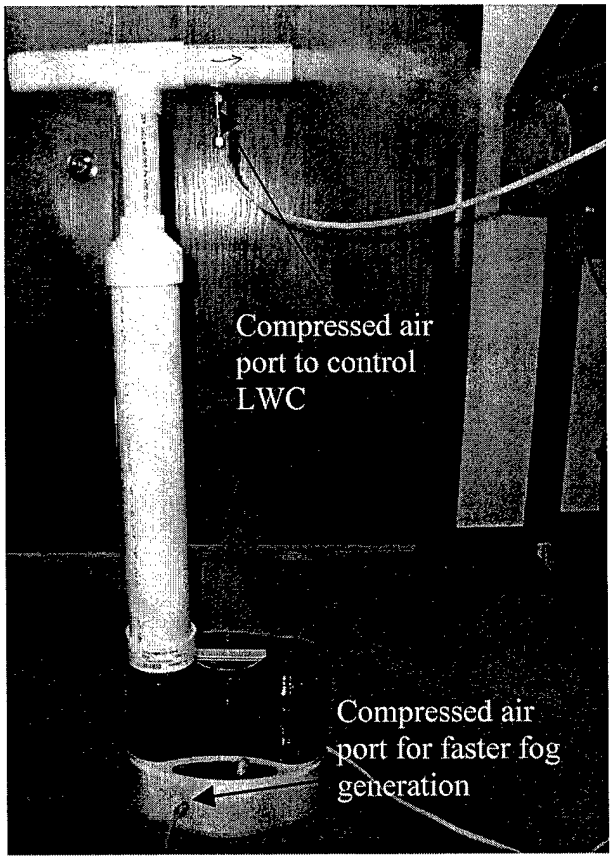

Figure 2.8 Humidifier setup for fog generation during Sim Lab tests.

After being satisfied with the fog generation, we proceeded to test the sensor in a variety of different configurations. The response of the sensor to simulated fog was examined by measuring attenuation, backscattered light, and different setups for forward-scattered light (see Figure 2.9).

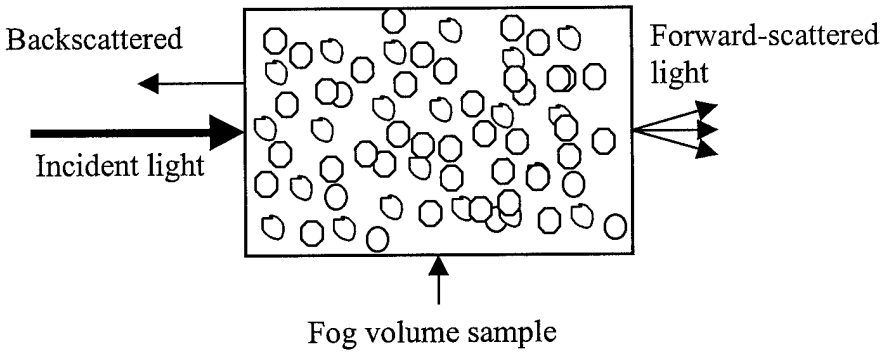

Figure 2.9 Schematic of backscattered and forward-scattered light.

The sensor response was calibrated prior to each configuration test as follows (see Appendix C for diagrams and for more in-depth calibration procedures). First, the null screw is adjusted just until the detector output LED's go out and only the power light remains on. Then, if needed we adjusted the null screw just until we got a zero reading on a voltmeter attached to the detector's analog output port. Next, fog was produced in the glove box (we consistently attempted to calibrate the sensor when the LWC was approximately 200 mg/m^3, as measured by the PVM) and adjusted the detector span setting until the reading matched the reading of the PVM. We then dried out the glove box, rechecked the zero adjustment, and if necessary repeated the entire procedure. The result of this calibration procedure was to calibrate each configuration of the CSU OFD at two points: a zero (no fog) and a span value corresponding to ~ 200 mg/m^3 LWC.

2.3.1 Backscatter configuration

The first test tried in the glove box was with the Banner components arranged in a backscatter configuration. This is the measurement configuration used by the Caltech IR fog sensor and promised to provide a very compact instrument configuration. For this test, the fiber optic cables were mounted on a single flat piece of metal (see Figure 2.10). The fiber optics were mounted approximately 1.3 centimeters apart. They were then placed inside the glove box with the PVM and the humidifier was activated. In this configuration the sensor was not sensitive enough to receive backscattered light from the fog; thus it was impossible to calibrate the sensor.

This configuration was tried a second time after it was calibrated in the attenuation mode. We still could not get a significant reading on the sensor even though the PVM was reading a LWC of over 500 mg/m^3. We concluded that the receiver was not sensitive enough to be used in this configuration.

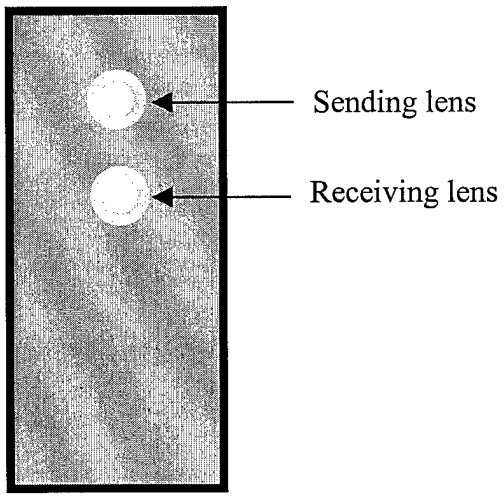

Figure 2.10 Schematic of optics setup for backscattering test.

2.3.2 Forward-scattered configuration

Two forward scattering configurations of the CSU OFD were tested. One utilized a slight angular displacement (near forward scattered) while the other was done with a dump spot blocking direct reception of the transmitted light beam.

2.3.2.1 Forward-scattered at an angular displacement

The angular displacement test was designed with an offset angle between the lenses. The sensor was calibrated initially with a 2° offset and this displacement was varied between 2°and 15° (see Figure 2.11). This was done in order to determine the best configuration. However, this configuration proved not to be very useful and no identifiable relationship seemed to exist between the voltage reading from the Banner components and the PVM LWC readings.

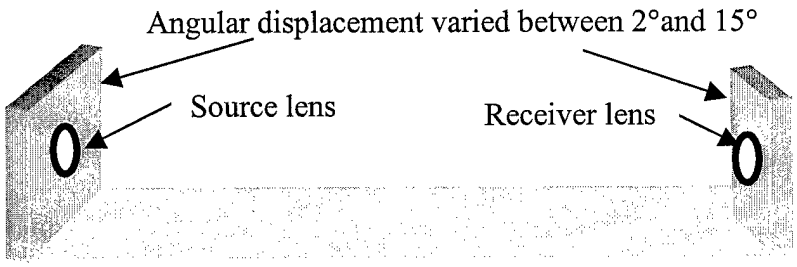

Figure 2.11 Setup of angular displacement test with lenses approximately 0.53 meters apart.

2.3.3 With dump spot

The next setup tested was the forward scattered with a dump spot (see Figure 2.12). For this test, numerous configurations were tried to determine what characteristics of the dump spot would work best. First, we tried to put the dump spot equally distant from both lenses as described by Mallant (1990). In this configuration,

we did not receive nearly as much signal as we had expected to receive. This may in part be due to not knowing the exact width of the source beam (Banner, the manufacture of the optics and IR sensor couldn't tell us the exact width either).

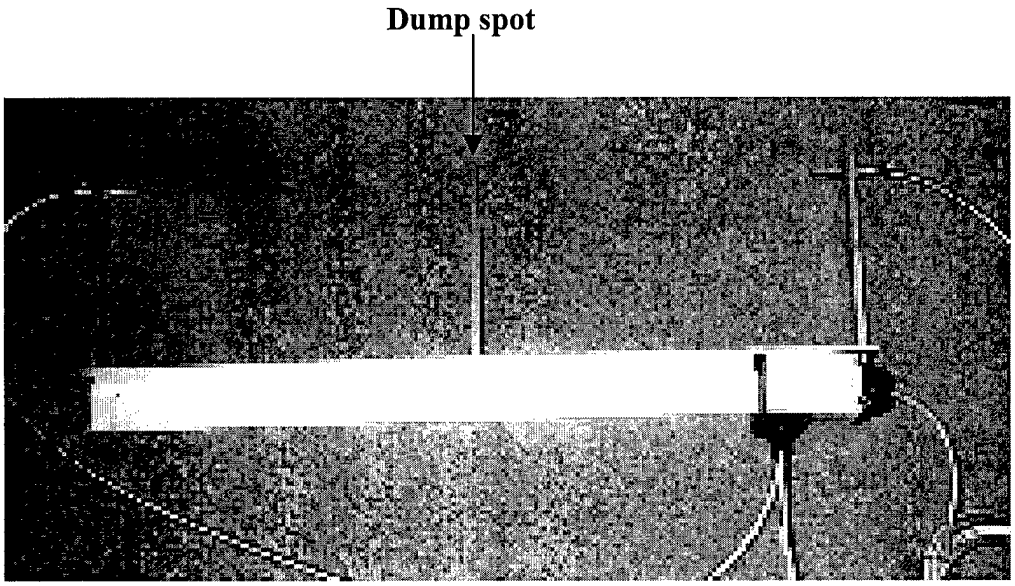

Figure 2.12 Components in dump spot configuration, after Mallant (1990).

Next, we tried to fashion a small dump spot (~ 2 millimeters wide) affixed ~ 2 centimeters in front of the receiving lens (see Figure 2.13). This was modeled after the configuration of the Gerber Scientific PVM.

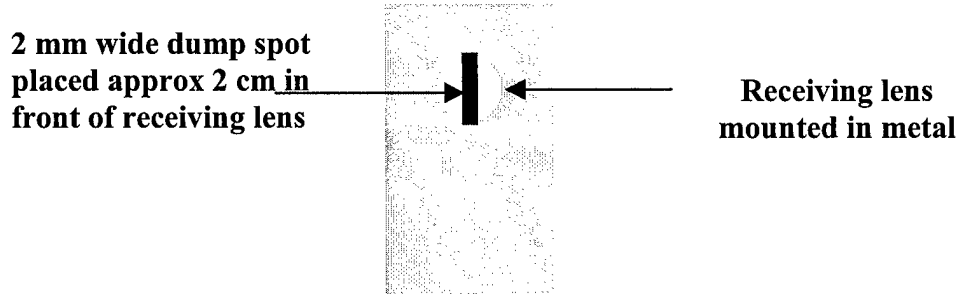

Figure 2.13 Small dump spot setup.

This configuration allowed us to receive more signal than before and to some extent, it tracked the LWC reading from the PVM (see Figure 2.14a and 2.14b),

especially up to the 200 mg/m^3 reading that was initially used to calibrate the sensor. However, it still did not track as well as desired at LWC values greater than 200 mg/m^3.

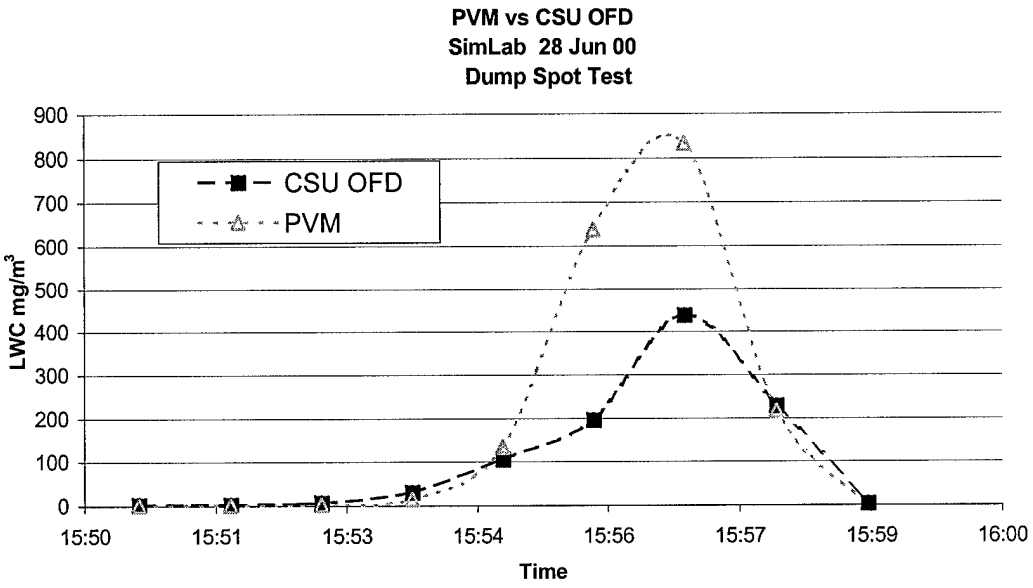

Figure 2.14a Dump spot test results with dump spot placed a few cm directly in front of receiving lens.

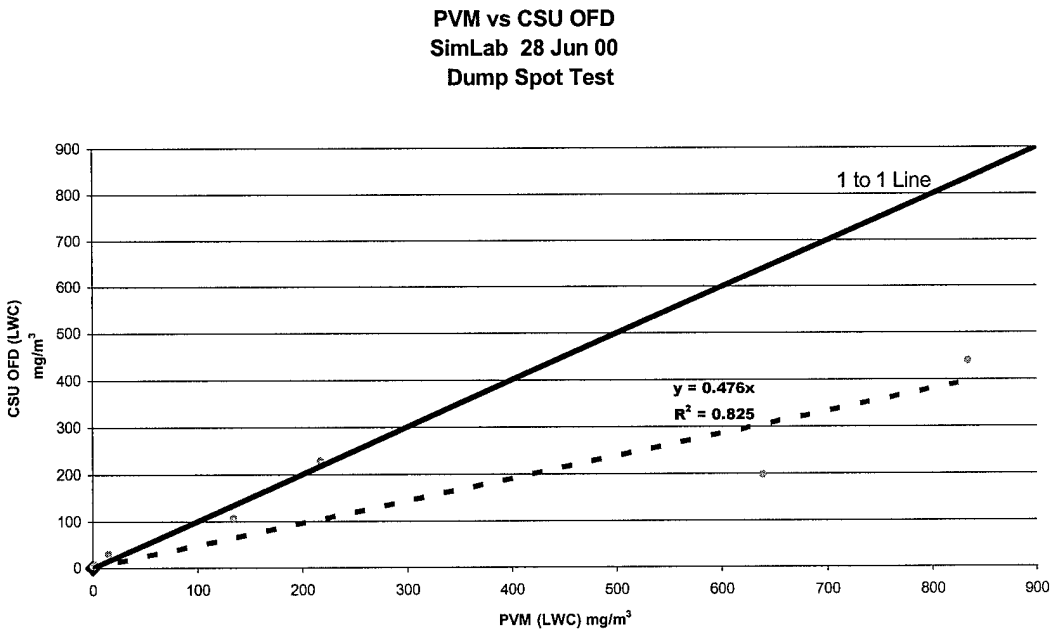

Figure 2.14b Comparison of PVM and CSU OFD LWC during the dump spot test with the dump spot placed a few cm directly in front of receiving lens.

2.3.4 Attenuation

For this test, the lenses were positioned 53.3 cm apart and opposed to each other with a 0° offset. This configuration would show full signal strength reaching the receiver in the absence of any obstructions. To make the voltage reading easier to read and to match the PVM reading more closely, the power setting was inverted on the OASBFX Analog OMNI-BEAM sensor. This would make full signal strength register as zero volts on the analog output. The output of this set up is an analog signal that appears to be proportional to LWC. The result of this test was very promising (see Figures 2.15a and 2.15b).

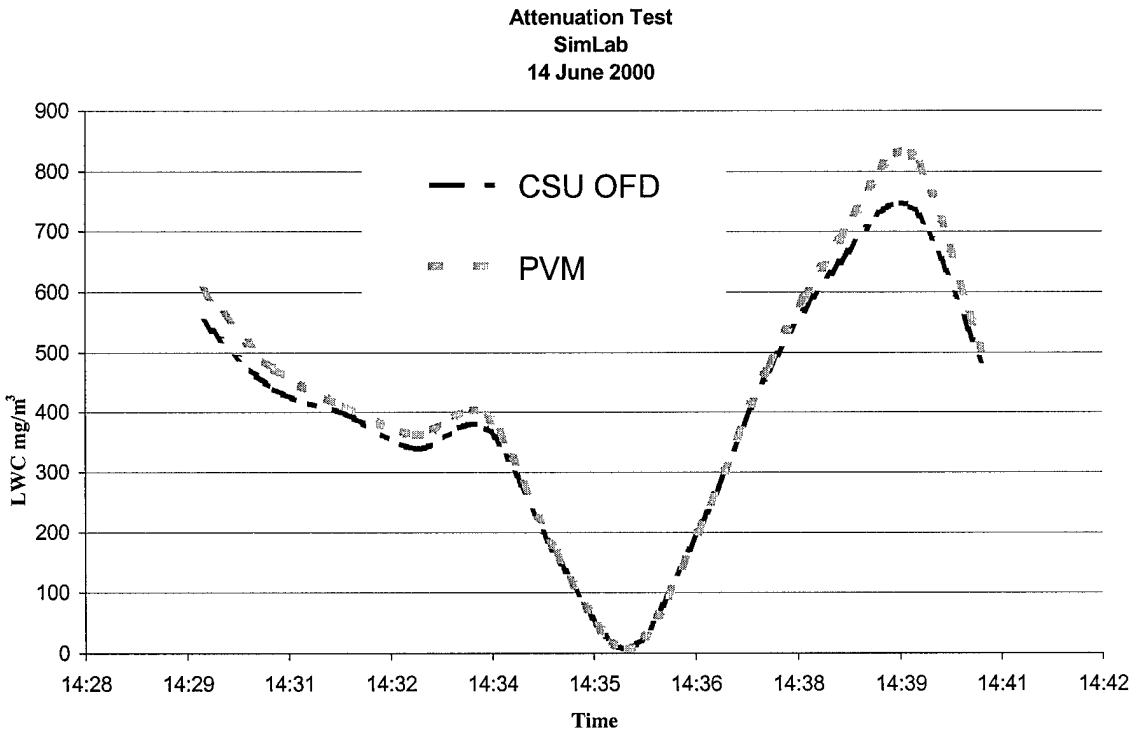

Figure 2.15a. Results of first attenuation test.

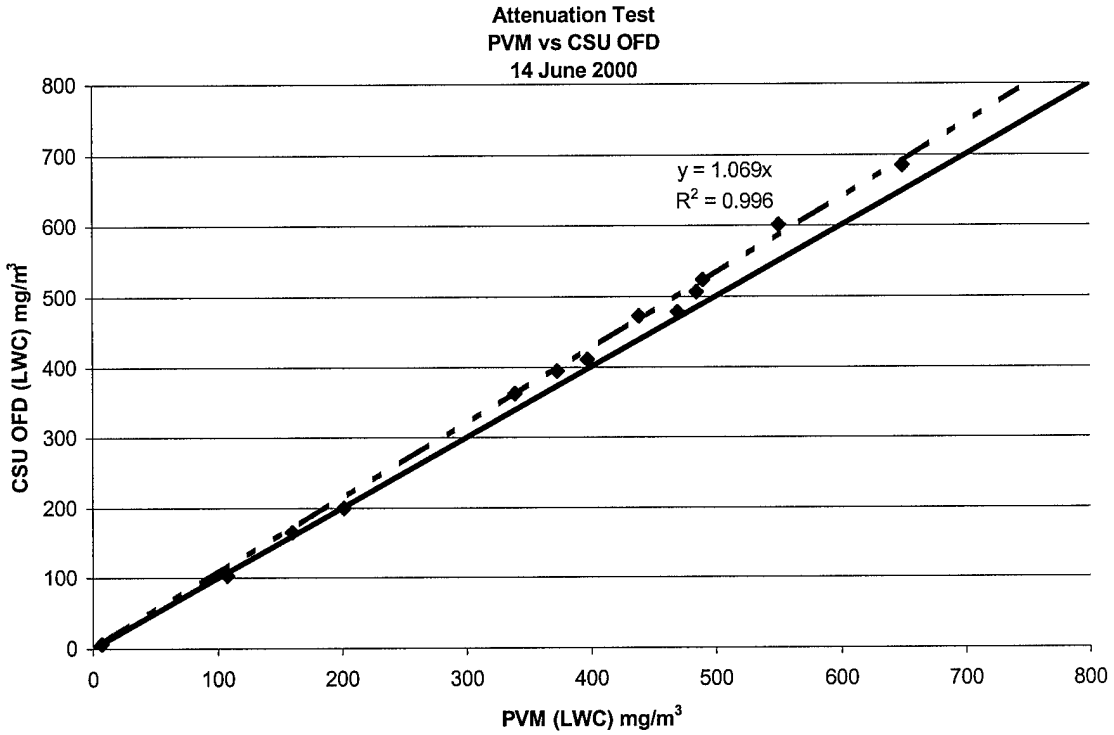

Figure 2.15b. One to one results from first attenuation test shows a very high linear correlation between the CSU OFD and the PVM.

The results show that the CSU OFD tracked exceptionally well with PVM, having an R^2 value (coefficient of determination) greater than 0.99 and a slope close to 1.0.

Next, we tested how the CSU OFD in its attenuation configuration would react when started in heavy fog with the fog quickly dissipating (see Figures 2.16a and 2.16b). The results again were very promising with the CSU OFD closely tracking the PVM until the fog dried out to approximately 10 mg/m^3. The linear correlation again was very good with an R^2 value greater than 0.99 and a slope of 1.01.

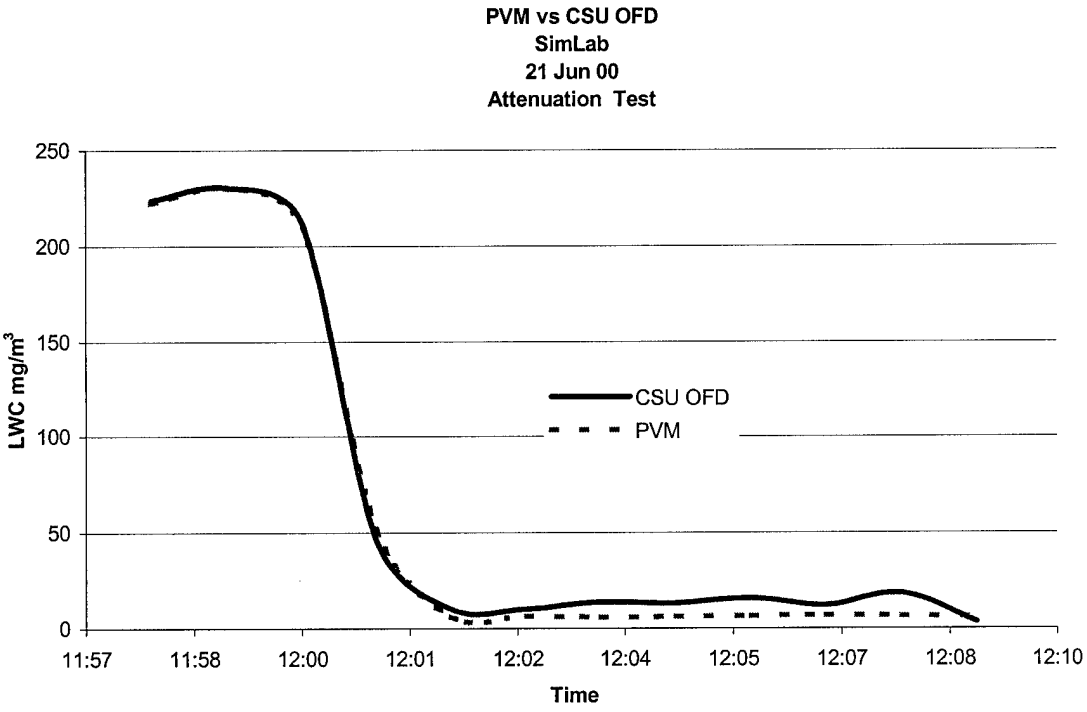

Figure 2.16a. Attenuation results starting in fog and drying out rapidly.

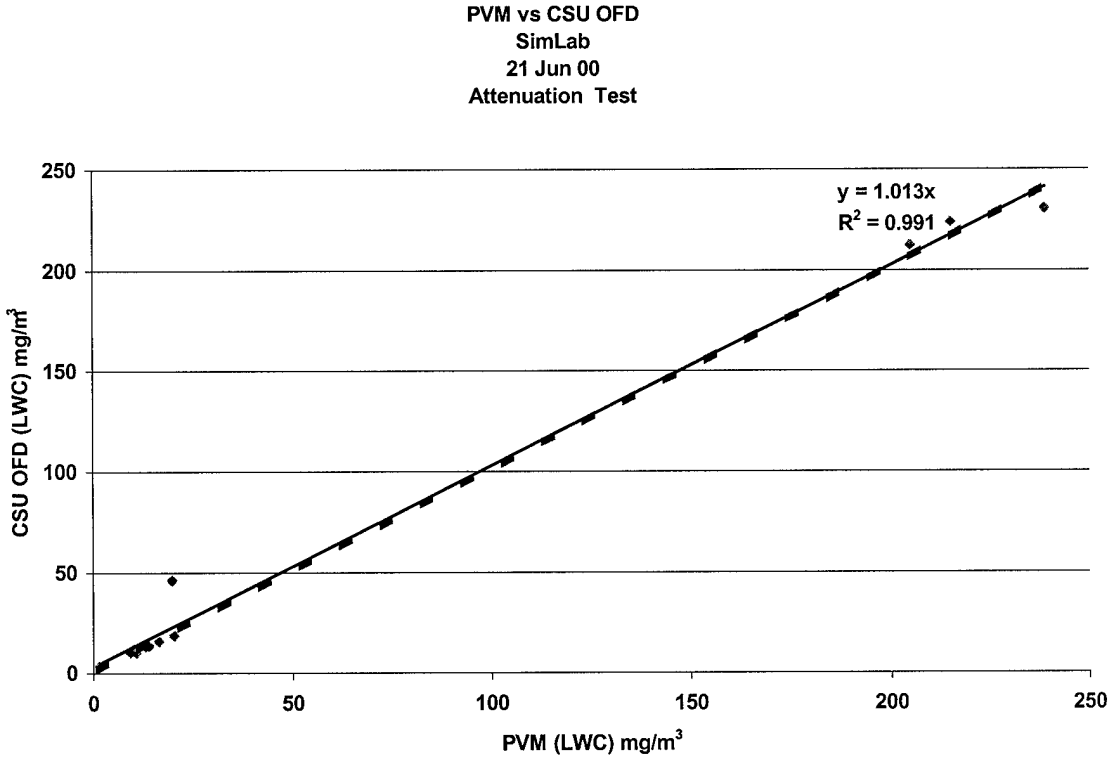

Figure 2.16b. One to one relationship of attenuation results starting in fog and drying out rapidly.

2.4.4.1 Attenuation test with focusing lenses

The results of the attenuation test were so promising it was decided that using the sensor in this mode was probably the best option. We decided to do another test in this mode utilizing focusing lenses that were attached (screwed on) to the sensing and receiving ends of the fiber optic cables. We thought this would possibly yield even better results (see Figures 2.17a and 2.17b). The configuration did produce results that showed the CSU OFD tracking reasonably well with the PVM but not as well as it did without the lenses.

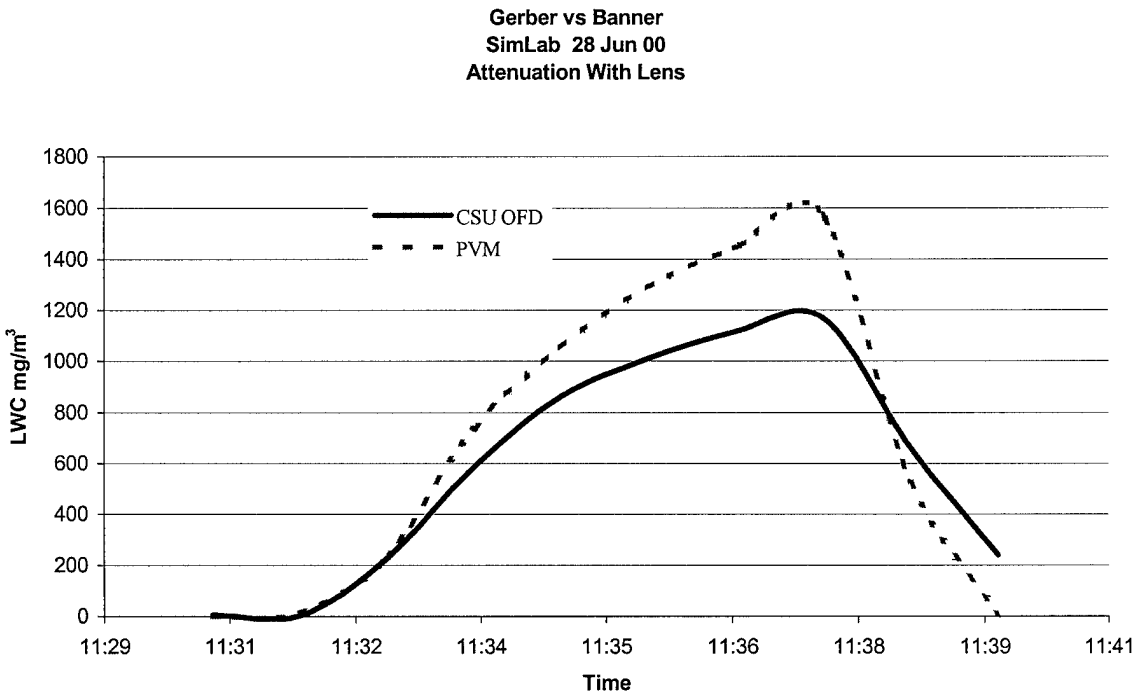

Figure 2.17a. Attenuation results with focusing lenses.

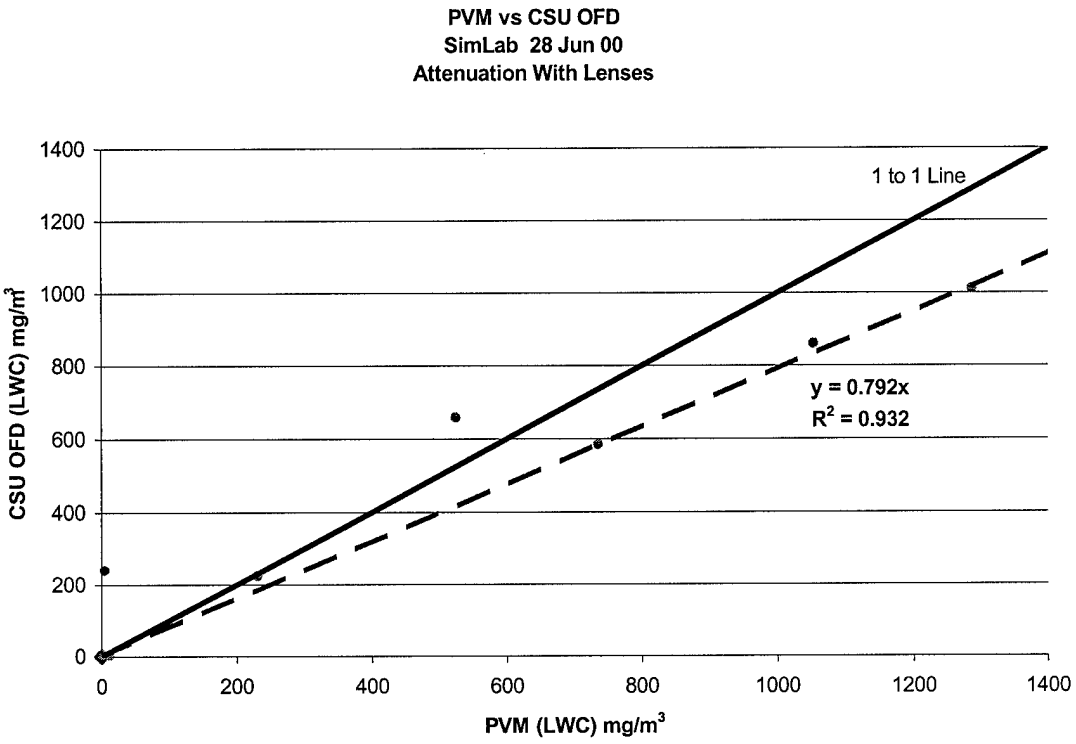

Figure 2.17b. One to one plot of attenuation results with lenses.

2.3.5 Design of CSU OFD for Storm Peak Lab tests

Storm Peak Lab (SPL) is located at 10,560 ft (3220 m) on Mt. Werner near Steamboat Springs, CO (see Figure 2.18). SPL is a high elevation, mountaintop atmospheric research facility readily accessible under all weather conditions. It is operated by the Desert Research Institute (DRI) Atmospheric Sciences Center (DRI, 2001). SPL maintains various meteorological sensors at the site.

Figure 2.18 Storm Peak Lab, mountaintop atmospheric research facility, Steamboat Springs, CO.

For the SPL field test, we used the attenuation setup without lenses. Three CSU OFD's were installed at SPL to verify whether the measurements of the CSU OFD were repeatable with multiple sensors.

2.4 Calibration tests and procedures

Before going to SPL, we developed a method for calibrating the sensors in the field. Up until this point, the sensors were calibrated using the PVM while they were both in the glove box. The initial OFD calibration procedure and its adaptation for field calibration are described below.

The following procedures were developed to initially calibrate a new sensor. The first adjustment to a new sensor, with no obstructions between the lenses, calls for turning the null screw just until the output LED's go out and only the power light remains on. Continue to slowly turn the null screw just until you get a near zero ($\pm 5mV$) reading on an attached voltmeter. If you cannot get it to this value, you may have to adjust the span screw until you get a near zero reading.

Now you need to produce fog and adjust the span setting until the reading matches the reading of the PVM (see Appendix C for current, more in-depth calibration procedures). Then dry out the glove box, recheck the zero adjustment, and if needed, repeat the entire procedure. The calibration of the CSU OFD is an iterative process.

Once we felt confident that one of the CSU OFDs was calibrated within reasonable limits ($\pm$ 5 mg/m^3) to the PVM, we developed a method to calibrate the other sensors without the use of the glove box. This procedure was required since it would not be feasible to take the glove box into the field.

Our first thought was to try to use the light diffusing calibration disk provided with the PVM. This disk was designed to work with the 780nm laser in the PVM. When it was placed in the path of the CSU OFD's 880nm infrared beam it would not allow any detectable light to pass through. Next, various plastic and glass lenses were tested to see what type of reading they would produce. We also had to ensure that the reading could be repeatably produced. We wanted something that could be easily replaced if broken or lost. It was discovered that an Avery 5177 Ink Jet Transparency consistently produced a reading of 330 mV on a voltmeter when placed in front of the receiving lens of the pre-calibrated CSU OFD (330 mV corresponds to 330 mg/m^3 when referring to LWC).

Several sheets of Avery 5177 Ink Jet Transparencies were tested and all produced similar results.

The other CSU OFDs were calibrated using the Avery transparency. All 3 CSU OFDs tracked very close to the PVM (in additional glove box testing). Therefore, a field calibration disk was made by placing a piece of transparency paper in a metal holder.

2.5 Storm Peak Lab experiment

The SPL experiment was scheduled when frequent cloud interception could be expected at the facility. August was chosen because climatologically, August has numerous cloud intercept days due to monsoonal flow and we hoped to test the CSU OFD in the presence of actual clouds.

2.5.1 Equipment setup

The equipment was set up on the roof of SPL (see Figure 2.19) and included three CSU OFDs, the PVM and a Campbell CR10X data logger. Unfortunately, data-logger problems precluded logging the particle surface area channel from the PVM.

The sensors were mounted on a railing and were set up virtually at the same height. This was done because small vertical position variations in a fog or cloud can yield large differences in LWC.

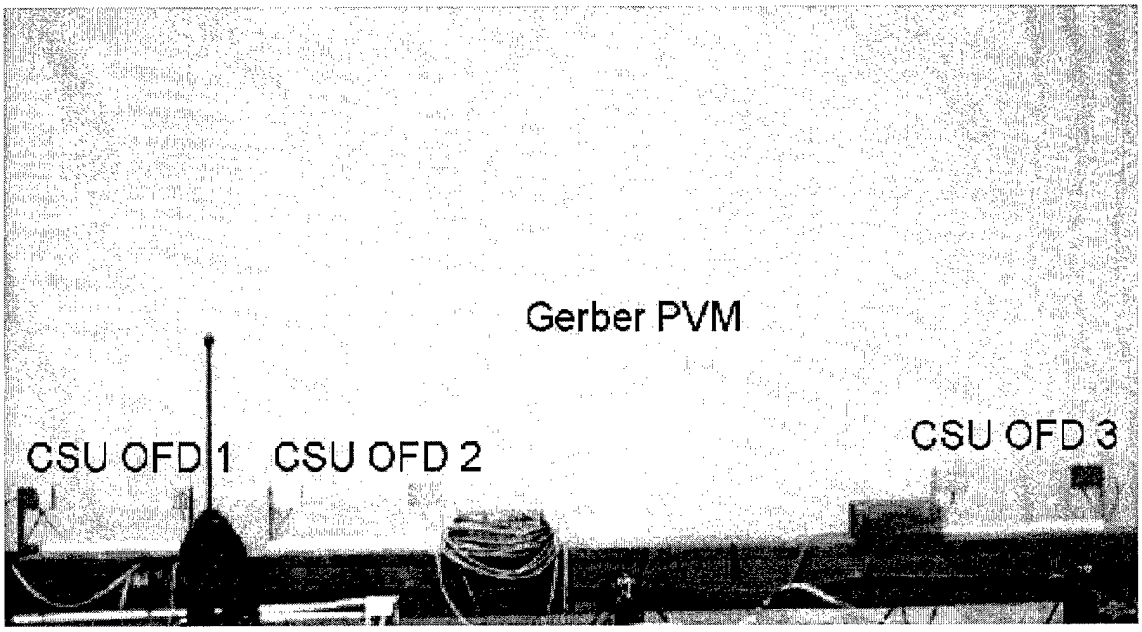

Figure 2.19. Equipment setup on SPL rooftop.

2.5.2 SPL test results

Overall, the results from the SPL experiment were excellent. However, it was discovered that one of the CSU OFDs was missing the O-ring that holds the fiber optics firmly in place. Since the optics were not held firmly in place, the sensor's readings tended to drift. Therefore, the data from that sensor (CSU OFD 1) were not reliable and were excluded from the comparisons.

There were three distinct cloud intercepts during the 4 weeks the sensors operated at SPL. The first event occurred on August 16-17, 2000 (see Figure 2.20) and lasted for 15 hours and 35 minutes. Both CSU OFDs tracked well with the PVM with the lowest linear correlation coefficient greater than 0.95 and slopes between 0.995 and 1.088. CSU OFD 2 slightly over-measured the LWC compared to the PVM while the CSU OFD 3 slightly under-measured it. The PVM measured a mean LWC, over the event, of 97 mg/m^3 with a maximum LWC of 608 mg/m^3.

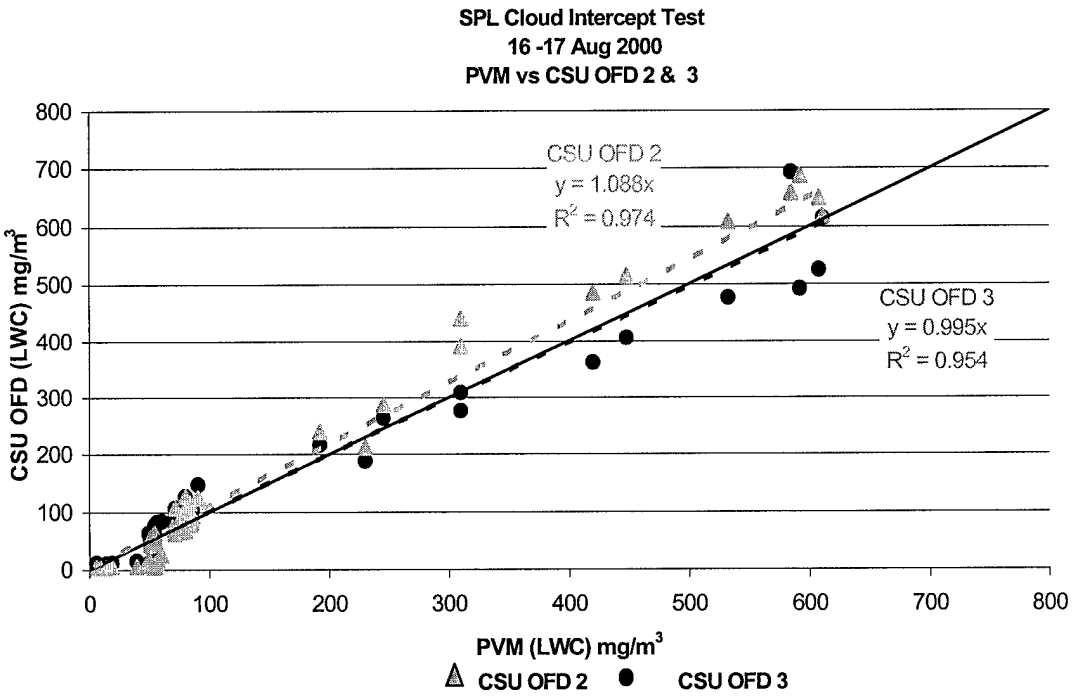

Figure 2.20. Relationship of CSU OFD versus PVM during the 16-17 Aug event.

The second cloud interception event occurred on August 20, 2000 (see Figure 2.21) and lasted for 4 hours and 20 minutes. The R^2 of CSU OFD 2 was 0.95 while CSU OFD 3 had an R^2 of 0.97, both showing a very high linear correlation for this event. During this event, CSU OFD 3 slightly over-measured the LWC (slope = 1.007) while CSU OFD 2 slightly under-measured it (slope = 0.955). The mean LWC reading from the PVM was 451 mg/m^3 with a wide range extending from near 0 to almost 1100 mg/m^3.

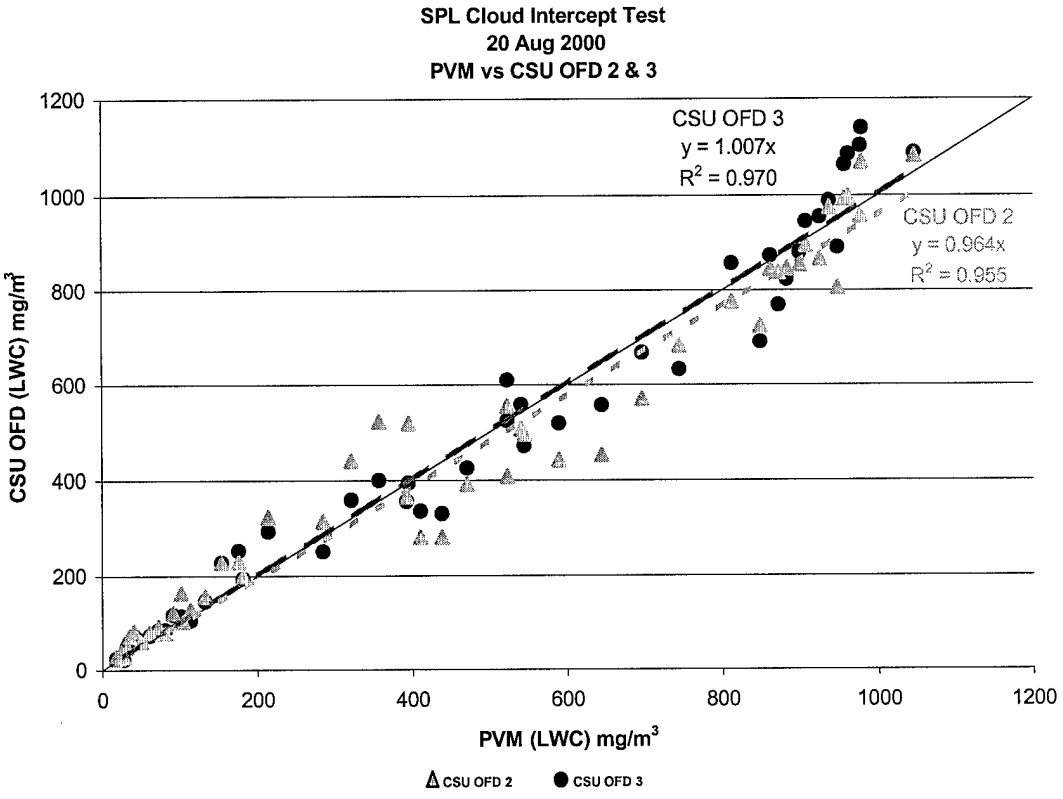

Figure 2.21. Relationship of CSU OFD versus PVM during the 20 Aug event.

The final event occurred on August 24-25, 2000 (see Figure 2.22) and lasted for 21 hours and 50 minutes. The linear correlation of both CSU OFDs fell off dramatically with CSU OFD 3 having the better R^2, which was only 0.84 (slope = 0.91). The slope and correlation coefficient for CSU OFD 2 were 1.03 and 0.81, respectively. The mean LWC reading from the PVM was 71 mg/m^3; the maximum LWC during the event was 443 mg/m^3.

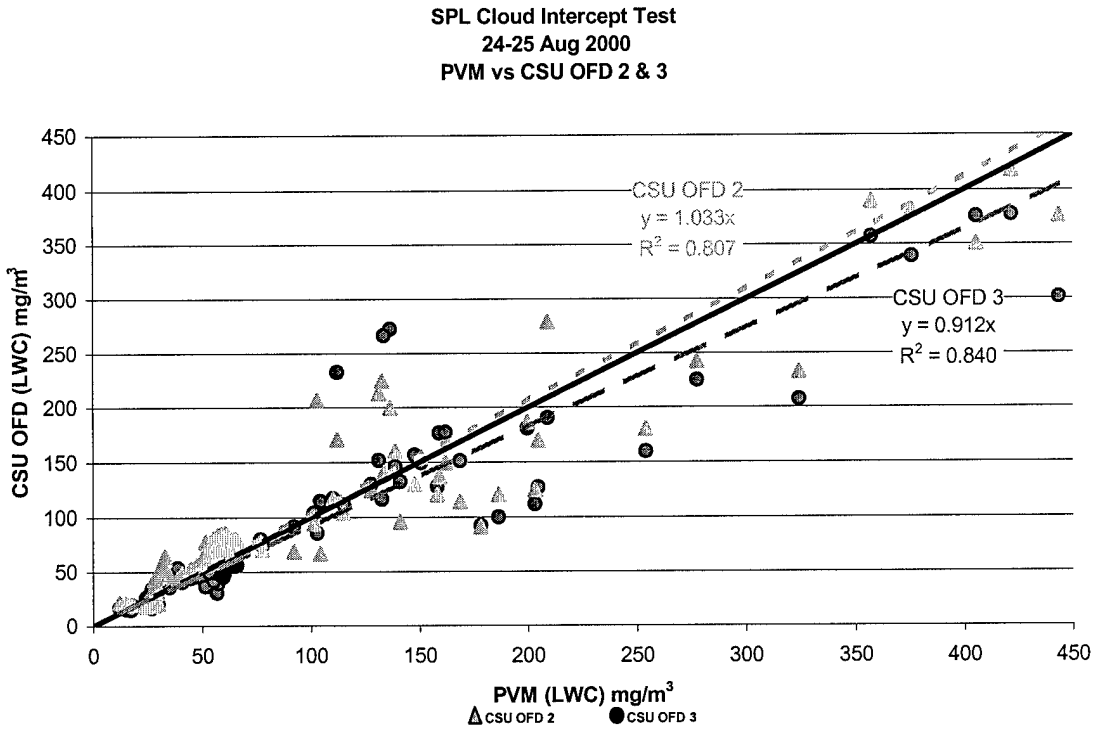

Figure 2.22. Relationship of CSU OFD versus PVM during the 24 – 25 Aug event.

The lower correlation during this event may be in part due to the accumulation of dirt on the optics over the 3 weeks that the sensors were installed. It is also possible that changes in the cloud drop size distribution during the event, and associated changes in OFD response, may have reduced the correlation in response between the OFD's and the PVM. Accumulation of water on the OFD sensor optics could also have affected the measured attenuation.

Changes in OFD response as the optics become dirty can be seen in figures 2.23a and 2.23b which depict results from a 12 day test done on the Sim Lab roof. For this test the sensors were all calibrated on September 8th then checked every few days to see how well the calibration held. The calibration held well the first few days but then began to

drift upward. We attributed this to dirt accumulating on the optics since after they were cleaned the readings went back to acceptable standards.

The dirt accumulation on the optics would cause the sensor to give false readings both in and out of cloud. Due to this, in the final design a filtered air pump was incorporated to blow clean air across the optics. We also decided to require the optics to be manually cleaned weekly.

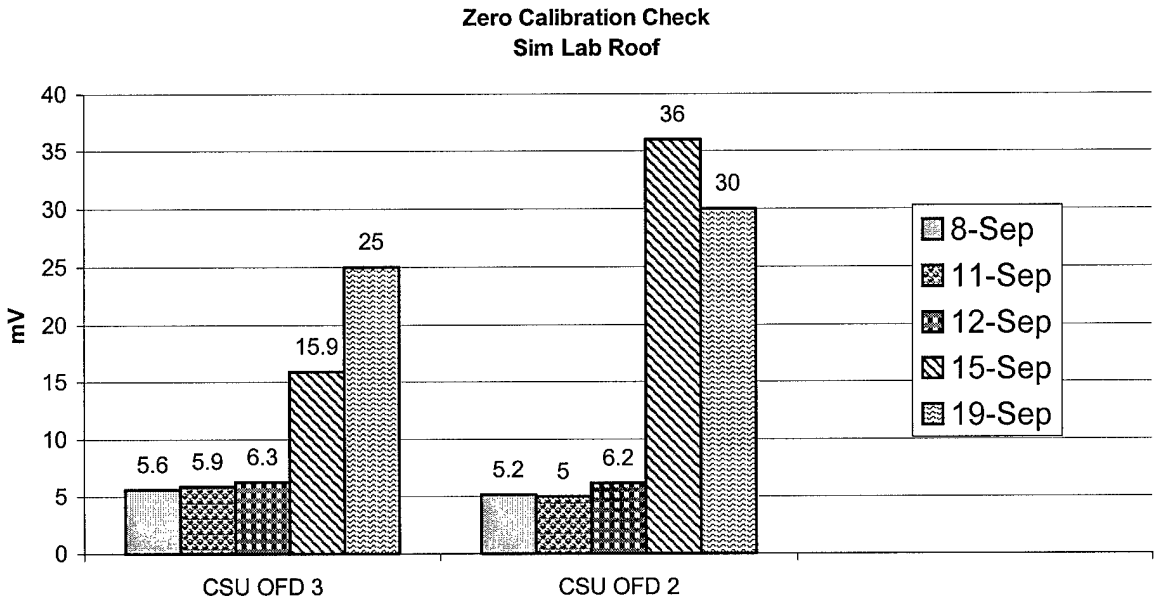

Figure 2.23a Calibration results from Sim Lab tests (zero calibration value should be 5 ± 3 mV). Increase in zero calibration value is attributed to accumulation of dirt on its optics.

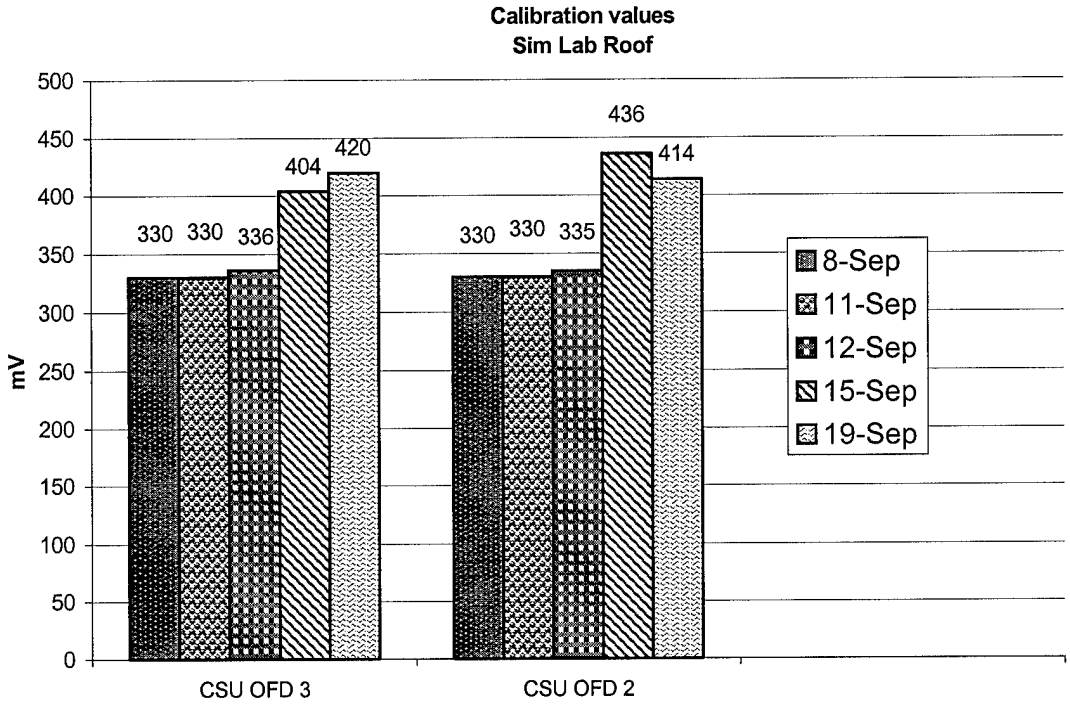

Figure 2.23b Calibration results from Sim Lab tests (calibration results should be 330 ± 3 mV). Increase in calibration value is attributed to accumulation of dirt on its optics.

Measurements from all three SPL cloud interception events are plotted in figure 2.24. A summary of linear regression results (OFD vs. PVM) is provided in Table 2.1. The CSU OFD's worked fairly well and neither sensor consistently gave high or low LWC readings. Combining results from both OFD's for all tests gave a regression equation of $LWC_{OFD} = 0.99 * LWC_{PVM}$ with a correlation coefficient of 0.92.

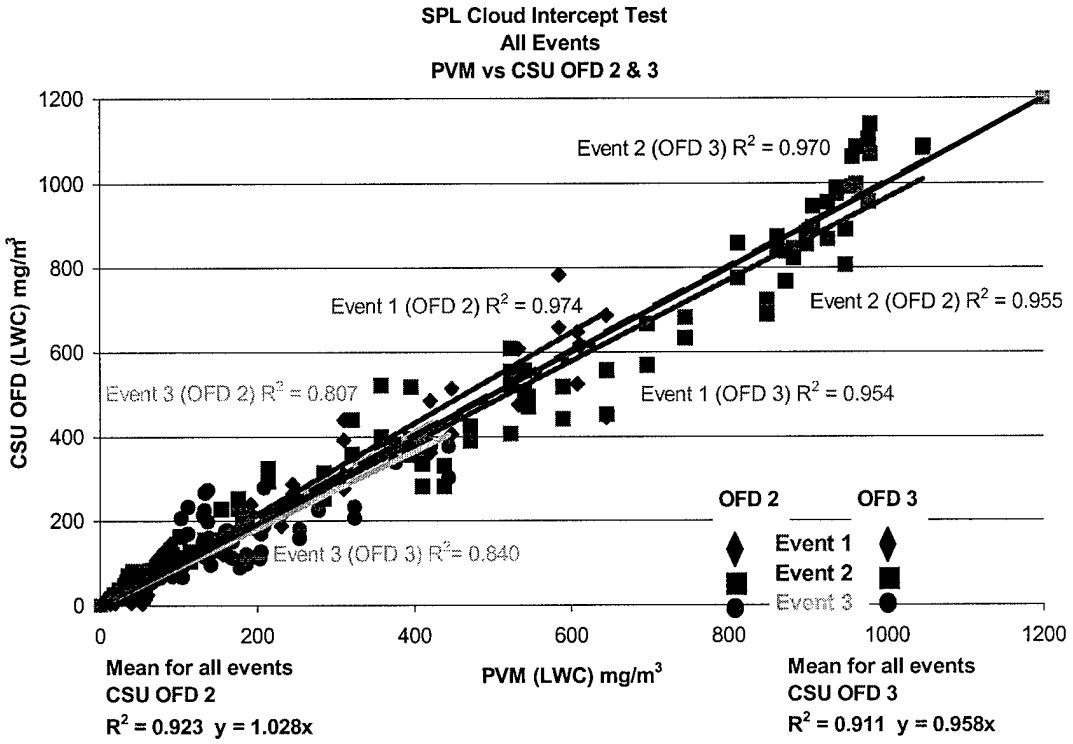

Figure 2.24. Relationship of CSU OFD versus PVM during all SPL events.

	Event 1 R^2	Event 2 R^2	Event 3 R^2	Event 1 y=	Event 2 y=	Event 3 y=
CSU OFD 2	0.973	0.955	0.841	1.088x	0.964x	1.033x
CSU OFD 3	0.954	0.973	0.807	0.955x	1.007x	0.912x

Table 2.1. Table of CSU OFD results from all SPL events.

We also wanted to see if the CSU OFDs exhibited any noticeable diurnal effects (see Figure 2.25), so a 3-day span was examined when there was not any fog/cloud detected at SPL. During this timeframe there does not seem to be a very noticeable diurnal effect. Measurement variability is within +/- 10 mg/m^3 for all three instruments, with the PVM showing the largest fluctuations.

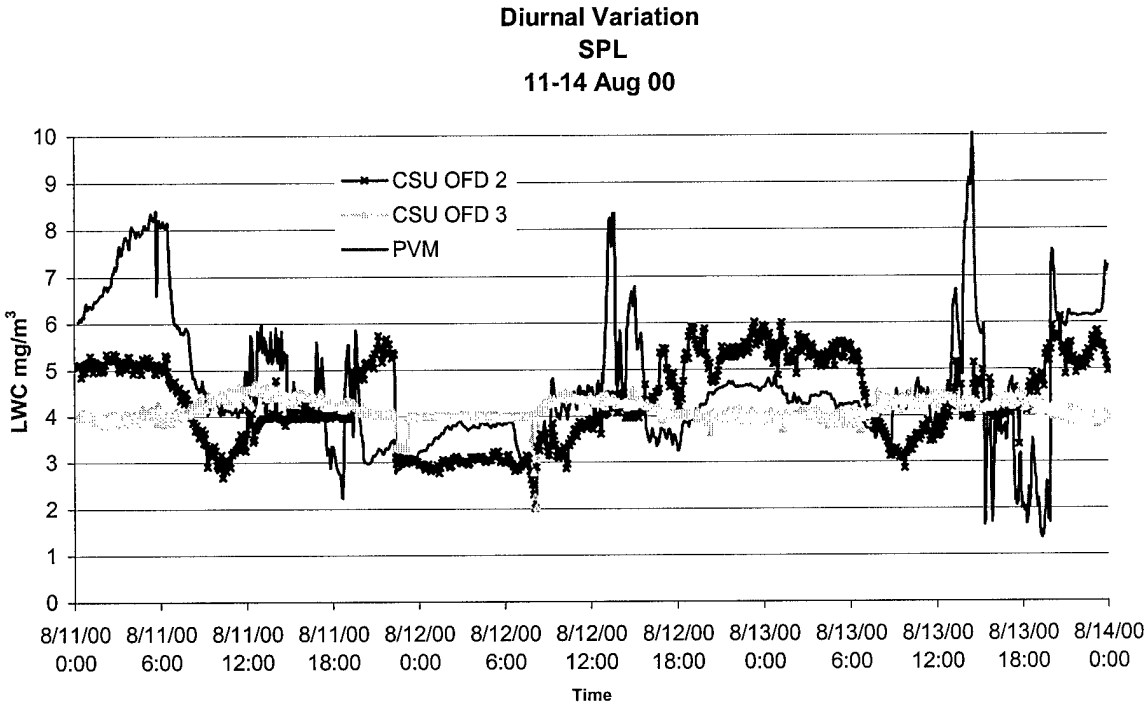

Figure 2.25. Diurnal variation test.

2.5.3 Lessons learned, precipitation effects, and minimum detection limit

The experimental results from SPL were very promising. We learned that the CSU OFD could definitely be used as a fog presence detector and, at least in the clouds at SPL, be used as an instrument capable of measuring LWC. We did discover that we needed to develop a method to help keep the optics clean.

We also wanted to see the effects that precipitation would have on the current configuration. Three CSU OFD's were again prepared for testing. Two of the sensors were modified by putting a roof over them to shield them from precipitation. The roof was made of metal and extended the entire length of the sensor. The long sides of the roof were bent at an approximate 30° angle to help shield the optics and sensing volume

from wind blown rain. The 30° angle brought the roofline down below the vertical position of the optics.

We also installed a filtered air pump to one of the modified, roofed sensors and the remaining unmodified CSU OFD and mounted resistors above the lenses (see Figure 2.26) on the roofed CSU OFDs to keep them from freezing and help to eliminate the accumulation of condensation.

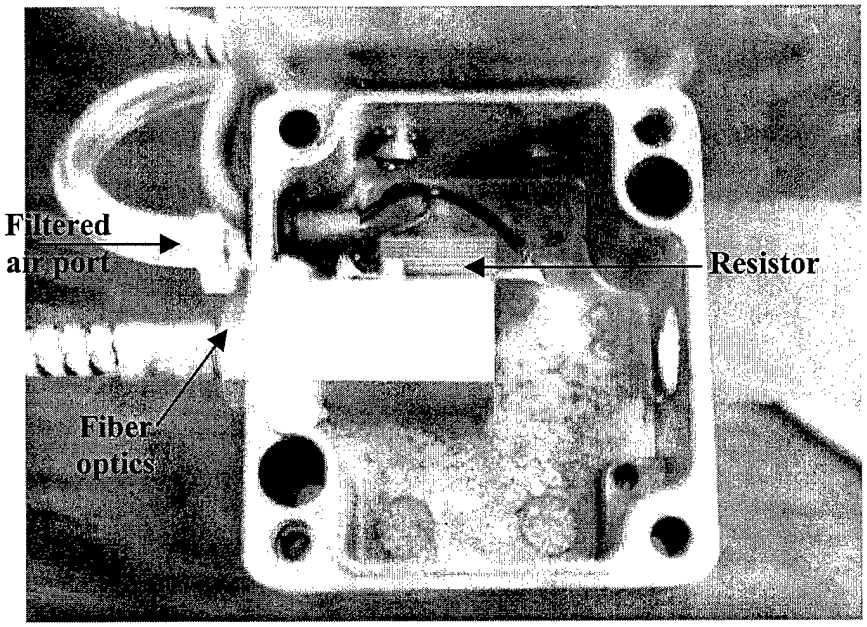

Figure 2.26 Heated and aspirated OFD receiver with cover removed.

The three sensors were mounted on the roof of the Sim Lab (see Figure 2.27). During the test period (2 – 6 Oct, 2000), we experienced a freezing precipitation event that caused the unshielded/unheated CSU OFD optics holders to freeze over (see Figure 2.27b), thus rendering this sensor incapable of an accurate measurement.

The sensor that was roofed and heated appeared to have had periods when precipitation was blown into the optics cover while the sensor that was roofed, aspirated, and heated showed no negative effects during the freezing precipitation event.

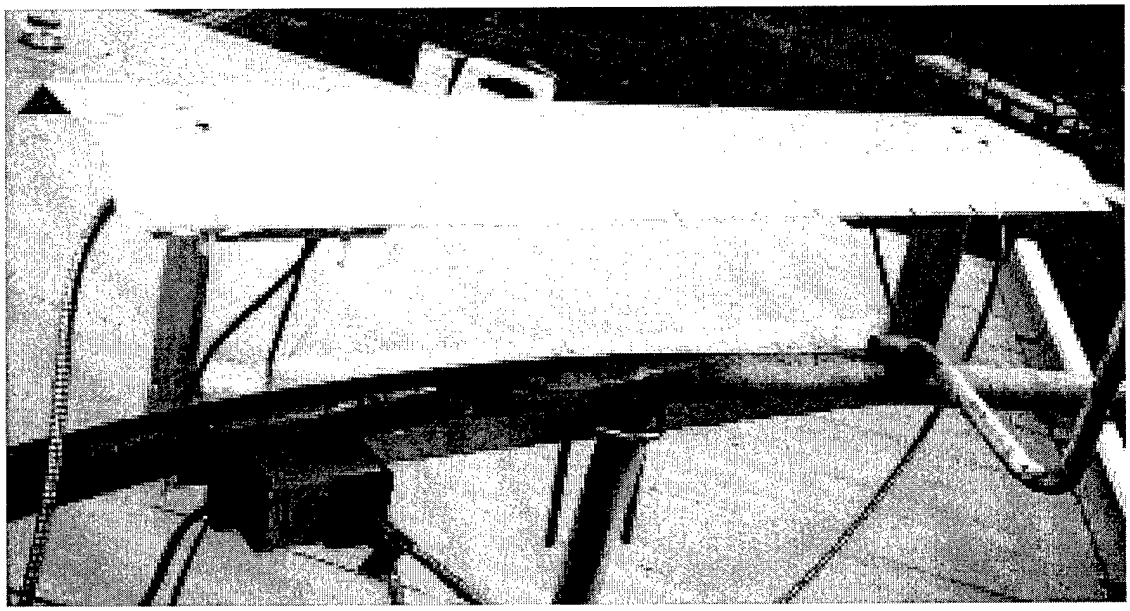

Figure 2.27a. Shielded and heated CSU OFD on Sim Lab roof during an October freezing precipitation event.

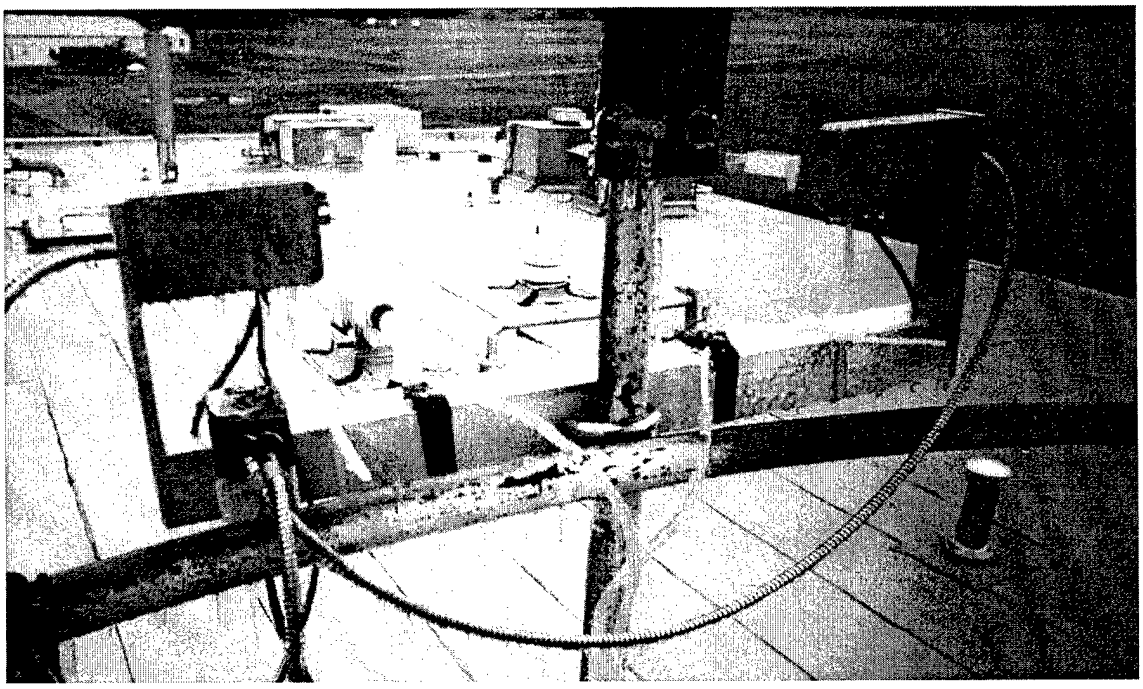

Figure 2.27b. Unshielded/heated CSU OFD on Sim Lab roof during an October freezing precipitation event.

Using data from the Sim Lab roof testing, the CSU OFD minimum detection limit (MDL) was determined by taking the mean signal and adding it to three times the standard deviation of the signal. The MDL was calculated based on a 24 hour time period (6 October, 2000) with the signal being recorded every 60 seconds. The results of the detection limit calculation are shown in Figure 2.28. The CSU OFDs have a theoretical MDL of 4.4 mg/m^3 compared to the PVM's MDL of 5.6 mg/m^3 (calculated by the same approach).

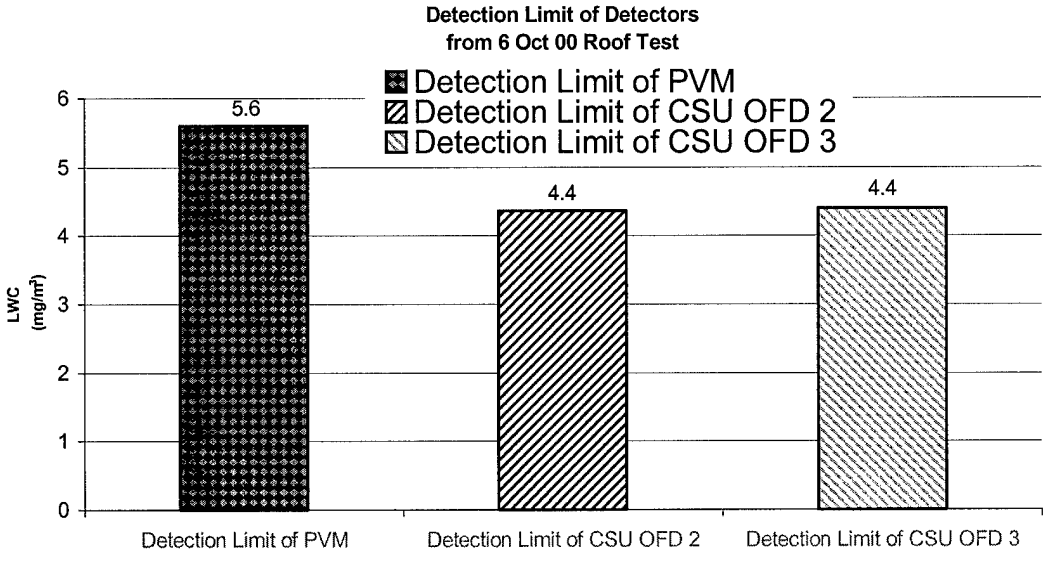

Figure 2.28. Calculated detection limit (signal to noise ratio) of PVM and the CSU OFD.

2.5.4 Final design of CSU OFD

The final design for the CSU OFD was based on the roofed, heated design including the filtered air. We had to make a few other minor modifications. The chief modification was turning the OFD upside-down in order to keep birds from possibly

perching on the metal bracket and setting off the sensor (see figure 2.29 for view from underside of CSU OFD).

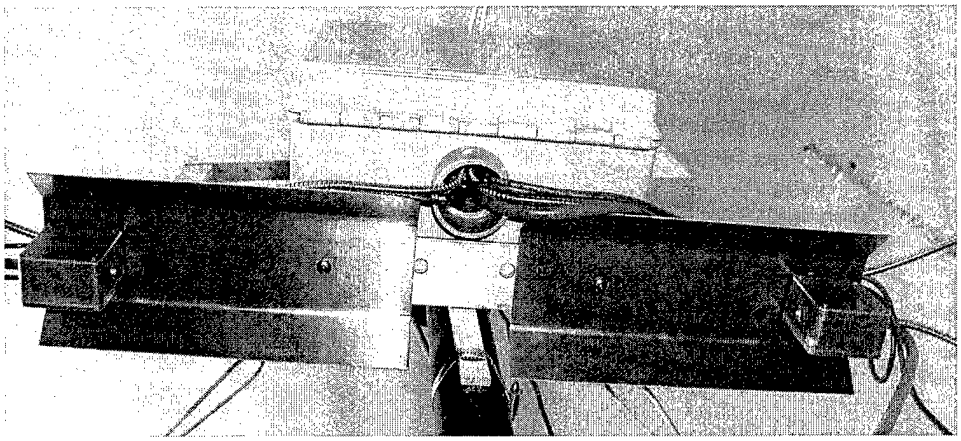

Figure 2.29. View from below CSU OFD. Inverting the sensor eliminated the possibility of birds perching below sensor and activating it.

We encased all the electrical components in a NEMA box (see Figures 2.30a and 2.30b). This alteration allowed for easy mounting while in the field, to limit the sensor's exposure to the environment, and to keep the design more compact (a list of major components can be found in appendix D).

Figure 2.30a. Wiring schematic and assembly of CSU OFD.

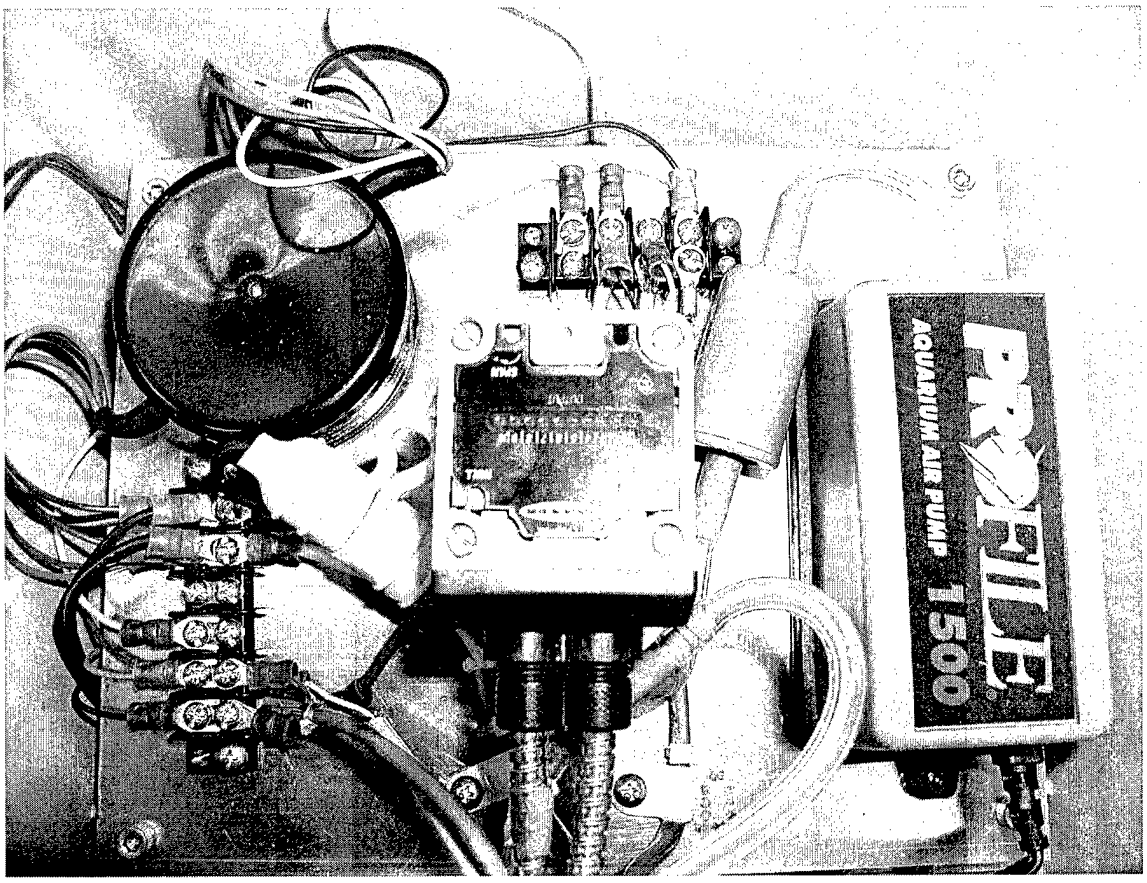

Figure 2.30b. Assembled electronic operating board of CSU OFD mounted in NEMA box.

The final design of the CSU OFD used for CRPAQS can be seen in figure 2.31.

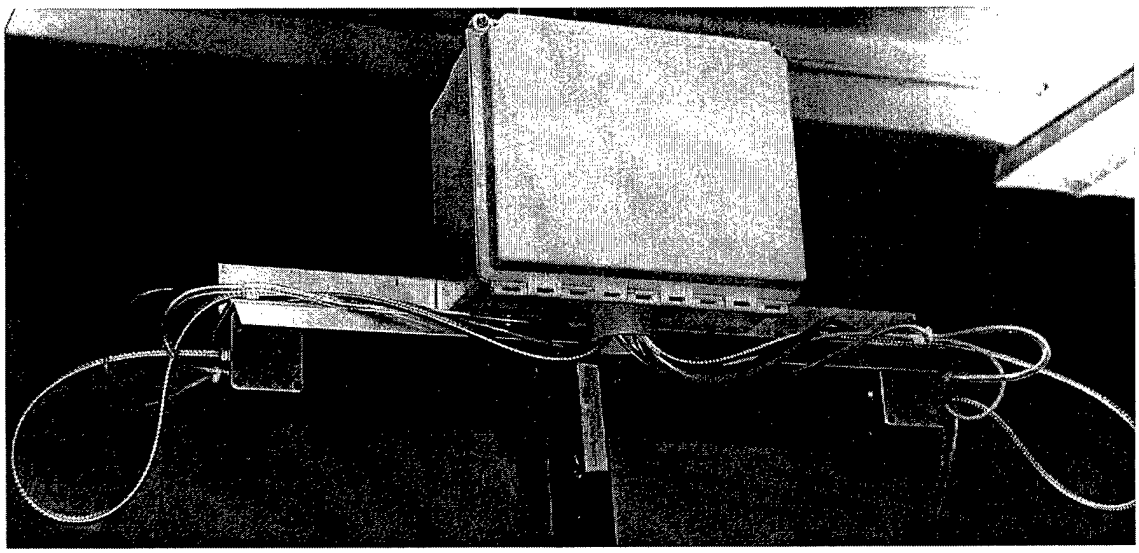

Figure 2.31. Completed model of the CSU OFD used for CRPAQS.

After the final design was decided, 8 CSU OFDs were built to be used during the California Regional Particulate Air Quality Study (CRPAQS). The sensors were all built, calibrated, and system checked before shipment to California. They were designed to be installed with minimal effort (e.g., plug in the power, attach cable to data logger and affix the sensor to the mounting pole with 2 clamps).

3 CRPAQS Experimental Approach

3.1 Overview

The main focus of this research was to develop a fog sensor that could be used during the California Regional Particulate Air Quality Study (CRPAQS). During CRPAQS, we evaluated how the CSU OFD worked as an inexpensive on/off switch to activate cloud/fog sampling devices. The results from the study also provided a method for evaluating the use of the sensor to measure/track LWC.

3.2 Equipment setup

The experimental setup for CRPAQS required the use of seven CSU Optical Fog Detectors (see Figure 3.1), most of which were used to activate various cloud/fog collectors. A method to test the accuracy and reliability of the CSU Optical Fog Detector also was needed. For this test, one CSU OFD was co-located with a PVM on a 3-meter pole at the main experiment site near Angiola, California. We also installed 3 CSU OFD's at different levels on a 100 meter tower at the same site and 3 at other San Joaquin Valley locations: McKittrick, Bakersfield and Helm. Results are presented here for Angiola and Helm as little or no fog formed at the other sites.

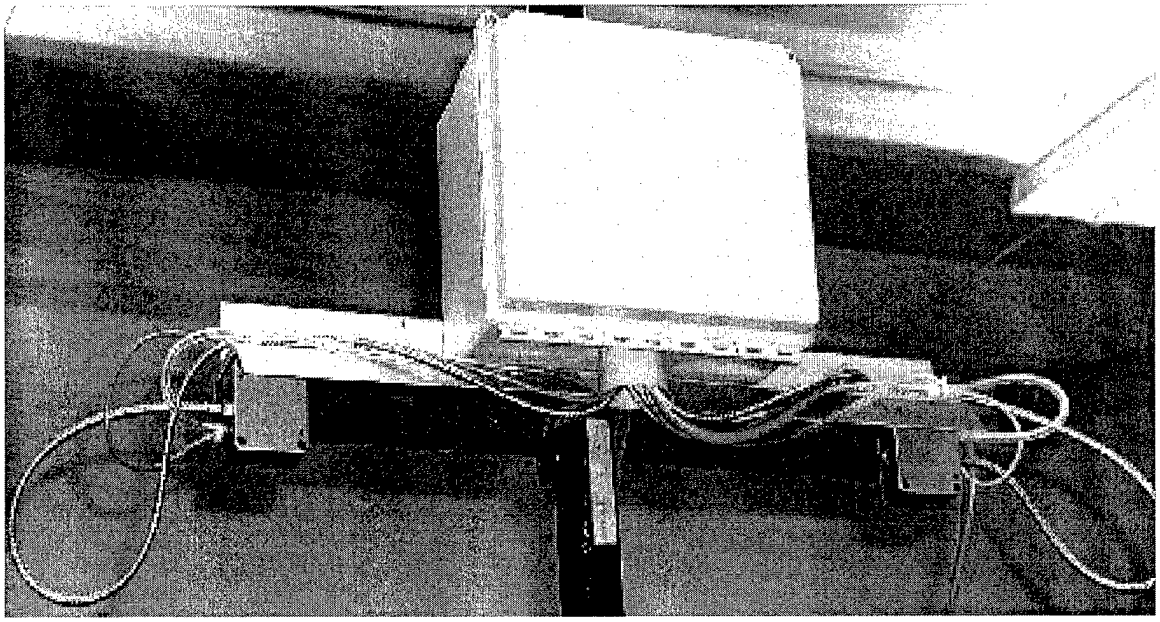

Figure 3.1 CSU Optical Fog Detector shown in the laboratory mounted on a 3-meter pole.

3.2.1 Remote setup at Helm

The experimental setup at Helm required erecting a 3-meter pole. A Caltech Active Strand Cloudwater Collector 2 (CASCC2, see Demoz et al., 1996) was mounted on the top of the pole to collect fogwater (see Figure 3.2). Underneath the CASCC2, a CSU Optical Fog Detector was mounted in addition to a relative humidity/temperature sensor (not seen in photo). The setup also included a Campbell CR10X data logger that was programmed to record the data every minute.

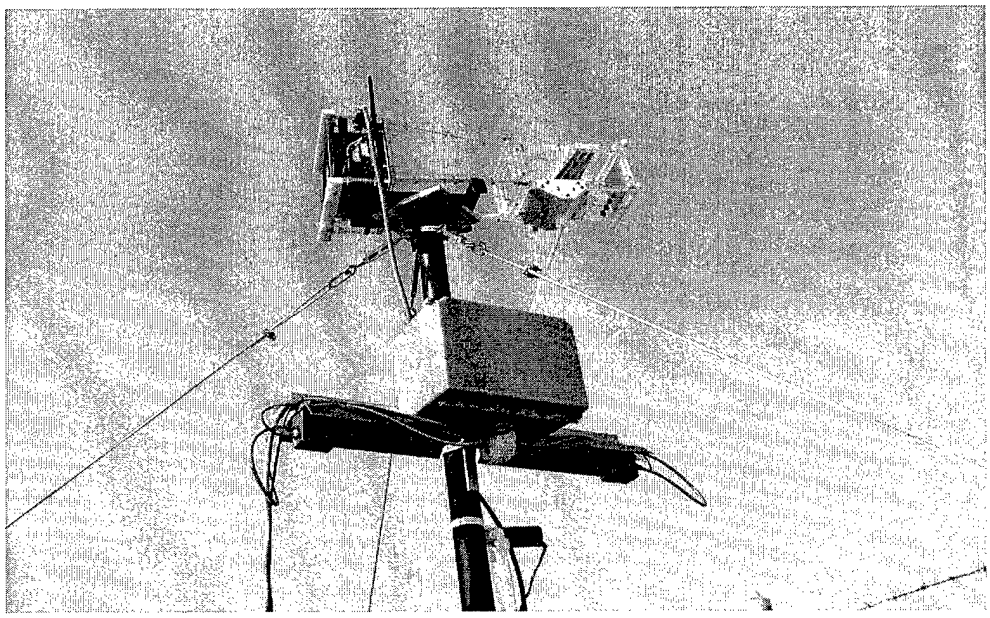

Figure 3.2 Setup of CSU Optical Detector and CASCC2 at Helm, CA.

This collection system is designed to function automatically in the presence of a fog that exceeds a specified liquid water content threshold value as measured by the CSU OFD. Each site utilized its own specific data logger program. This was done because some sites had modems (programmed to call and notify of fog conditions) while other sites had differing versions of the data logger that required different programming. The program for Helm can be found in Appendix E. A brief description of the program functions will be given here.

The collector is triggered to sample by the CSU OFD fog monitor. The program sets a threshold reading from the CSU OFD that will open the collector doors and start the fan. This liquid water content threshold value was initially set to 30 mg/m^3, but it could be easily changed. We suggested the value stay in the 30 – 50 mg/m^3 range.

Once the CSU OFD measures a liquid water content of greater than or equal to 30 mg/m^3 for a specified amount of time, sample collection will begin. The threshold time was set to 5 minutes. After the threshold values have been reached the fan on the CASCC2 is turned on and its doors are opened.

Once the CSU OFD detects a liquid water content of less than the threshold value for 150 seconds the collector is considered to be 'OUT OF FOG' and the doors of the CASCC2 collector will close. If the CSU OFD again detects a LWC of greater than or equal to $30mg/m^3$ for more than five minutes within the next 1 hour, sampling will resume on the same 1 liter bottle. This process of going in and out of fog on the same bottle will continue until the sampler has been 'OUT OF FOG' for more than one hour. At this point a solenoid valve will turn, switching to a new bottle.

If the collector then goes back IN FOG before it has been serviced, it will sample on the second bottle. The program will perform the same operations with the second bottle sampling. Again, this bottle will be used until the collector goes OUT OF FOG for more than an hour. At this point both bottles have been used for sampling and the program will not allow the collector to sample again until the site has been serviced and a program flag has been reset.

3.2.1.1 Sample retrieval

Upon arrival at the site, the operator must take note of how many 1 liter bottles were used to sample. He should then remove the bottles, cap them and place them in a cooler. (All weighing, pH measurement and testing was done at the sample processing trailer in Angiola).

Once the samples have been taken care of, the collector must be cleaned. To do this the collector does not need to be removed from the pole. Using a ladder and a backpack sprayer the collectors can be adequately cleaned. The operator must manually open the collector doors using the manual switch in the control box (down position). With the doors open the sprayer is used to thoroughly rinse the inside of the collector with deionized (DI) water, paying special attention to all collection surfaces. This procedure is done with one of the 1 liter bottles attached to catch all of the DI water.

Once the collector has been cleaned, a blank needs to be taken. To take the blank, a small spray bottle is used to spray a few hundred milliliters of Nanopure DI water onto the collection strands in the collector. The 1 liter bottle is emptied and reattached and additional water is sprayed onto the collection surfaces. Once there is enough DI water collected in the 1 liter bottle (about 50 – 100ml) this blank is transferred into a labeled 100ml bottle.

3.2.2 Tower setup

Three CSU Optical Fog Detectors were attached to a 100 meter tower (see Figure 3.3) at different heights. They were all installed with a new Teflon coated Aluminum CASCC2, featuring an automated cover (see Figure 3.4), a carousel collection system and a Campbell CR10X data logger (see Figure 3.5). The sensors were placed at 8, 23, and 91 meters above the ground.

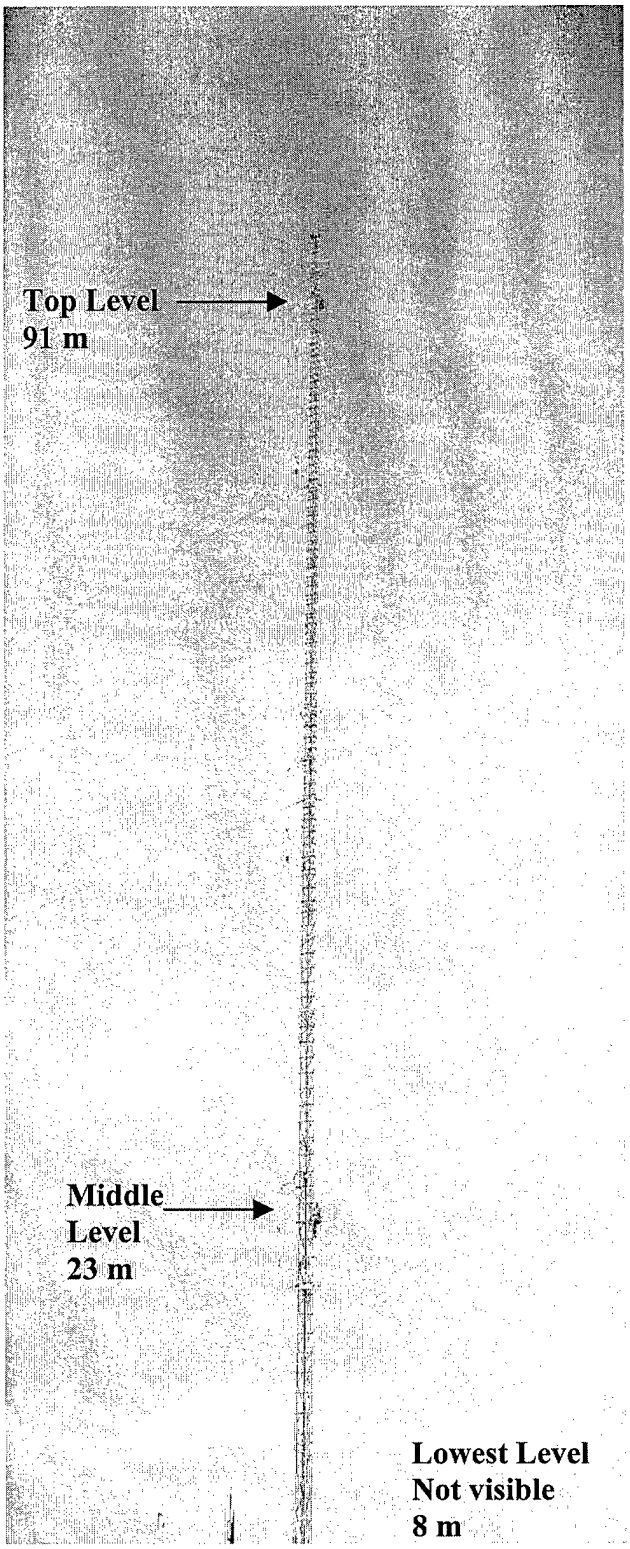

Figure 3.3 100 meter tower at Angiola, CA.

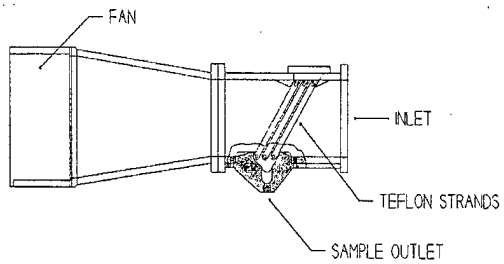

Figure 3.4 The CASCC2 collects bulk cloudwater samples (from Demoz et al., 1996).

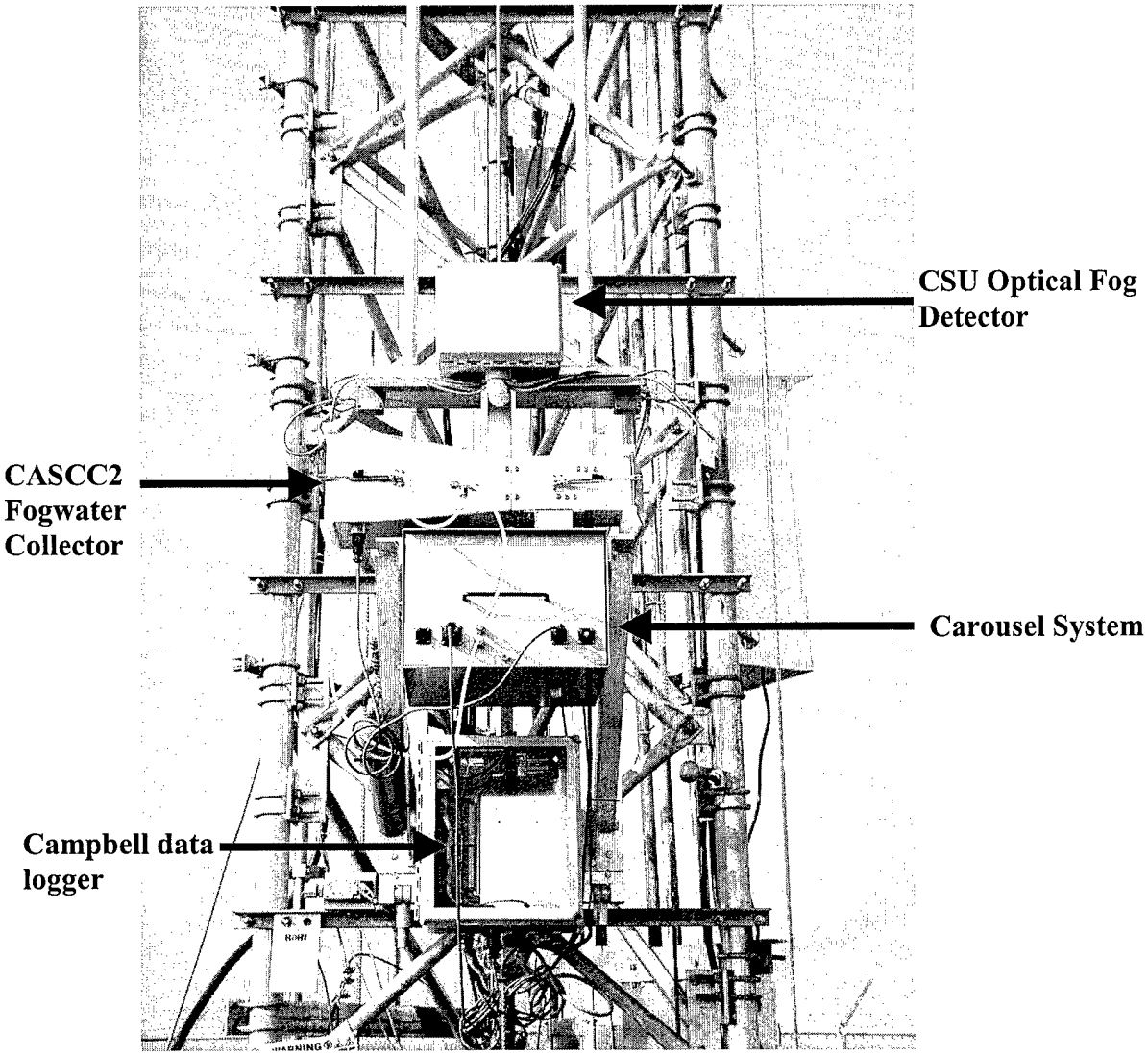

Figure 3.5 Setup of tower sampling system (Lower level).

3.2.3 Main site (base) setup

The Angiola main site setup (see Appendix F) was designed to be the control for the experiment. The CSU Optical Fog Detector was mounted on a 3-meter pole with the Gerber PVM-100. The setup had the PVM mounted at the top of the pole and the CSU detector mounted about 1 meter below the PVM (see Figure 3.6). This configuration was chosen in order to have both sensors sample approximately the same segment of the fog

since small spatial differences in fog, both in the vertical and horizontal, might produce large differences in LWC and PSA.

A Caltech Active Strand Cloudwater Collector (CASCC) and a size-fractionating CASCC (see Demoz et al., 1996) were also located at the main site atop 3 m poles. Fogwater volumes collected from these instrument were measured at 1-2 hr intervals.

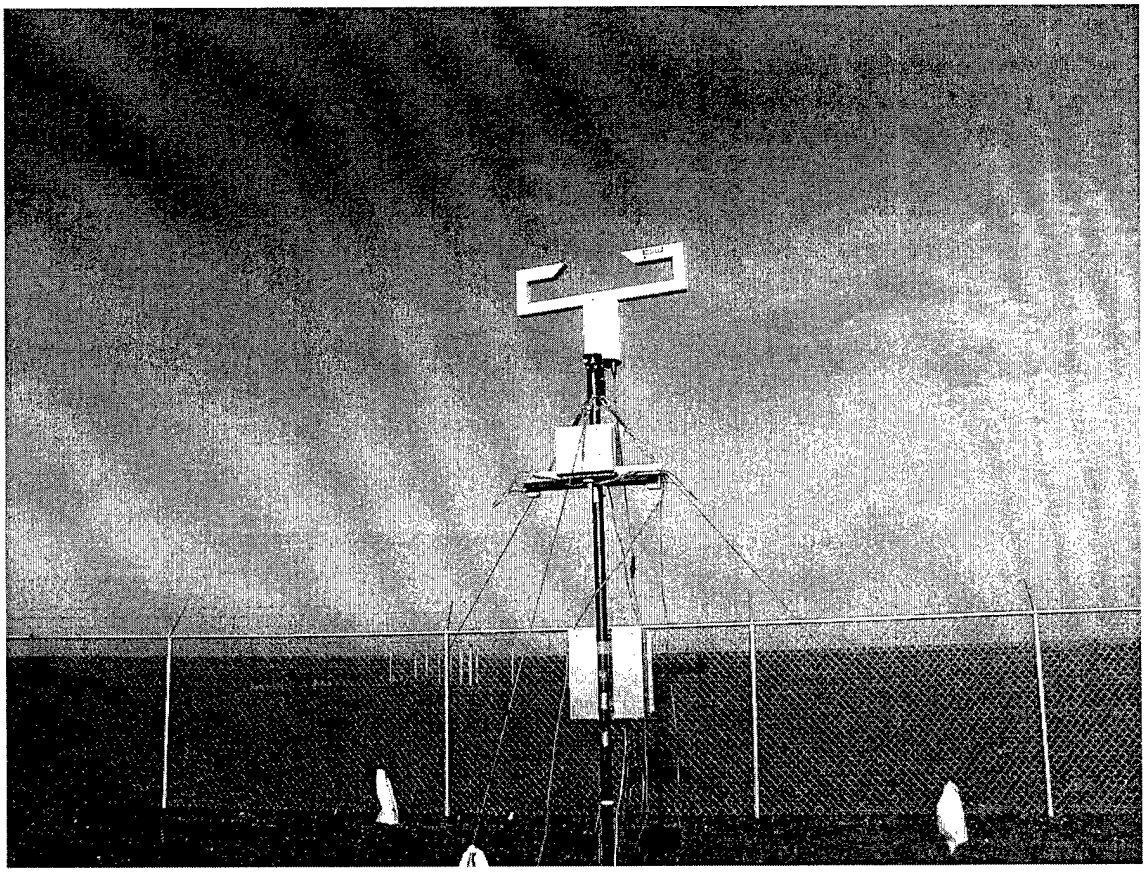

Figure 3.6 Gerber Scientific PVM 100 and CSU Optical Fog Detector at main site in Angiola, CA.

3.3 Calibration and field maintenance

Correct calibration of the CSU Optical Fog Detector is required to get accurate results. To calibrate the CSU Optical Fog Detector in the field a flathead screwdriver, phillips screwdriver, small flathead screwdriver, calibration disc, and either a laptop

loaded with Campbell Data Logger software or a voltmeter are required (see Appendix C for in-depth details).

The calibration process is an iterative process. The goal for the initial setting is to try to get the reading within 0 ± 5 to 10 millivolts by adjusting only the NULL adjustment screw. After this is achieved a SPAN calibration is performed. To check the span value, a calibration disk (see Figure 3.7) is attached to the receiving terminal with the film side facing the lens (see Figure 3.8).

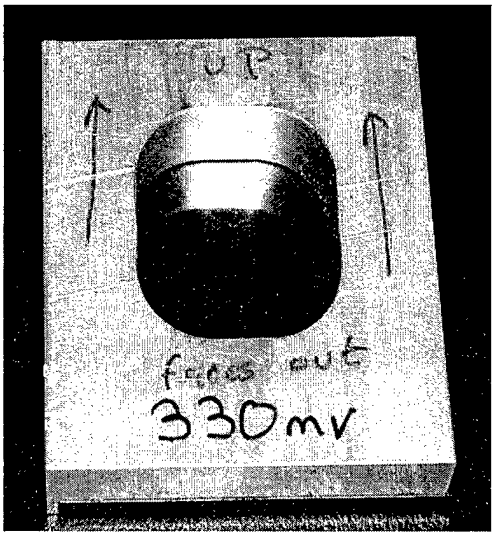

Figure 3.7 Calibration disk.

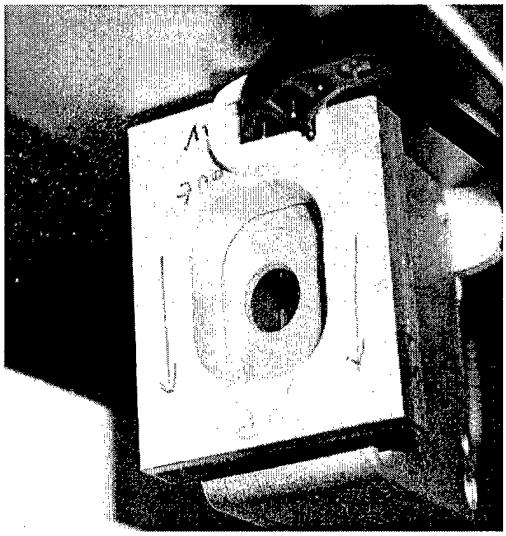

Figure 3.8 Proper placement of calibration disk for SPAN adjustment.

The calibration disk should give a reading of 330mv. The calibration screw labeled SPAN must be adjusted to get the reading on the control panel within ± 5 to 10 mv of the desired 330 mv.

The disk is then removed and the operator must wait for the readings to fall back down to near zero. This is because adjusting the SPAN value may have affected the NULL or ZERO value (the reverse is also true - that is, adjusting the NULL value has an

effect on the SPAN), so the NULL (ZERO) value may require further adjustment using the NULL calibration screw and then the SPAN may require further adjustment using the SPAN screw. The calibration process is repeated until the values are within ± 1.5 mv of the calibration value. Once these values have been obtained the CSU Optical Fog Detector calibration is done.

Field maintenance requires weekly calibration checks and cleaning of the fiber optics. Occasionally the optics housing will attract insects like spiders, which can interfere with the proper operation of the sensor. The optics also tend to get dirty after 7 to 10 days of operation, depending on the area where the sensors are placed. To clean the optics the operator will need Q-tips and isopropyl alcohol. The operator must dip a Q-tip into the alcohol and gently rub on each fiber optic lens followed by rubbing with a dry Q-tip. Repeating process until it comes out clean.

3.4 Experimental procedure

The experimental procedures varied for each location. At the Angiola site the ground based CSU OFD was to be compared directly to the PVM. The CSU sensor that was co-located with the PVM had a broken connection inside the control box. Unfortunately, this was not fixed until the study was almost over. The sensor was shipped back to CSU where it was repaired and returned. After it was returned to the field, it was remounted and we were able to capture one useful event.

The experimental procedure for the CSU Optical Fog Detectors on the tower was designed to compare the actual amount of cloudwater collected to the theoretical collection rate and secondly to the PVM's LWC reading. At Helm, the CSU Optical Fog Detector was the only sensor used to measure the fog, and thus was used to activate the

CASCC2. The CASCC2 fogwater collection rate was compared to the theoretical collection rate based on the CSU OFD estimated LWC.

3.4.1 Theoretical cloud LWC collection rate calculations

The fog sample collection rate by a CASCC2 fog collector, Cr, is dependent on the liquid water content and the drop size distribution of fog being sampled. It also depends on the flow rate, Q, of air through the CASCC2 (m^3/min), the fraction of air that is actually sampled (η_2), and the volume fraction of the initial (ambient) drop distribution collected (η_1). It is expressed in $\frac{ml}{\min}$. From Demoz et al. (1996), the collection rate may be written as

$$Cr = (\eta_1)(\eta_2)Q(LWC) \qquad \text{(Eq'n 3.1)}$$

According to this equation, Cr and LWC are related if η_1, η_2 and Q are known (for the CASCC2 used at Helm, Q = 5.84 m^3/min) The fraction of air sampled is calculated using the equation from Demoz et al, (1996)

$$\eta_2 = \{1 - (1 - \frac{d_c}{x})^r\} \qquad \text{(Eq'n 3.2)}$$

where d_c is the strand diameter, r is the number of rows, and x is the strand spacing. From Demoz et al. (1996), η_2 for the CASCC2 is 86%.

In order to calculate η_1, information about the shape of the drop size distribution is needed. In most field situations, drop size distributions are not known. In this absence, one can utilize parameterizations of cloud drop size distributions as a function of liquid water content. Demoz et al. (1996) calculated drop size distributions for various LWC

values, based on the parameterization according to Best, as referenced in Demoz et al. (1996). They discovered a linear relationship between η_1 and LWC for LWC values above 0.175 g/m^3. Therefore, for values of LWC $\geq$ 0.175 g/m^3, η_1 can be assumed to be linearly dependent on LWC and substituted in equation 3.1 to yield

$$Cr = 0.493 \times (LWC)^2 + 4.73 \times (LWC) \text{ for } 0.175 < LWC \leq 0.5 \text{ g/m}^3. \quad \text{(Eq'n 3.3)}$$

For LWC values below 0.175 g/m^3, η_1 can be expressed by a 5th order polynomial (Demoz et al., 1996) and substituted into Eq'n 3.1 to yield

$$Cr = 1318 \times (LWC)^6 - 1957 \times (LWC)^5 + 1102 \times (LWC)^4 - 293 \times (LWC)^3 +$$

$$37.2 \times (LWC)^2 + 2.97 \times (LWC) \text{ for } 0.025 \leq LWC < 0.175 \text{ ml/m}^3. \quad \text{(Eq'n 3.4)}$$

The collection rate as a function of LWC for the CASCC2, calculated from Eq'n 3.3 and 3.4, can be found in Appendix G.

3.5 Results

Experimental results for the CSU Optical Fog Detector look very promising. When comparing the theoretical collection rates with the actual collection rates we see how the CSU OFD may function as a LWC sensor. However, there are some uncertainties with this comparison. Some uncertainty is due to the lack of knowledge of how some collectors were oriented to the wind. Depending upon their orientation, the drop size distribution and the ambient wind speed, we could have many factors that affect the collector's overall sampling efficiency. If the wind speeds were always low (e.g. < 2 m/s as is typical in these fog episodes) this probably would not matter too much but if the wind speeds were higher the larger droplets might not be able to make the turn

into the collector. More uncertainties are introduced by uncertainty in the flow rate of air through the CASCC2 and the shape of the drop size distribution. Therefore, the theoretical collection rate should only be used as an approximate surrogate for the actual fog LWC.

3.5.1 Helm results

The results from Helm were very encouraging with numerous samples collected (see Table 3.2).

No.	Sample Number	Sampling Date	Sampling Time On	Sampling Time Off	Time Period (min) CSU Fog Sensor	CSU Fog Sensor (Mean) LWC mg/m^3	Retrieval Date	Sample Volume (g)
1	**R1PC135301**	12/17/00	2:30	9:35	425.0	211.0	12/18/00	**284.0**
2	**R1PC135502**	12/19/00	4:55	6:00	65.0	125.2	12/20/00	**37.5**
3	**R1PC100101**	12/31/00	7:50	9:40	110.0	88.6	01/01/01	**27.9**
4	**R1PC100102**	01/01/01	1:40	4:00	140	62	01/01/01	**98.2**
5	**R1PC100201**	01/02/01	4:10	9:10	280* *Collector off for 20 min	89.7	01/02/01	**90.0**
6	**P1PC101202**	01/10/01	5:00	7:00	120	120	01/12/01	**43.0**

Table 3.1 Selected Events from Helm, CA.

The December 17, 2000 event (see Figure 3.9) lasted 425 minutes and had an average collection rate of 40.1 ml/hr. Comparing this to the theoretical collection efficiency of the CASCC2 as a function of drop diameter, the theoretical collection

should be 1.02 ml/min while the actual amount collected was 0.67 ml/min. This suggests that the CSU OFD may have overestimated the LWC.

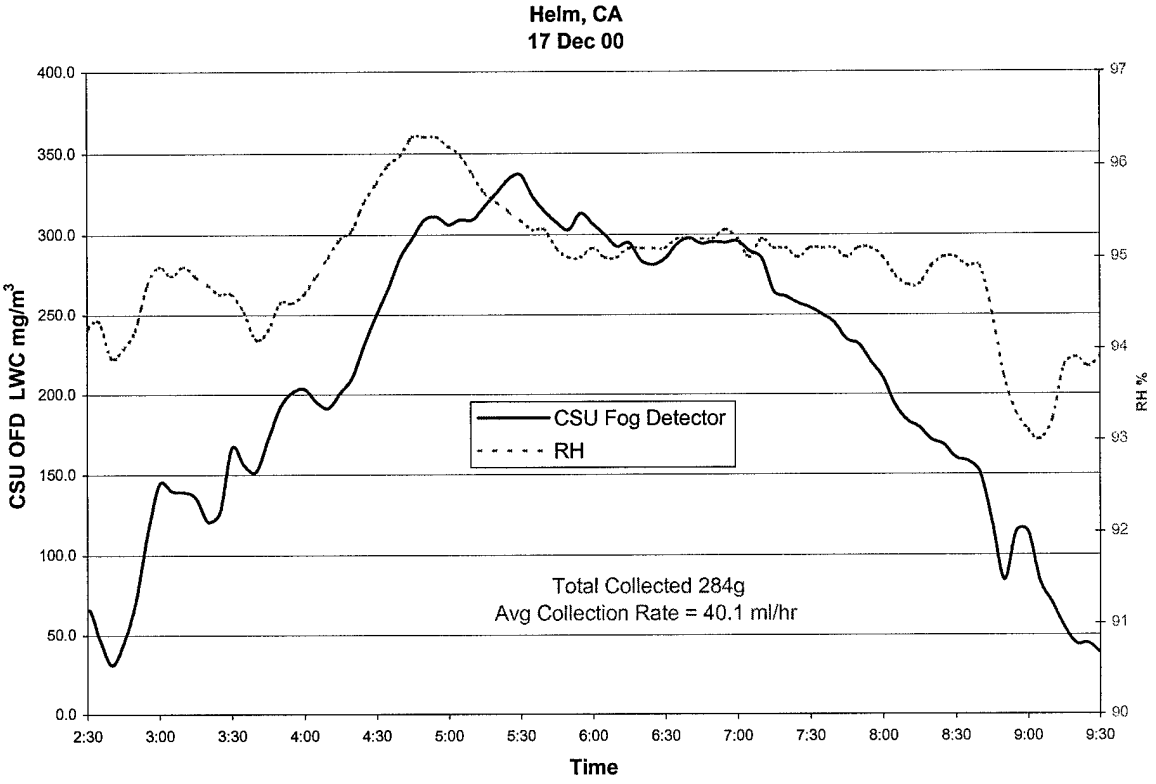

Figure 3.9 Event from Helm, CA. December 17, 2000.

The December 19, 2000 event (see Figure 3.10) lasted 65 minutes and had an average collection rate of 34.6 ml/hr. The theoretical collection should be 0.6 ml/min while the actual amount collected was 0.6 ml/min. For this event the CSU OFD appears to have done an excellent job of measuring the LWC. It would have been very instructive to examine the drop size distribution for these events if it were available.

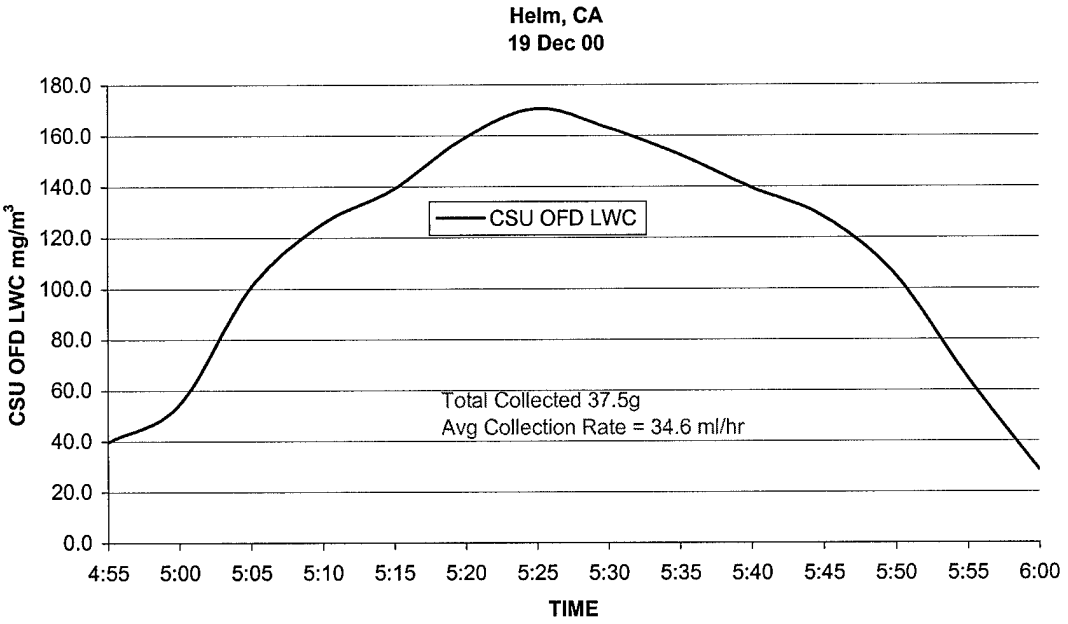

Figure 3.10 Event from Helm, CA. December 19, 2000.

The December 31, 2000 event (see Figure 3.11) lasted 110 minutes and had an average collection rate of 27.9 ml/hr. The theoretical CASCC2 collection rate is 0.40 ml/min while the actual amount collected was 0.25 ml/min.

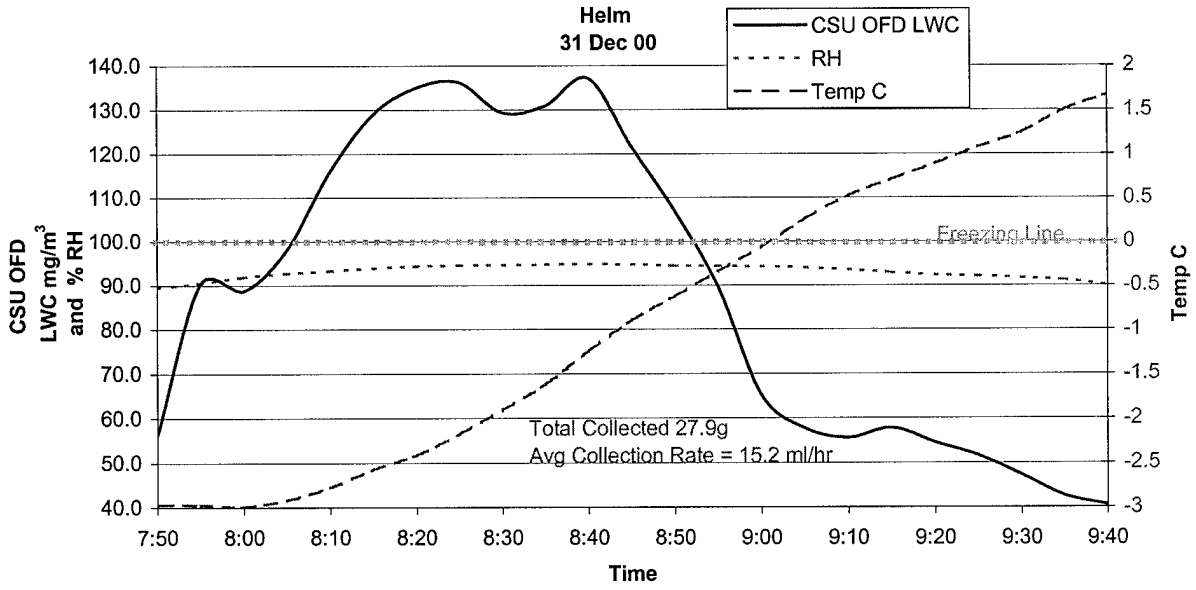

Figure 3.11 Event from Helm, CA. December 31, 2000.

The January 1, 2001 event (see Figure 3.12) lasted 140 minutes and had an average collection rate of 42.1 ml/hr. The theoretical CASCC2 collection rate is 0.27 ml/min while the actual amount collected was 0.70 ml/min.

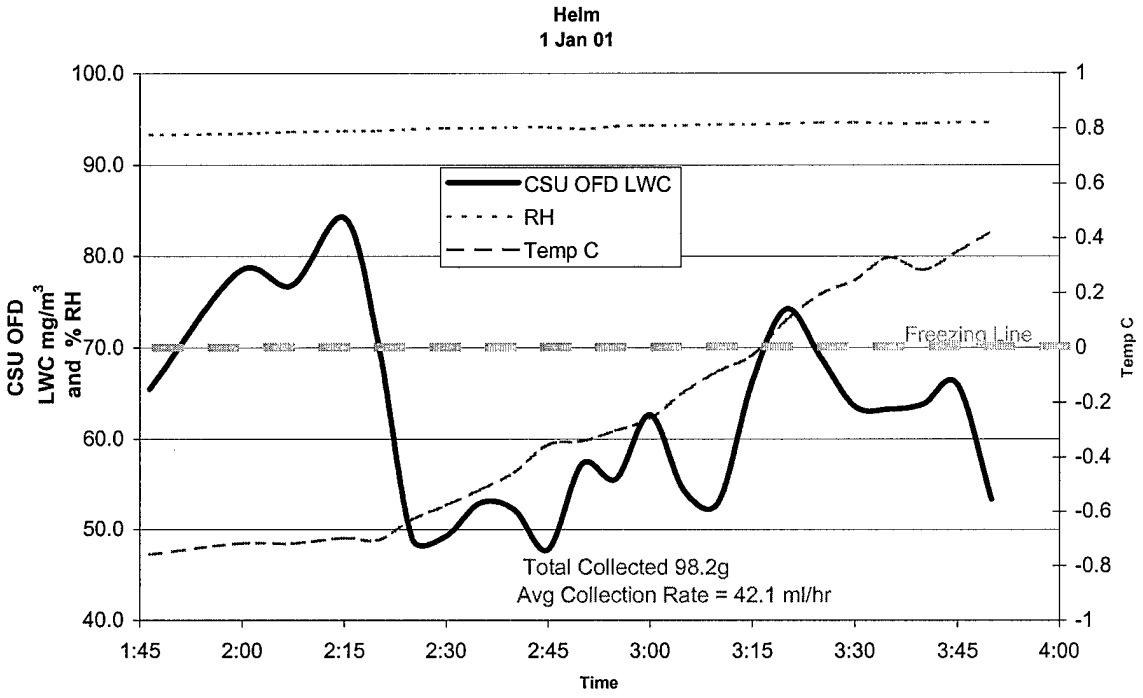

Figure 3.12 Event from Helm, CA. January 1, 2001

The January 2, 2001 event (see Figure 3.13) lasted 280 minutes and had an average collection rate of 19.3 ml/hr. The theoretical CASCC2 collection rate is 0.42 ml/min while the actual amount collected was 0.32 ml/min.

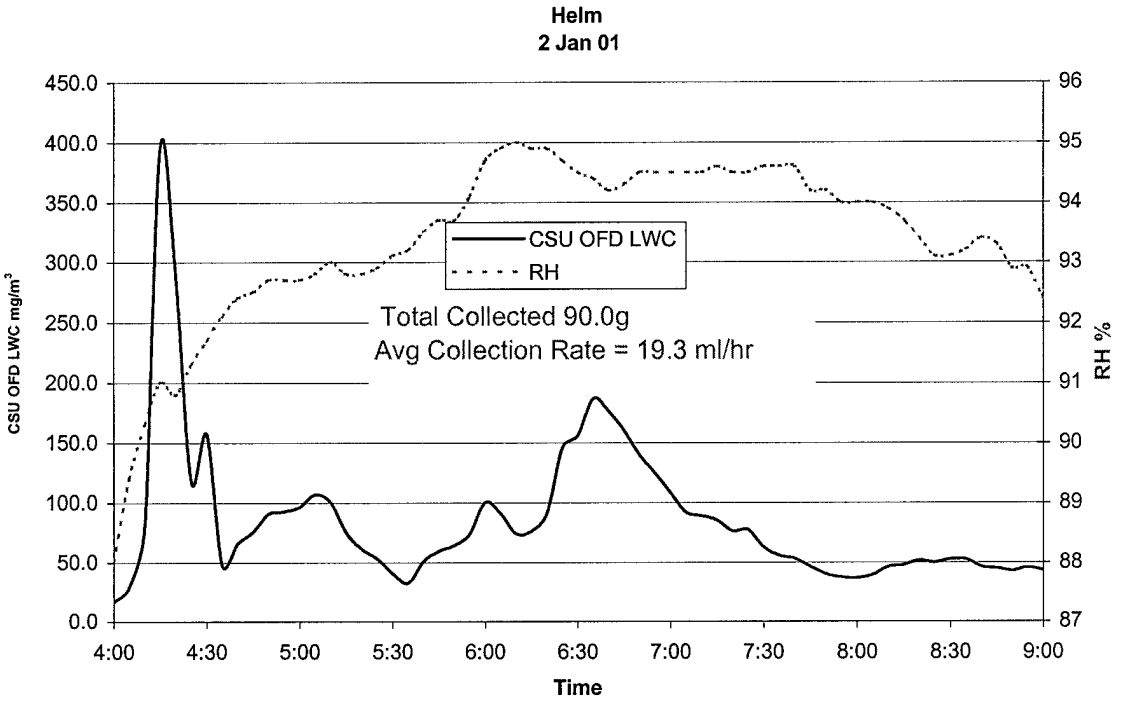

Figure 3.13 Event from Helm, CA. January 2, 2001

The January 10, 2001 event (see Figure 3.14) lasted 120 minutes and had an average collection rate of 21.5 ml/hr. The theoretical CASCC2 collection rate is 0.57 ml/min while the actual amount collected was 0.36 ml/min.

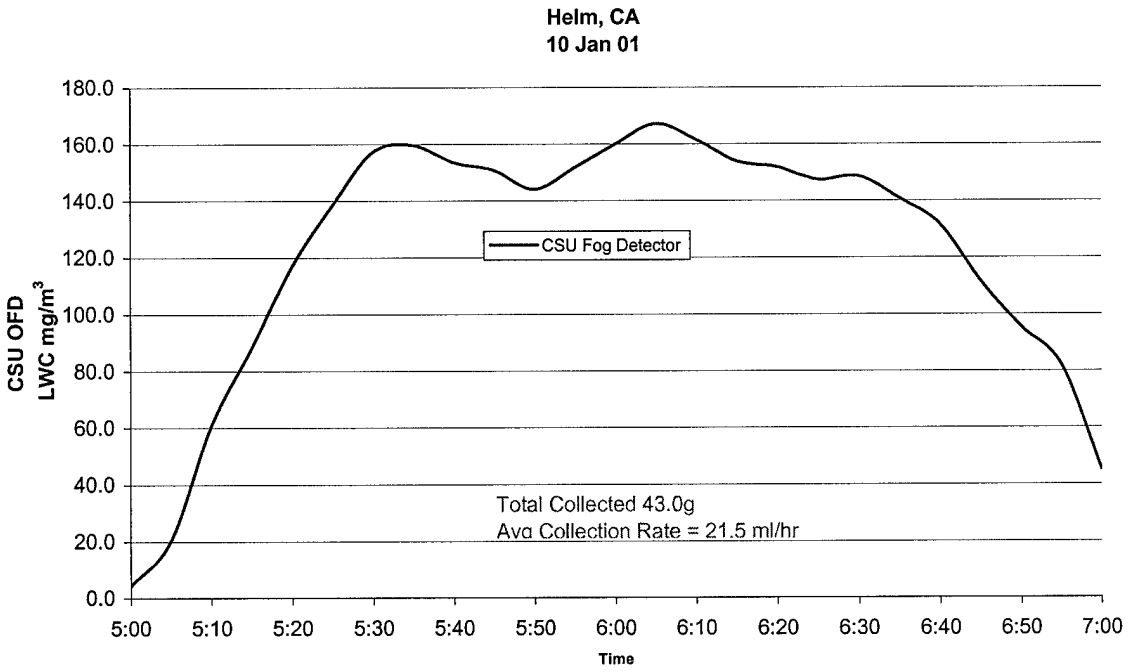

Figure 3.14 Event from Helm, CA. January 10, 2001

The combined collection results for Helm are presented in figure 3.15.

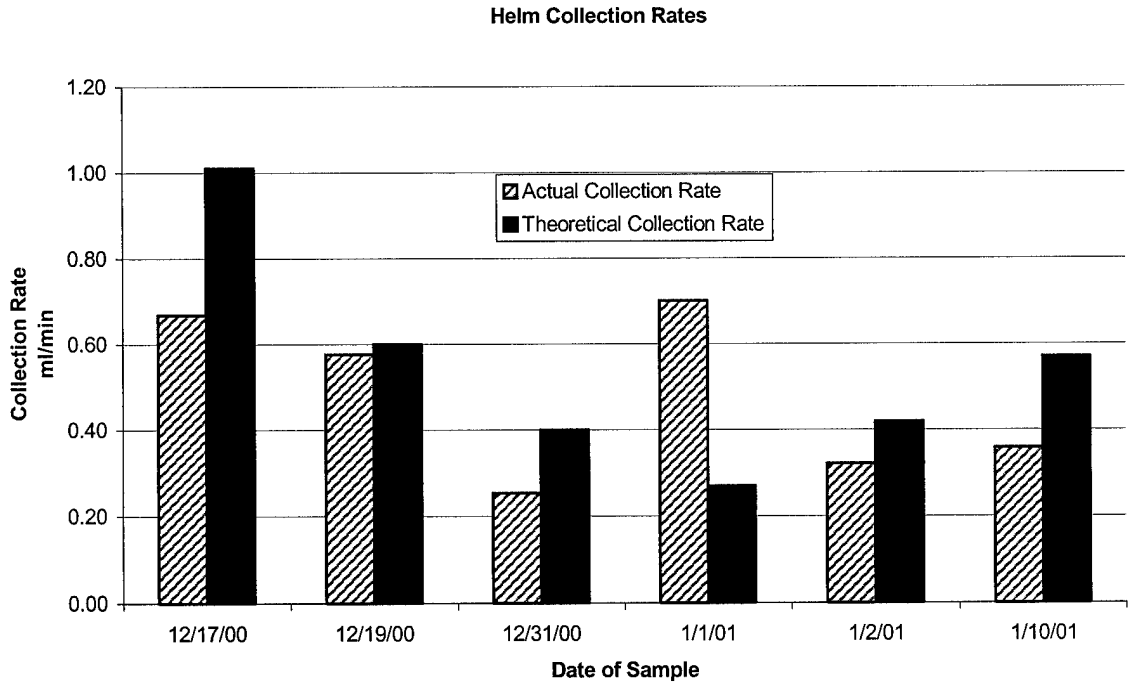

Figure 3.15 Collection rates from Helm, CA.

When comparing these events we see that the theoretical collection rates are higher than the actual collection rates for all but the January 1, 2001 event. This event was a freezing event where the temperature was below 0°C for the majority of the event. Therefore, it is possible that this sample contained frozen fog water from a previous sample. This could happen if the CASCC2 or the tube, leading from the CASCC2 to the collection bottle, had frozen water in it when the solenoid switched to the new bottle.

The results from Helm seem to suggest that the CSU OFD may be overestimating the LWC for these events. Figure 3.16 shows a scatter plot of OFD-predicted vs. observed CASCC2 collection rates, excluding the sub-freezing January 1 event. The data are positively correlated (R^2=0.77) and the slope of a linear regression line suggests an average difference of 36% between the two values.

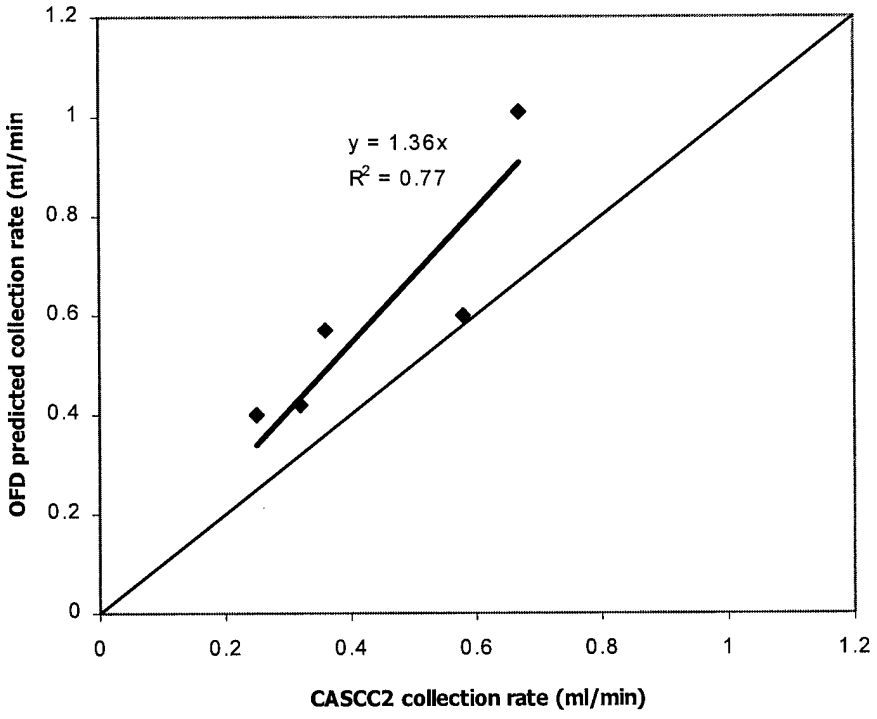

Fig. 3.16 OFD-predicted vs. observed CASCC2 fogwater collection rates at Helm, CA.

3.5.2 Tower results

There are only 2 days from the tower that will be analyzed. The first day (actually 2 separate fog events) was on December 17, 2000 and is compared against the ground based PVM (see Figure 3.17). Because of the possible large differences in the vertical structure of fog it is impractical to make an exact LWC comparison between the ground based PVM and the CSU OFD on the tower. However, it is somewhat instructive to see if we can identify when the fog was forming and dissipating at the different levels.

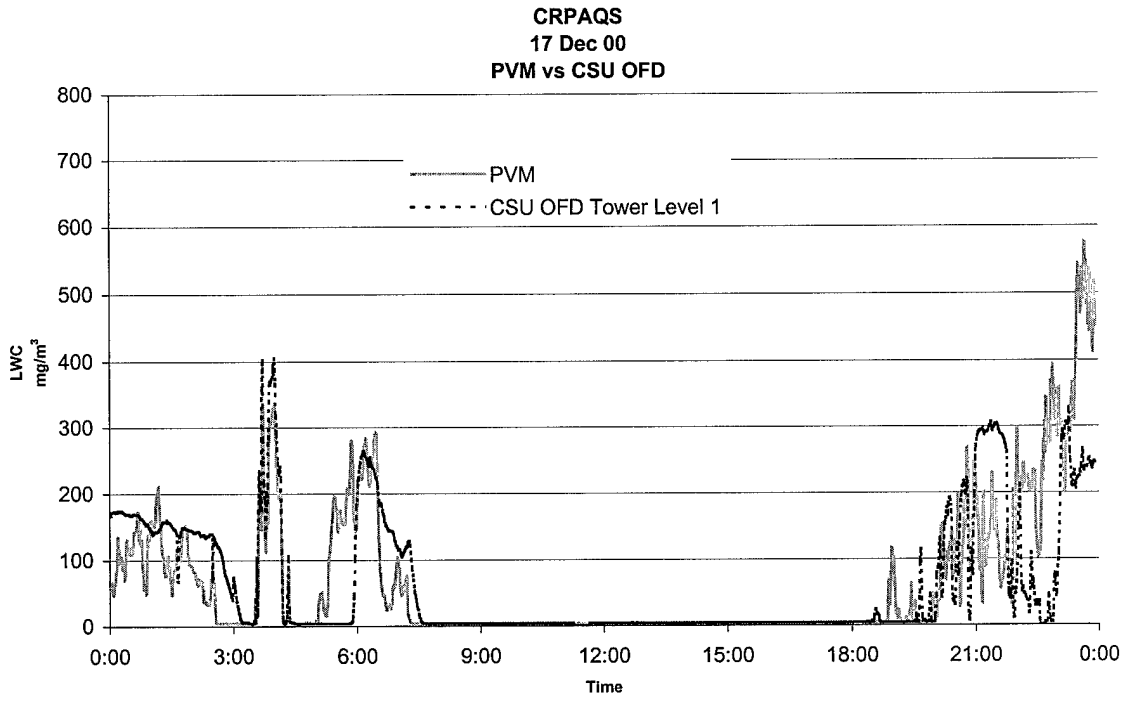

Figure 3.17 CRPAQS Angiola, CA. December 17, 2000

Even with the special differences, this event shows that the CSU OFD tracked the event LWC similar to the PVM. Figure 3.18 compares the LWC values from the ground based PVM and the CSU OFD on tower level 1. The day's events are divided into 2

separate events for analysis (00:00-07:45 and 18:30-23:55). In the first period the OFD-estimated LWC was approximately 23% higher than the PVM while the PVM showed a 38% higher average LWC during the second period. Note that this comparison is influenced by the fact that the PVM and OFD do not appear to be in-fog during the exact same time periods.

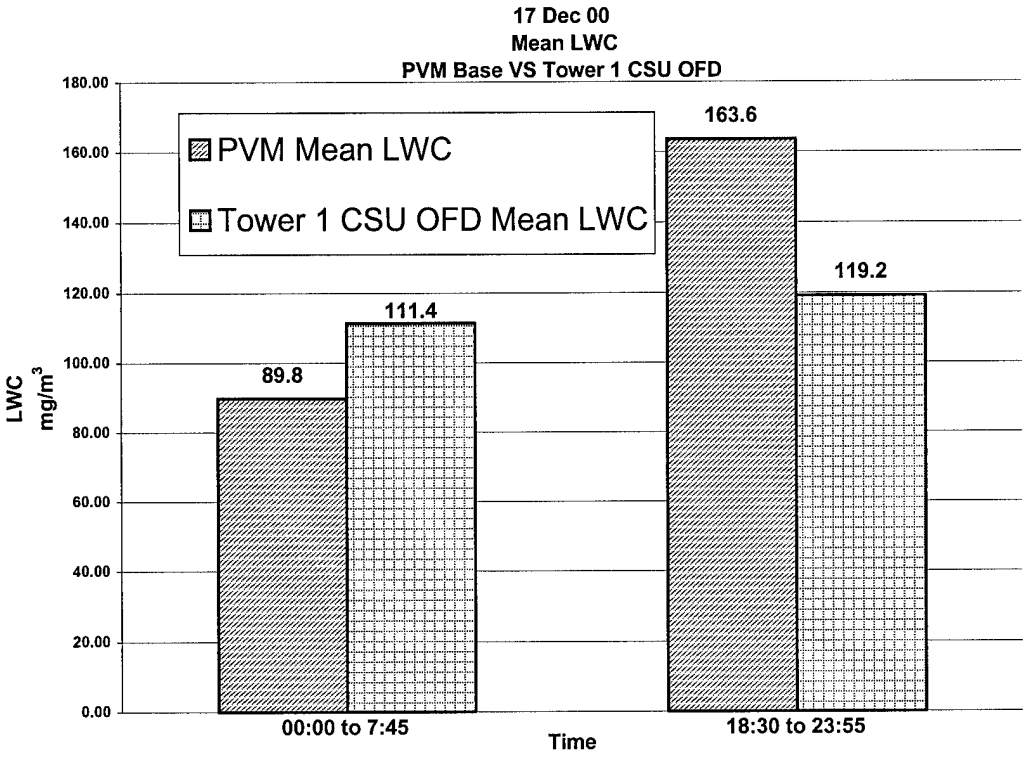

Figure 3.18 Mean LWC values from PVM and CSU OFD Tower Level 1, December 18, 2000

During the December 19, 2000 event all 3 tower CSU OFD were in fog. These are compared against each other and the PVM in Figure 3.19. Levels 2 and 3 tracked fairly closely with each other even though they were 68 meters apart in the vertical (see Figure 3.20).

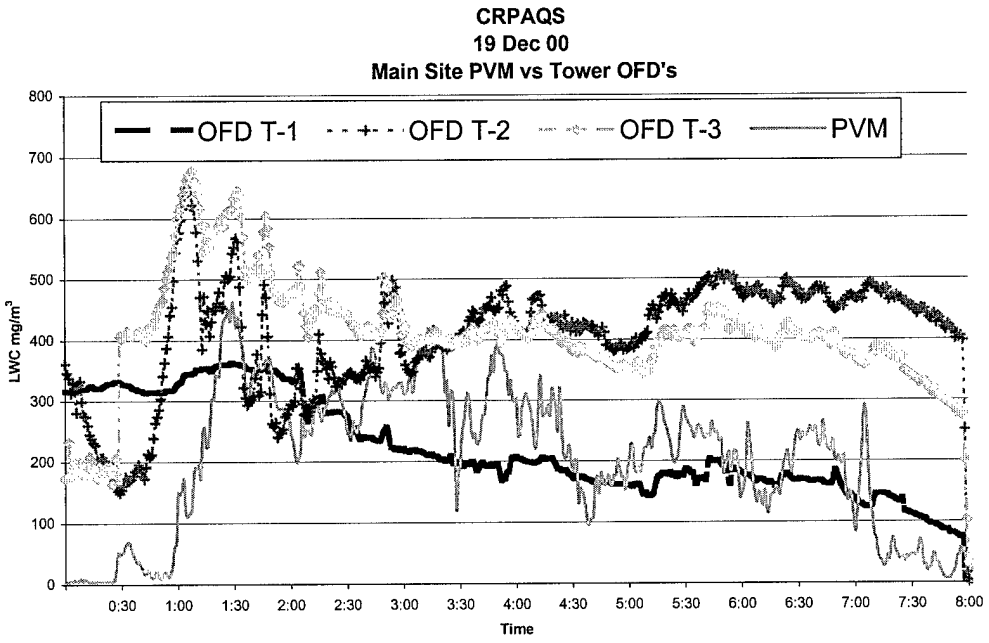

Figure 3.19 CRPAQS Angiola, CA. December 19, 2000. T-1 (8 m), T-2 (23 m), T-3 (91 m) and PVM (3 m).

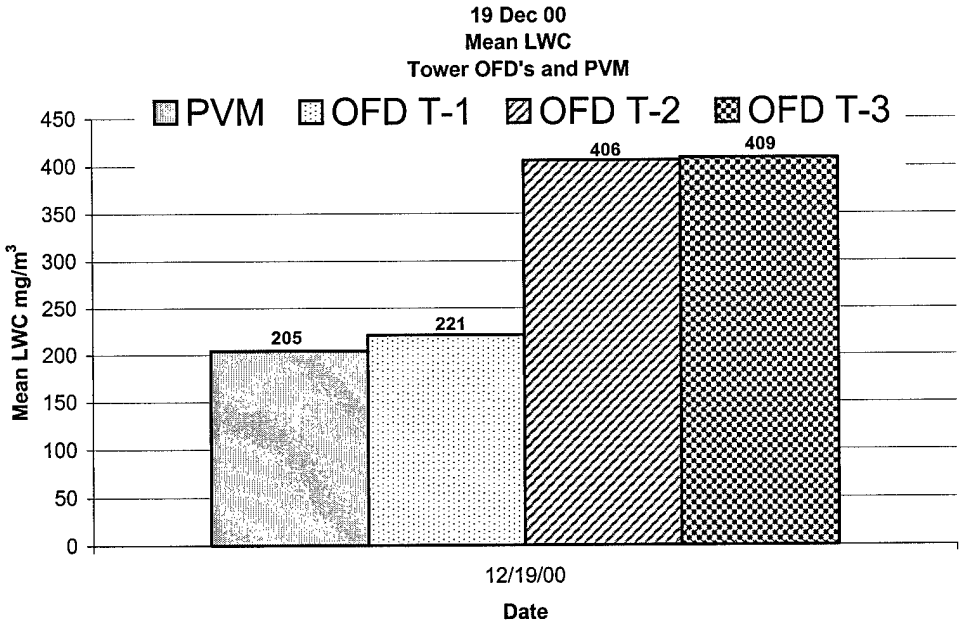

Figure 3.20 CRPAQS Angiola, CA. December 19, 2000 (00:00 – 08:30). T-1 (8 m), T-2 (23 m), T-3 (91 m) and PVM (3 m).

The average LWC values from each sensor for the time period 00:00-08:30 on 19 December, 2000 are depicted in Figure 3.20. The PVM at 3 m and the OFD at 8 m yielded similar LWC estimates of 205 and 221 mg/m^3, respectively. The average LWC reported by the higher OFD's were also close to each other, 406 vs. 409 mg/m^3, but quite a bit higher than the LWC values closer to the ground.

3.5.3 Main site (base) results

Results from the main site (base) consist of only one favorable event (see Figure 3.21) due to the inoperability of the base CSU OFD (mounted with the PVM) for the majority of the field campaign.

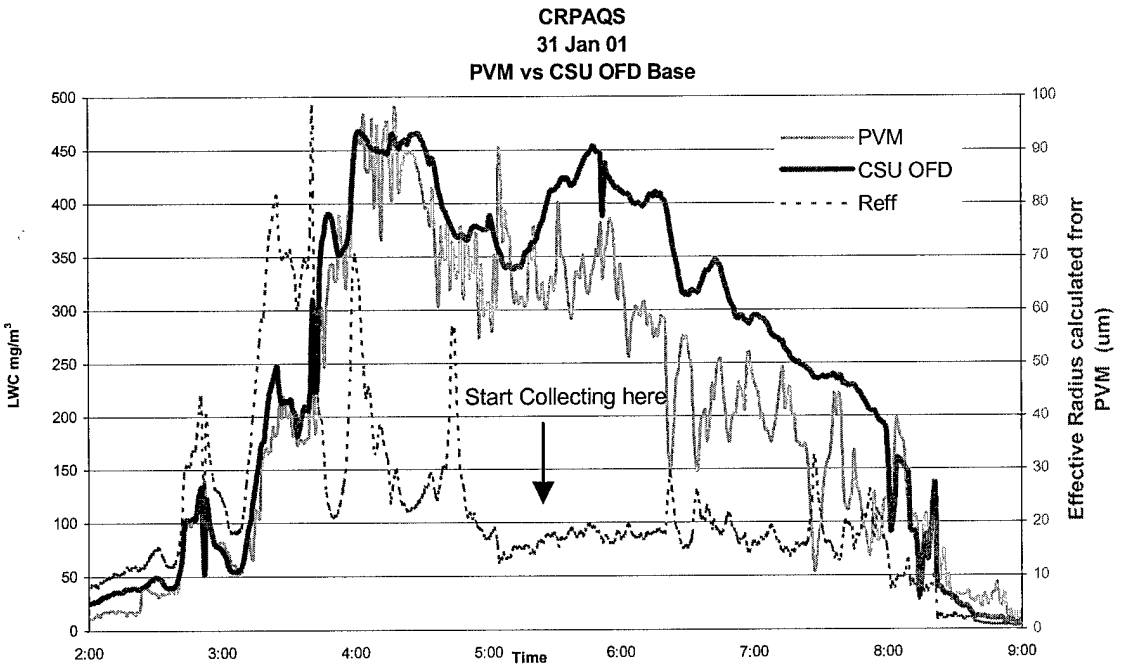

Figure 3.21 January 31, 2001 event. Comparison of LWC and effective radius.

For this event, the LWC from the CSU OFD and the PVM were compared directly. The LWC comparisons look very good for the large drops present before 04:45 but after this time the CSU OFD has some possible LWC discrepancies, with respect to the PVM.

The effective radius was calculated from the PVM data to see how the range of drop size distributions varied in time. Equation 3.5, modeled from Gerber (1993), shows how to calculate the R_{eff},

$$R_{eff} = 30\frac{V}{SA} \qquad \text{(Eq'n 3.5).}$$

where R_{eff} is in [μm], V is the volume which is proportional to the LWC [mg/m^3] and the SA is the particle surface area [cm^2/m^3].

The LWC comparisons look very good for the large drops present before 04:45 but after this time the CSU OFD has some discrepancies, with respect to the PVM. If we assume the PVM is accurate, the CSU OFD may have over-estimated the LWC.

It was also instructive to see the effective radius as calculated from the PVM because the PVM is designed to respond to droplets from 3- to 50 -μm diameter (Gerber et al., 1991). From Figure 3.21 we see that during this event from approximately 2:45 to 4:45 the drop sizes were at times larger than the PVM was designed to efficiently sample. When drops exceed 50 μm diameter it is likely that the PVM underestimates LWC. Keep in mind, too, that when large drops are present the effective radius reported by the PVM is also probably too small (see Appendix I for theoretical vs. actual collection rate results). Because of this, the data was divided in to two parts; when the effective radius was < 20 μm and when the effective radius was > 20 μm. The result can be seen in Figure 3.22.

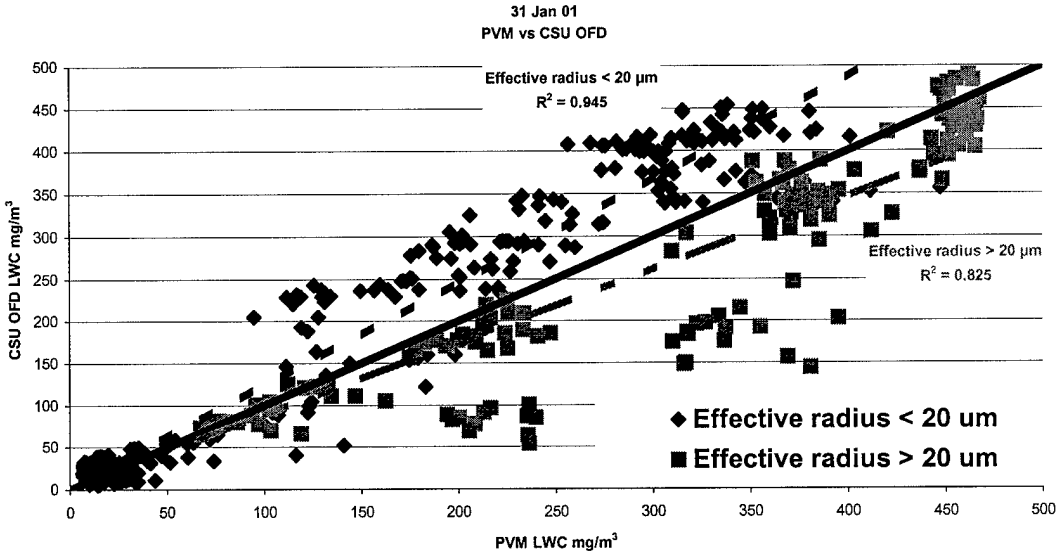

Figure 3.22 January 31, 2001 event. PVM vs. CSU OFD.

From this, we see that when the effective radius was < 20μm the linear correlation (R^2) was 0.95. When the effective radius was > 20 μm the linear correlation fell to 0.83. This shows that the CSU OFD tracked well (compared to the PVM) when the effective radius was < 20μm.

The theoretical CASCC and sf-CASCC collection rates (see Demoz et al., 1996) were calculated for both detector LWC measurements and compared to the actual CASCC and sf-CASCC collection rates (see Appendix H). This suggests that the CSU OFD and the PVM probably did overestimate the LWC during this event, although it is possible that the CASCC did not efficiently sample the very large fog drops that appeared to comprise an important fraction of the LWC. It is also very likely the flow rate (Q), could be different than the one used for the original calculation since it has not been verified recently. For the CASCC and sf-CASCC calculations we roughly compensated for a lower than accepted power supply voltage and it brought both the CSU OFD and PVM theoretical rates closer to what was actually collected (Appendix H).

4 Conclusions

An evaluation of the use of commercially available optical components for fog detection has been performed. Numerous fog detector design configurations were tested and the current attenuation design of the CSU optical fog detector (OFD) was deemed successful in that it provided, at a minimum, an inexpensive (~ $400) switch capable of automating remote fog sensing equipment. It also provided useful information concerning fog LWC.

Results from laboratory tests in a glove box filled with artificially generated fog proved that optical components purchased from Banner Engineering were capable of monitoring changes in fog LWC when operated in a light attenuation mode. After an initial calibration, the LWC signal from the CSU OFD was found to correlate strongly with LWC measured by a Gerber Scientific PVM-100. The linear correlation of the first laboratory attenuation test had an R^2 value greater than 0.99 and a slope (OFD vs. PVM) of 1.07.

Theoretical calculations of attenuation of 880 nm light passing through a population of fog drops suggest the OFD response to fog LWC should vary with the ambient fog drop size distribution. The results indicated extinction decreases as the drops are shifted to larger sizes (with a fixed LWC and lognormal distribution). Accordingly, it is expected that the response of the CSU OFD will vary with mean fog/cloud drop size.

An optical disk was constructed to provide a means of field calibration of the OFD. Two calibrated OFD's were compared to PVM LWC measurements during initial field tests of orographic clouds at Storm Peak Laboratory (SPL) in Steamboat Springs, Colorado. Combined analysis of 3 distinct cloud intercept events showed the OFD LWC signal to be strongly correlated with PVM LWC (correlation coefficient of 0.92) with no bias on average ($LWC_{OFD} = 0.99*LWC_{PVM}$).

Tests performed in the absence of fog on top of our laboratory in Fort Collins provided a measure of OFD baseline noise. Analysis of the observed noise yielded a minimum detection limit of 4.4 mg m^{-3} for the OFD and a comparable value (5.6 mg m^{-3}) for the PVM. During this same testing period it was discovered that the heated, roofed/aspirated OFD does not respond to precipitation. During this test, we had periods of strong winds (in excess of 12 meters/sec) with blowing rain and the heated, roofed/aspirated OFD was not falsely activated by the precipitation.

The OFD was incorporated into several automated fog sampling systems deployed in California's San Joaquin Valley as part of the California Regional Particulate Air Quality Study (CRPAQS). The CSU OFD performed well as a fog sensor and provided some insight into fog LWC.

Comparison of fog collector water collection rates with OFD estimated LWC at Helm, CA suggested that the OFD may have overestimated the LWC of fog events at this location. When comparing the OFD-predicted and the observed CASCC2 collection rates, excluding the sub-freezing January 1 event, we see the data are positively correlated (R^2=0.77) and the slope of a linear regression line suggests an average difference of 36% between the two values. Comparison of an OFD co-located with a

PVM in fogs sampled at Angiola, CA indicated the CSU OFD also may have over-estimated the LWC. The linear correlation (R^2) for the CSU OFD was 0.91 while the slope was 1.16.

This work served to develop an inexpensive sensor capable of automating remote fog/cloud sampling sites. The CSU OFD, at a cost of approximately $400, fills this requirement. Further, it appears that the OFD holds the potential of providing at least semi-quantitative estimates of fog/cloud LWC although additional evaluation of this capability under a variety of conditions is needed.

5 Future Work

From this work, several avenues for future tests and possible improvements exist. These are summarized briefly here.

- Additional measurements of the drop size distribution of artificial fogs used for laboratory testing of the OFD are recommended. If the drop size could be varied, it would be possible to test the relative responses of the OFD and PVM across a variety of conditions likely to be encountered in the environment. If a bias was found, with certain drop size distributions, it may be possible to develop a correction factor that could be applied to the CSU OFD's LWC reading.
- Tests should be done of the calibration disk (Avery transparency) to check its transmission spectrum vs. λ (880 nm for the OFD). This would help to characterize what type of response we should expect and may lead to a better method to calibrate the CSU OFD.
- Further study could possibly be done in a wind tunnel to better evaluate the OFD response to LWC. During these tests, the drop size distribution and LWC should be independently varied so a record of the CSU OFD's response can be made. Given the varying response of the PVM across large drop sizes, it should also be evaluated during these tests. Results

from these tests would define the ability of the OFD (and PVM) to measure LWC associated with different drop distributions.

- Future work may also include additional investigation into the OFD's response to precipitation (rain and snow). In our testing, there were some cases where heavy rain appeared to trigger the OFD-operated remote sampling system at McKittrick. Response to snow has not been tested. At present, careful screening of LWC observations for false values associated with precipitation is suggested.
- Additional field-testing of the OFD is needed. In particular, OFD response should be compared with PVM LWC and measured drop size distributions in a variety of fogs and clouds. More tests are recommended of a forward scattering OFD configuration with a dump spot. If adequate signal can be measured in this configuration then many possible obstruction problems can be prevented (e.g. birds or insects blocking the beam in the attenuation mode). The problems would be prevented because in the dump spot configuration, the sensor is only activated when fog is present to scatter the beam around the dump spot.
- Finally, additional investigation is warranted to ensure no condensation accumulates on the optics. If condensation occurs, it may bias the values reported by the OFD. The addition of a heat strip near the optics, similar to the PVM design, might prove useful.

References

Andrews, E., Collett, J. L. Jr., and Kreidenweis, S. M., (1997). On the use of commercial visibility sensors for cloud observations. Unpublished report.

Arends B G., Kos G. P. A., Wobrock W., Schell D., Noone K. J., Fuzzi S., and Pahl S. (1992). Comparison of techniques for measurements of fog liquid water content. *Tellus* **44B**: 604-611

Banner Spec Sheet (2001). https://www.buybanneronline.com/pdf/03579.pdf

Collett, J. L. Jr., Daube, B. C. Jr., and Hoffmann, M. R. (1990). The Chemical Composition of Intercepted Cloudwater in the Sierra Nevada. *Atmospheric Environment:* Vol. 24A, No. 4, pp. 952–972.

Belfort (2001). http://www.belfortinstrument.com/VisM6100.htm

Bohren, C.F., Huffman, D.R., (1983). Fortran program to calculate the absorption and scattering of light by small particles.

Desert Research Institute (2001). Storm Peak Laboratory
http://www.dri.edu/Projects/SPL/

Demoz, B.B., Collett, J. L. Jr., and Daube, B. C. Jr. (1996). On the caltech active strand cloudwater collectors. *Atmos. Res.* **41**:47-62.

Gerber, H. (1991). Direct measurement of suspended particulate volume concentration and far-infrared extinction coefficient with a laser-diffraction instrument. *Applied Optics*-LP, Vol. 30 Issue 33 4824-4831.

Gerber, Scientific INC. (1993). Particulate Volume Monitor Operator's Manual for Model PVM-100.

Hinds, William C., (1999). Aerosol Technology Properties, Behavior, and Measurement of Airborne Particles: Second Edition, pp. 349–373.

Hoffmann, M.R., Collett, J.L. Jr., and Daube, B.C. Jr. (1989). Characterization of cloud chemistry and frequency of canopy exposure to clouds in the Sierra Nevada. Final report prepared for the California Air Resources Board, Sacramento, CA.

Jaycor (2001). http://www.jaycor.com/eme/vsm.htm

Korolev, A. V., J. W. Strapp, G. A. Isaac, A. N. Nevzorov, (1998). The Nevzorov Airborne Hot-Wire LWC–TWC Probe: Principle of Operation and Performance Characteristics. *Journal of Atmospheric and Oceanic Technology*: Vol. 15, No. 6, pp. 1495–1510.

Mallant, Ronald K. A. M. (1988). Poor man's optical fog detector. *Annalen der Meteorologie*. No. 25, Vol. 1, p. 333-334.

PMS Technical Note (1989). Particle Measuring Systems, INC. 1855 South 57th Court. Boulder, CO 80301. P/N 10022-5

Appendix A – Modified Bohren and Huffman (1983) Fortran program for scattering calculations

```
                PROGRAM SCATTER
This code calculates scattering coefficients
using Mie theory and summed Number bins. You must
compile with : f77 -K -o file.exe file.f -lslatec if you use
the ERF option

c nline should be 262
c ndata should be 50, ndiam should be 100
      parameter (nline=262, Ndata=40, Ndiam=1000)
      real  refre, refim, wavel,
     *      x,tot1,tot2,ans1,ans2,bext,bsca,tot,
c    *      Data(Ndata),Dp(Ndata),Dpm(Ndata),
     *      Diammd(Ndiam),DlogDp(Ndiam),Diam(Ndiam),
     *      F(Ndiam),bin(Ndiam),totN,sigma,Dpgn,
     *      max, min,totV,Dpgv
      integer lenb
      complex refrel, s1(2000),s2(2000)
      character*50 filename
      character*80 char80
      pi = acos(-1.0)
      wavel = .880
      tot =0.0
      sqrt2 = sqrt(2.)
c **** refmed is the refractive index surrounding the medium
      refmed = 1.0
      refim = 0.0
c     close(12)
      close(14)
c ***************************************************************
c   nang = number of angles between 0 and 90 degrees.
c   Matrix elements calculated at 2 * nang - 1 angles
c   including 0, 90, 180 degrees.
c ***************************************************************
       nang = 91
```

```
      dang = 1.570796327 / float(nang - 1)

c---------- opening  directory files ---------------------------------
      open(unit=14, file = 'fog.out', status = 'unknown')

c-- unit 2 holds all the names of the files to be analyzed.

c Changed 2/23/01 to use with CSU OFD, for fog drop distribution

c     write(*,*)"input lognormal parameters: Vtot, Dpgv, sigma, m"
      write(*,*)"input lognormal parameters:  sigma"
c     read(*,*)totV,Dpgv,sigma,refre
      read(*,*)sigma

      refre = 1.33
c     sigma = 1.5
      totV = 0.2
      totV = totV*1.e6
      Dpgv = 45.
      refim = 0.0
c     write(*,*)totN,Dpgn,sigma,refre
      write(*,*)totV,Dpgv,sigma,refre


ccccccccccccccccccccccccccccccccccccccccccccccccccccccccccccc
c---- loop to read in data from data files ---------


      refrel = cmplx( refre, refim)/refmed


c Convert Volume to Number

      totN = (totV/Dpgv**3.)*(6./pi)
      Dpgn = Dpgv/(EXP( 1.5* (ALOG(sigma))**2.))

      write(*,*)totN, Dpgn


*------ DETERMINE DIAMETERS for LOGNORMAL ------------------
*------ using log scale for diameter      ------------------

       min = 0.5
       max = 100

      delDp = (alog(max)-alog(min))/100.
```

```
      Diam(1)=min
      Diam(100)=max

C------ starting to calculate lognormal diameters

      tot1 = 0.
      tot2 = 0.
      ans1 = 0.
      ans2  = 0.

c      write(*,*) 'starting scattering calcs'
c---- LOOP To CALCULATE LOGNORMAL SCATTERING VALUES ---------

       DO 200 j=1,100,1
        Diam(j+1)=exp( alog(Diam(j)) + delDp)
        Diammd(j) = (Diam(j)*Diam(j+1))**0.5
        DlogDp(j) = alog10(Diam(j+1)) - alog10(Diam(j))

c--  'mid'  size parameter for bhmie code, using the midpoint
diameter of the 'bin'
       x=pi*Diammd(j)*refmed/wavel

c--------------------

c      write(*,*)'About to start Error Function'

*--- USE ERROR FUNCTION TO DETERMINE BIN AREAS ----------------
       sqrt2 = 2.**0.5
       x1 = (alog(Diam(j)/Dpgn))/(sqrt2*alog(sigma))
       erfun1 = erf(x1)
c        write(*,*)Diam(j),Dpgn,sigma,x1,erfun1
       x2 = (alog(Diam(j+1)/Dpgn))/(sqrt2*alog(sigma))
       erfun2 = erf(x2)
       F(j) = totN/2. + (totN/2.)*erfun1
       F(j+1) = totN/2. + (totN/2.)*erfun2
c       write(*,*)F(j),F(j+1)
       if (j.eq.99) then
           F(j+1)= totN/2. + (totN/2.)*erfun2
       endif
       bin(j) = F(j+1)-F(j)
c       write(*,*)x,bin(j),refrel
c       write(*,*)'about to call BHMIE'
*** CALL BHMIE SUBROUTINE ************************
       call bhmie(x, refrel, nang, s1, s2, qext,qsca,qback)
c       write(11,66)Dpm(j),qsca
c 66     format(' ', f6.3,3x,f10.4)
```

```
*** CALCULATE BSCAT ******************************

      bext = (pi/4.)*bin(j)*qext*Diammd(j)**2.
      bsca = (pi/4.)*bin(j)*qsca*Diammd(j)**2.

      tot1 = bext + tot1
      tot2 = bsca + tot2

c       write(14,67)Diammd(j),bsca,bsca/DlogDp(j)
 67     format(' ',f6.3,3x,f9.5,3x,f9.5)
c
 200  continue
c  ans1 = bext,
c  ans2 = bscat
c  ans3 = babs

      ans1 = 1e-3*tot1
      ans2 = 1e-3*tot2
      ans3 = ans1 -ans2

      write(*,*)'answer is: bext,bsca:'
      write(*,*)ans1,ans2


C------WRITE TO FILES--------

      write(*,*)'write to files:'


c       write(12,350)stjd,ans1,ans2,ans3,refre
c 350    format(' ',f7.3,3x,3(f9.5,3x),f6.4)

       write(14,350)totV/1.e6,Dpgv,sigma,ans1
  350    format(' ',4(f20.5,3x))


      write(*,*)'have written to files'
c     goto 10

      stop
      end

c ***************************************************************
c   Subroutine BHMIE calculates amplitude scattering matrix
c   elements and efficiencies for extiction, total scattering
c   and backscattering for a given size parameter and
```

```
c   relative refractive index.
c ***************************************************************
      subroutine bhmie ( x, refrel, nang, s1, s2, qext, qsca, qback )
      dimension amu(2000), theta(2000), pi(2000), tau(2000),
     *          pi0(2000), pi1(2000)
      complex d(3000), y, refrel, xi, xi0, xi1, an, bn, s1(2000),
     *        s2(2000)
      double precision psi0, psi1, psi, dn, dx
c jlh
c       write(*,*)'in BHMIE'
c jlh      write(*,*)x,refrel
      dx = x
      y = x * refrel
c ***************************************************************
c   Series terminated after nstop terms.
c ***************************************************************
      xstop = x + 4. * x ** .3333 + 2.0
      nstop = xstop
      ymod = cabs(y)
      nmx = amax1( xstop, ymod ) + 15
      dang = 1.57096327 / float( nang - 1 )
      do 555 j = 1, nang
       theta(j) = ( float(j) - 1. ) * dang
555    amu(j) = cos( theta(j) )
c ***************************************************************
c   Logarithmic derivative d(j) calculated by downward
c   recurrence beginning with initial value 0.0 + i * 0.0
c   at j = nmx.
c ***************************************************************
      d(nmx) = cmplx( 0.0, 0.0 )
      nn = nmx - 1
       do 120 n = 1, nn
        rn = nmx - n + 1
120    d(nmx - n) = (rn / y) - ( 1. / ( d(nmx - n + 1) + rn / y ) )
      do 666 j = 1, nang
       pi0(j) = 0.0
666    pi1(j) = 1.0
      nn = 2 * nang - 1
      do 777 j = 1, nn
       s1(j) = cmplx(0.0,0.0)
777    s2(j) = cmplx(0.0,0.0)
c ***************************************************************
c   Ricatti - Bessel functions with real argument x
c   calculated by upward recurrence.
c ***************************************************************
      psi0 = dcos(dx)
```

```
      psi1 = dsin(dx)

      chi0 = -sin(x)
      chi1 = cos(x)
      apsi0 = psi0
      apsi1 = psi1
      xi0 = cmplx(apsi0, -chi0)
      xi1 = cmplx(apsi1, -chi1)
      qsca = 0.0
      n = 1
200   dn = n
      rn = n
      fn = ( 2. * rn + 1. ) / ( rn * (rn + 1.) )
      psi = ( 2. * dn - 1. ) * psi1 / dx - psi0
      apsi = psi
      chi = ( 2. * rn - 1. ) * chi1 / x - chi0
      xi = cmplx(apsi, -chi)
      an = ( d(n) / refrel + rn / x ) * apsi - apsi1
      an = an / ( ( d(n) / refrel + rn / x ) * xi - xi1 )
      bn =  ( refrel * d(n) + rn / x ) * apsi - apsi1
      bn = bn / ( ( refrel * d(n) + rn / x ) * xi - xi1 )
      qsca = qsca + (2. * rn + 1.) * (cabs(an) * cabs(an) + cabs(bn)
     + * cabs(bn) )
      do 789 j = 1, nang
       jj = 2 * nang - j
       pi(j) = pi1(j)
       tau(j) = rn * amu(j) * pi(j) - ( rn + 1. ) * pi0(j)
       p = (-1.) ** ( n - 1 )
       s1(j) = s1(j) + fn * ( an * pi(j) + bn * tau(j) )
       t = (-1.) ** n
       s2(j) = s2(j) + fn * ( an * tau(j) + bn * pi(j) )
       if ( j.eq.jj ) go to 789
       s1(jj) = s1(jj) + fn * ( an * pi(j) * p + bn * tau(j) * t )
       s2(jj) = s2(jj) + fn * ( an * tau(j) * t + bn * pi(j) * p )
789   continue
      psi0 = psi1
      psi1 = psi
      apsi1 = psi1
      chi0 = chi1
      chi1 = chi
      xi1 = cmplx(apsi1, -chi1)
      n = n + 1
      rn = n
      do 999 j = 1, nang
      pi1(j) = ( ( 2. * rn - 1. ) / ( rn - 1. ) * amu(j) * pi(j) )
      pi1(j) = pi1(j) - rn * pi0(j) / ( rn - 1. )
```

```
  999    pi0(j) = pi(j)
         if ( n - 1 - nstop ) 200, 300, 300
  300    qsca = ( 2. / ( x * x ) ) * qsca
         qext = ( 4. / ( x * x ) ) * real( s1(1) )
c jlh


         qback = ( 4. / ( x * x ) ) * cabs( s1(2 * nang - 1) )
     +  * cabs( s1( 2 * nang - 1 ) )
         return
         end
```

Appendix B – Scattering results from Fortran Program

Numerical results from scattering calculations based on a modified program written by Bohren and Huffman (1983).

LWC g/m^3	Mean size (um)	Breadth (um)	Extinction coefficient	(I/Io) Attenuated light
0.2	5	1.5	116.60	0.94
0.2	10	1.5	55.91	0.97
0.2	15	1.5	36.45	0.98
0.2	20	1.5	26.97	0.99
0.2	25	1.5	21.37	0.99
0.2	30	1.5	17.66	0.99
0.2	35	1.5	14.99	0.99
0.2	40	1.5	12.92	0.99
0.2	45	1.5	11.23	0.99
0.2	50	1.5	9.81	0.99
0.2	55	1.5	8.56	1.00
0.2	60	1.5	7.46	1.00
0.05	15	1.5	9.11	1.00
0.1	15	1.5	18.23	0.99
0.2	15	1.5	36.45	0.98
0.3	15	1.5	54.68	0.97
0.4	15	1.5	72.91	0.96
0.5	15	1.5	91.13	0.95
0.05	30	1.5	4.42	1.00
0.1	30	1.5	8.83	1.00
0.2	30	1.5	17.66	0.99
0.3	30	1.5	26.49	0.99
0.4	30	1.5	35.33	0.98
0.5	30	1.5	44.16	0.98
0.05	45	1.5	2.81	1.00
0.1	45	1.5	5.62	1.00
0.2	45	1.5	11.23	0.99
0.3	45	1.5	16.85	0.99
0.4	45	1.5	22.47	0.99
0.5	45	1.5	28.09	0.98

0.2	15	1.1	42.59	0.98
0.2	15	1.2	41.67	0.98
0.2	15	1.3	40.18	0.98
0.2	15	1.4	38.40	0.98
0.2	15	1.5	36.45	0.98
0.2	15	1.6	34.42	0.98
0.2	15	1.7	32.36	0.98
0.2	30	1.1	20.65	0.99
0.2	30	1.2	20.19	0.99
0.2	30	1.3	19.49	0.99
0.2	30	1.4	18.64	0.99
0.2	30	1.5	17.66	0.99
0.2	30	1.6	16.57	0.99
0.2	30	1.7	15.40	0.99
0.2	45	1.1	13.65	0.99
0.2	45	1.2	13.31	0.99
0.2	45	1.3	12.83	0.99
0.2	45	1.4	12.13	0.99
0.2	45	1.5	11.23	0.99
0.2	45	1.6	10.26	0.99
0.2	45	1.7	9.29	0.99

Appendix C – CSU OFD Calibration Procedures

Correct calibration of the CSU Optical Fog Detector is required to get accurate results. To calibrate the CSU Optical Fog Detector in the field you will need a flathead screwdriver, Phillips screwdriver, small flathead screwdriver, calibration disk, and either a laptop loaded with Campbell Data Logger software or a voltmeter.

Open cover on the data logger and detach the blue serial connection cable from the modem in the control box mounted on the pole (if site is utilizing a modem). Attach the long end of the blue serial communication cable to the Campbell SC32A (Optically Insulated RS232 Interface) that in turn connects to the laptop's serial port. Turn on the laptop then open Campbell Software. Next, open the control panel of the program corresponding to the CSU Optical Fog Detector. Establish communication between the computer and the Campbell system in the control box by clicking on the 'CONNECT' icon in the software.

In the left hand column of the display find the heading for the sensor. This value is the reading from the fog detector. If nothing is in between the transmitting and receiving sides of the detector, it should be displaying a value fairly close to zero.

To calibrate the sensor, open the face of the gray box by loosening the two screws at the top. The inside of the CSU Optical Fog Detector should appear as in Figure C.1.

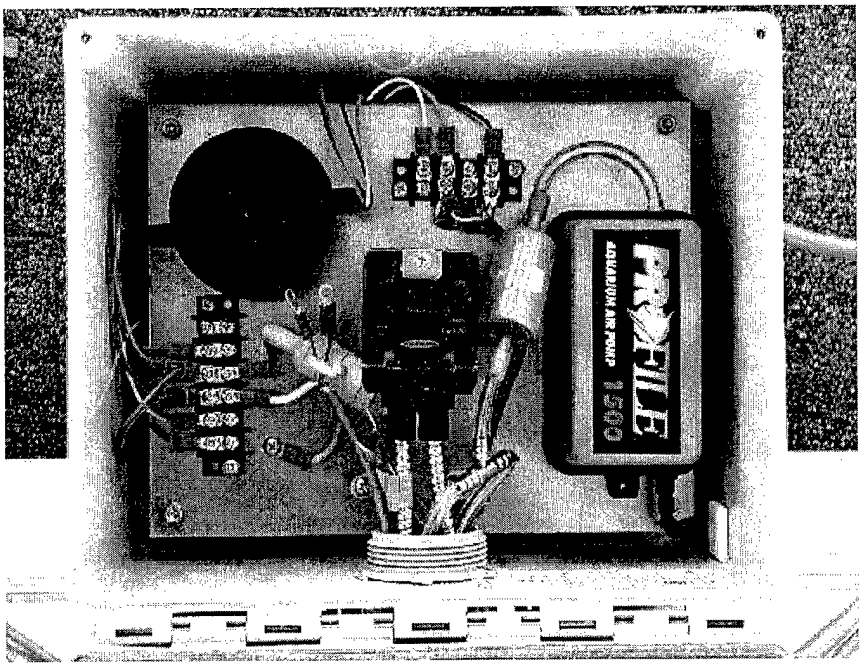

Figure C.1 Inside view of the CSU Optical Fog Detector control box.

Now open the face of the small yellow Banner (OASBFX) box that contains LED's. This is done by removing the Phillips head screw at the top of the clear plastic faceplate and then sliding the plate out. Once this is removed the calibration screws should be visible (see Figure C.2). There is one labeled NULL and one labeled SPAN.

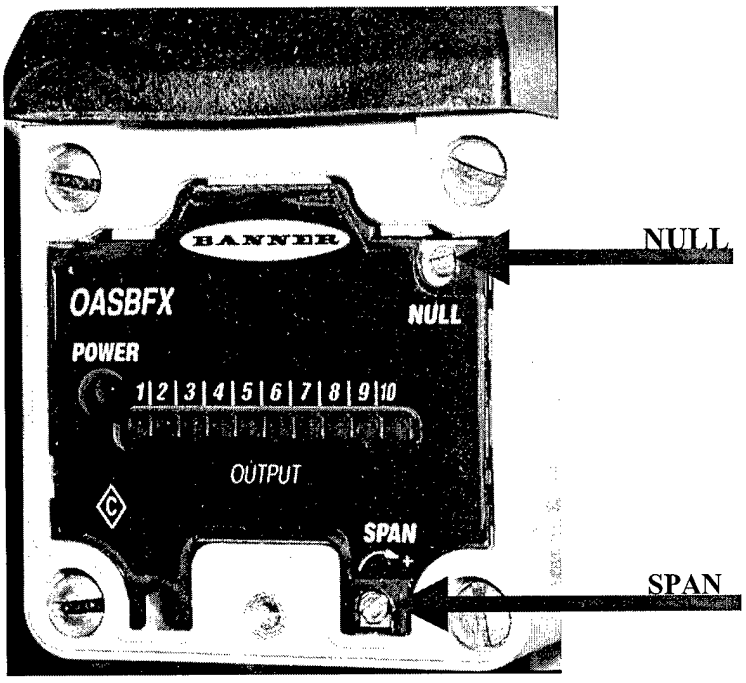

Figure C.2 The picture to the right is the yellow Banner control box. The RED arrows indicate the calibration screws. Note the Figure shows the Banner box upright. The NULL adjustment screw is at the top with the SPAN adjustment screw below it. Note when you calibrate the sensor this will be upside down.

Position the laptop in such a way that you are able to read the CSU OFD display from the program's control panel while you are adjusting the calibration screws on the yellow box. Use the small flat head screwdriver to adjust these screws. Make sure there are no objects between the sending and receiving arms of the sensor. You can now begin the NULL or ZERO calibration. The calibration screws are very sensitive, if you are close to the desired value (zero in this case) use very slight movements.

The calibration process is an iterative process so for the first attempt just try to get the reading within ± 5 to 10 millivolts (this is the value that is being displayed on the control panel or volt meter) of 0mv (zero). You should be able to achieve this range by adjusting only the NULL adjustment screw. After this is achieved move onto the SPAN calibration. To check the span value, attach the calibration disk (see Figure C.3) to the receiving terminal (on the right), with the lens side facing the terminal (see Figure C.4).

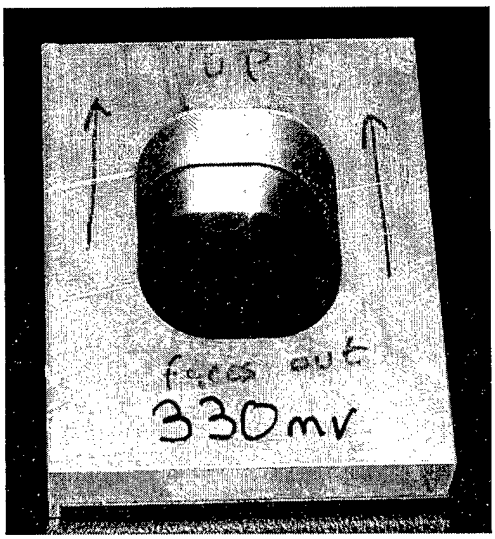

Figure C.3 Calibration disk.

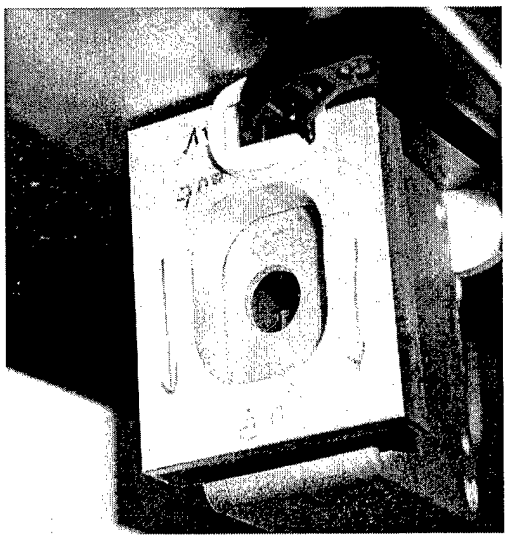

Figure C.4 Proper placement of calibration disk for SPAN adjustment.

The control panel display should show that the sensor reading is now much higher, make sure you allow the sensor enough time (at least 30secs) for the readings to

adjust to the disk. Again, make sure that there is no interference between the terminals other than the calibration disk.

The calibration disk should give a desired reading of 330mv. To achieve this reading adjust the calibration screw labeled SPAN, to get the reading on the control panel within ± 5 to 10mv of the desired 330mv.

Remove the disk and again wait for the readings to fall back down to near zero. Notice that the zero reading may have changed from what you just set it to. This is because adjusting the SPAN value has an effect on the NULL or ZERO value. The reverse is also true (that is, adjusting the NULL value has an effect on the SPAN).

Again adjust the NULL (ZERO) value using the NULL calibration screw and then the SPAN using the SPAN screw. Repeat the calibration process until the values are within ± 1.5mv. of the calibration value (see Table C.1). The zero reading should bounce between positive and negative values.

CALIBRATION VALUES

TYPE	VALUE
NULL	**0±1.5mv**
SPAN	**330±1.5mv**

Table C.1 CSU OFD calibration values

Once these values have been obtained the CSU Optical Fog Detector calibration is done. Replace the clear plastic faceplate onto the yellow Banner box. Then screw the face back onto the gray box. Make sure this is screwed on tightly to protect the interior from rain and other damaging elements.

Field maintenance requires weekly calibration checks and cleaning of the fiber optic lenses. Occasionally the lens housing will attract insects like spiders which can interfere with the proper operation of the sensor. The lenses also tend to get dirty after 7 to 10 days of operation, depending on the area the sensors are placed.

To clean the lenses you will need Q-tips and isopropyl alcohol. Dip the Q-tips into the alcohol and gently rub on each fiber optic lens then with a dry Q-tip and repeat until it comes out clean.

Appendix D – Major Components

Manufacturer/ Vendor	Description	Part Number	Approximate Cost
Banner	OASBFX Analog OMNI-BEAM Infrared (880nm) high power sensor	27601	$116.00
Banner	OPBA3 Power block	27415	$63.00
Banner	Two each IT2.53S, opposed mode glass fiber optic cables	17344	$75.00
Duala	Toroidal transformer	170667	$8.00
	1/4' Polyflow tubing		
Newark Electronics	Fiberglass NEMA enclosure	95F2769	$48.00
Newark Electronics	Bud NEMA utility box	95F936	$6.00
Newark Electronics	DAL RH-5 270 ohm resistor	02F-2487	$2.50
Newark Electronics	DAL RH-5 500 ohm resistor	02F-2497	$2.50
Profile	Aquarium Pump	1500	$6.00
Balston	Filter Tube	DFU	
McMaster Carr Supply	Waterproof inline fuse holder	7696K31	$4.00

Appendix E – Campbell Control Program for Helm, CA

A copy of the automated fog sampler code from Helm will follow this brief introduction to some of the major features of the program. First note important port functions:

PORT	FUNCTION
1	Open Doors (HIGH)
2	Fan ON (HIGH)
3	Turn Bottle Solenoid (HI)

Also note Flag functions:

FLAGS	FUNCTIONS
1	Manual and Initial Startup Reset
2	Manual Prevent Calls for Testing
3	Used for LWC Counter to Start Sampling
4	Used to Make Start Call
5	Used to Stop Sampling After 2nd Bottle Has Been Used
6	Used to Make End Call
7	Used for Delay to Go on to 2nd Bottle
8	Used to Open Doors and Start Fans

All values that can be changed are marked by a line of plus signs (+++++++). These are preceded (three lines above) by a line of equal signs (==========). Generally reading the code will allow you to determine what parameter you are changing. Here is a short list:

Line 30,84,87: Minimum Liquid Water Content needed for collection (if one of these is changed, they all should be)

Line 37: Amount of time (in sec) required to be at or above the minimum LWC before sampling begins

Line 55: Amount of time (in sec) to pass before switching to the second sample bottle

Line 90: Amount of time (in sec) to pass while under the LWC threshold

before the sampling will stop

Also when changing the number to be dialed (Line 76, 77), use the code 44 for a delay.

```
;{CR10}
*Table 1 Program
 01: 1.0000    Execution Interval (seconds)

1: If Flag/Port (P91)
 1: 21      Do if Flag 1 is Low
 2: 30      Then Do

   2: Do (P86)
    1: 11      Set Flag 1 High ;MANUAL AND INITIAL STARTUP RESET

   3: Do (P86)
    1: 23      Set Flag 3 Low ;USED FOR LWC COUNTER TO START SAMPLING

   4: Do (P86)
    1: 25      Set Flag 5 Low ;USED TO STOP SAMPLING AFTER 2ND BOTTLE
HAS BEEN USED

   5: Do (P86)
    1: 27      Set Flag 7 Low ;USED FOR DELAY TO GO ON TO 2ND BOTTLE

   6: Do (P86)
    1: 28      Set Flag 8 Low ;USED TO OPEN DOOR AND START FANS


   7: Z=F (P30)
    1: 0       F
    2: 0       Exponent of 10
    3: 10      Z Loc [ LWCCOUNTR ]

   8: Z=F (P30)
    1: 0       F
    2: 0       Exponent of 10
    3: 11      Z Loc [ ENDCOUNTR ]

   9: Z=F (P30)
    1: 0       F
    2: 0       Exponent of 10
    3: 12      Z Loc [ BOTCOUNTR ]
```

```
  10:  Z=F (P30)
   1: 1       F
   2: 0       Exponent of 10
   3: 15      Z Loc [ BOTTLE    ]

11:  End (P95)

;**********ANALOG VOLTAGE MEASUREMENTS

12:  Volt (SE) (P1)
 1: 1       Reps
 2: 25      2500 mV 60 Hz Rejection Range
 3: 7       SE Channel
 4: 3       Loc [ BANNER    ]
 5: 1.0     Mult
 6: -15     Offset

13:  Volt (SE) (P1)
 1: 1       Reps
 2: 25      2500 mV 60 Hz Rejection Range
 3: 5       SE Channel
 4: 4       Loc [ RH        ]
 5: .1      Mult
 6: 0.0     Offset

14:  Volt (SE) (P1)
 1: 1       Reps
 2: 25      2500 mV 60 Hz Rejection Range
 3: 6       SE Channel
 4: 5       Loc [ TEMP      ]
 5: .1      Mult
 6: -40     Offset

15:  Low Pass Filter (P58)
 1: 1       Reps
 2: 5       Sample Loc [ TEMP      ]
 3: 16      Loc [ FILTER_T_ ]
 4: 0.020   Weighting Factor

;OUTPUT TO FINAL STORAGE EVERY 5 MINUTES
16:  If time is (P92)
 1: 0       Minutes (Seconds --) into a
 2: 5       Interval (same units as above)
 3: 10      Set Output Flag High

17:  Set Active Storage Area (P80)
```

```
1: 1      Final Storage Area 1
2: 111    Array ID

18: Real Time (P77)
1: 1110   Year,Day,Hour/Minute (midnight = 0000)

19: Average (P71)
1: 3      Reps
2: 3      Loc [ BANNER   ]

20: Standard Deviation (P82)
1: 1      Reps
2: 3      Sample Loc [ BANNER   ]

21: Sample (P70)
1: 1      Reps
2: 10     Loc [ LWCCOUNTR ]

22: Sample (P70)
1: 1      Reps
2: 15     Loc [ BOTTLE   ]

;****************************** CONTROL STUFF

23: If Flag/Port (P91)
1: 25     Do if Flag 5 is Low
2: 30     Then Do

   24: If (X<=>F) (P89)
;=============================================================
   1: 16     X Loc [ FILTER_T_ ]
   2: 3      >=
   3: -.5    F
;+++++++++++++++++++++++++++++++++++++++++++++++++++++++++++++++
   4: 30     Then Do

      25: If (X<=>F) (P89)
;=============================================
      1: 3      X Loc [ BANNER   ]
      2: 3      >=
      3: 40     F
;+++++++++++++++++++++++++++++++++++++++++++++++++
      4: 13     Set Flag 3 High

      26: If Flag/Port (P91)
      1: 13     Do if Flag 3 is High
```

```
      2: 30     Then Do

        27: Z=Z+1 (P32)
         1: 10     Z Loc [ LWCCOUNTR ]

      28: End (P95)

      29: If Flag/Port (P91)
       1: 23     Do if Flag 3 is Low
       2: 30     Then Do

        30: Z=F (P30)
         1: 0      F
         2: 0      Exponent of 10
         3: 10     Z Loc [ LWCCOUNTR ]

      31: End (P95)

      32: If (X<=>F) (P89)
;=============================================================
       1: 10     X Loc [ LWCCOUNTR ]
       2: 1      =
       3: 300    F
;+++++++++++++++++++++++++++++++++++++++++++++++++++++++++++++
       4: 30     Then Do

         33: Do (P86)
          1: 18     Set Flag 8 High

      34: End (P95)

   35: End (P95)

;***** AUTOMATED CASCC OPERATION

   36: If Flag/Port (P91)
    1: 18     Do if Flag 8 is High
    2: 30     Then Do

;OPEN DOORS
      37: Do (P86)
       1: 41     Set Port 1 High

      38: Beginning of Loop (P87)
       1: 2      Delay
       2: 1      Loop Count
```

```
      39:  End (P95)

;TURN FAN ON
      40:  Do (P86)
       1: 42      Set Port 2 High

   41:  End (P95)

   42:  If Flag/Port (P91)
    1: 28      Do if Flag 8 is Low
    2: 30      Then Do

;CLOSE DOORS
      43:  Do (P86)
       1: 51      Set Port 1 Low

;TURN FAN OFF
      44:  Do (P86)
       1: 52      Set Port 2 Low

   45:  End (P95)

   46:  If Flag/Port (P91)
    1: 17      Do if Flag 7 is High
    2: 30      Then Do

      47:  If Flag/Port (P91)
       1: 28      Do if Flag 8 is Low
       2: 30      Then Do

         48:  Z=Z+1 (P32)
          1: 12      Z Loc [ BOTCOUNTR ]

         49:  If (X<=>F) (P89)
;=================================================
          1: 12      X Loc [ BOTCOUNTR ]
          2: 3       >=
          3: 3600    F
;+++++++++++++++++++++++++++++++++++++++++++++++++++++++++++++++
          4: 30      Then Do

            50:  Do (P86)
             1: 27      Set Flag 7 Low

            51:  Z=F (P30)
```

```
            1: 0      F
            2: 0      Exponent of 10
            3: 12     Z Loc [ BOTCOUNTR ]

;TURN ON SOLENIOD FOR SECOND BOTTLE
          52: Do (P86)
            1: 43     Set Port 3 High

          53: Z=Z+1 (P32)
            1: 15     Z Loc [ BOTTLE    ]

        54: End (P95)

        55: If (X<=>F) (P89)
          1: 15     X Loc [ BOTTLE    ]
          2: 3      >=
          3: 3      F
          4: 15     Set Flag 5 High

      56: End (P95)

      57: If Flag/Port (P91)
        1: 18     Do if Flag 8 is High
        2: 30     Then Do

          58: Do (P86)
            1: 27     Set Flag 7 Low

          59: Z=F (P30)
            1: 0      F
            2: 0      Exponent of 10
            3: 12     Z Loc [ BOTCOUNTR ]

      60: End (P95)

    61: End (P95)

    62: If Flag/Port (P91)
      1: 28     Do if Flag 8 is Low
      2: 30     Then Do

        63: Z=F (P30)
          1: 0      F
          2: 0      Exponent of 10
          3: 11     Z Loc [ ENDCOUNTR ]
```

```
      64:  If (X<=>F) (P89)
;=============================================================
       1: 3       X Loc [ BANNER    ]
       2: 4       <
       3: 40      F
;+++++++++++++++++++++++++++++++++++++++++++++++++++++++++++++
       4: 23      Set Flag 3 Low

   65:  End (P95)

   66:  If Flag/Port (P91)
    1: 18      Do if Flag 8 is High
    2: 30      Then Do

      67:  If (X<=>F) (P89)
;=============================================================
       1: 3       X Loc [ BANNER    ]
       2: 4       <
       3: 40      F
;+++++++++++++++++++++++++++++++++++++++++++++++++++++++++++++
       4: 30      Then Do

         68:  Z=Z+1 (P32)
          1: 11      Z Loc [ ENDCOUNTR ]

      69:  End (P95)

      70:  If (X<=>F) (P89)
;=============================================================
       1: 3       X Loc [ BANNER    ]
       2: 3       >=
       3: 40      F
;+++++++++++++++++++++++++++++++++++++++++++++++++++++++++++++
       4: 30      Then Do

         71:  Z=F (P30)
          1: 0       F
          2: 0       Exponent of 10
          3: 11      Z Loc [ ENDCOUNTR ]

      72:  End (P95)

      73:  If (X<=>F) (P89)
;=============================================================
       1: 11      X Loc [ ENDCOUNTR ]
       2: 1       =
```

```
        3: 150     F
;+++++++++++++++++++++++++++++++++++++++++++++++++++++++++++++++
        4: 30      Then Do

          74:  Do (P86)
           1: 28      Set Flag 8 Low

          75:  Do (P86)
           1: 17      Set Flag 7 High

        76:  End (P95)

     77:  End (P95)

     78:  If (X<=>F) (P89)
      1: 10      X Loc [ LWCCOUNTR ]
      2: 1       =
      3: 4100    F
      4: 30      Then Do

        79:  Z=F (P30)
         1: 5       F
         2: 2       Exponent of 10
         3: 10      Z Loc [ LWCCOUNTR ]

     80:  End (P95)

81:  End (P95)

*Table 2 Program
 01: 0.0000    Execution Interval (seconds)

*Table 3 Subroutines

End Program

-Input Locations-
1 _____ 1 0 0
2 _____ 0 0 0
3 BANNER   1 6 1
4 RH       1 1 1
5 TEMP     1 2 1
6 _____ 0 0 0
7 _____ 0 0 0
8 _____ 0 0 0
9 _____ 0 0 0
```

10 LWCCOUNTR 1 3 4
11 ENDCOUNTR 1 1 4
12 BOTCOUNTR 1 1 4
13 STARTCALL 1 0 0
14 ENDCALL 1 0 0
15 BOTTLE 1 2 2
16 FILTER_T_ 1 1 1
17 _____ 0 0 0
18 _____ 0 0 0
19 _____ 0 0 0
20 _____ 0 0 0
21 _____ 0 0 0
22 _____ 0 0 0
23 _____ 0 0 0
24 _____ 0 0 0
25 _____ 0 0 0
26 _____ 0 0 0
27 _____ 0 0 0
28 _____ 0 0 0
29 _____ 0 0 0
30 _____ 0 0 0
31 _____ 0 0 0
32 _____ 0 0 0
33 _____ 0 0 0
34 _____ 0 0 0
-Program Security-
0000
0000
0000
-Mode 4-
-Final Storage Area 2-
0

Appendix F – Angiola setup

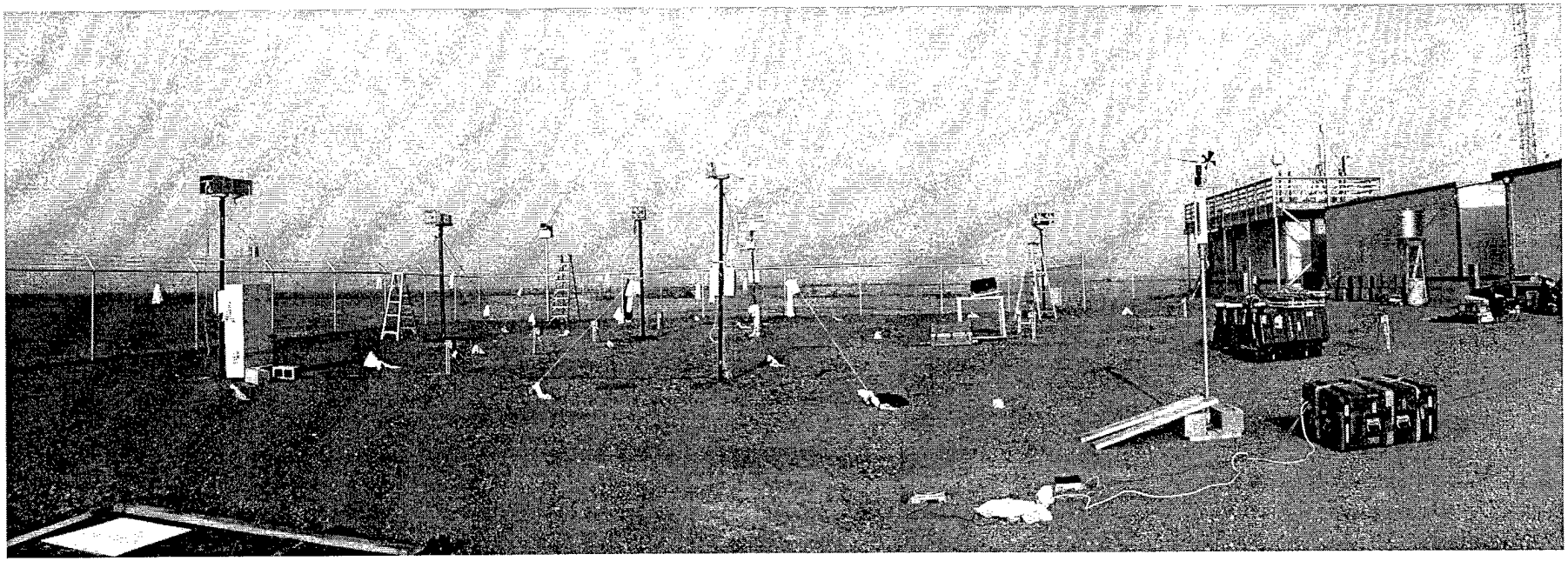

Appendix G – Theoretical CASCC2 Collection Rate

The theoretical collection rate for the CASCC is calculated below.

LWC	Q = 5.84 m^3/min Demoz et al., (1996)	$n_2 = \{1-(1-d_c/x)^r\}$ Friedlander (1977)	Cr = 1318*LWC^6-1957*LWC^5+1102*LWC^4-293*LWC^3+37.2*LWC^2+2.97*LWC for 0.025≤ LWC ≤ 0.175 Demoz et al., (1996)	Cr = 0.493*LWC^2 + 4.93*LWC for 0.175< LWC ≤ 0.5 Demoz et al., (1996)
g/m^3	Q	n_2	Cr (ml/min) for 0.025≤ LWC ≤ 0.175	Cr (ml/min) for 0.175< LWC ≤ 0.5
0.025	5.84	0.86	0.09	
0.03	5.84	0.86	0.12	
0.035	5.84	0.86	0.14	
0.04	5.84	0.86	0.16	
0.045	5.84	0.86	0.19	
0.05	5.84	0.86	0.21	
0.055	5.84	0.86	0.24	
0.06	5.84	0.86	0.26	
0.065	5.84	0.86	0.29	
0.07	5.84	0.86	0.31	
0.075	5.84	0.86	0.34	
0.08	5.84	0.86	0.36	
0.085	5.84	0.86	0.39	
0.09	5.84	0.86	0.42	
0.095	5.84	0.86	0.44	
0.1	5.84	0.86	0.47	
0.105	5.84	0.86	0.49	
0.11	5.84	0.86	0.52	
0.115	5.84	0.86	0.54	
0.12	5.84	0.86	0.57	
0.125	5.84	0.86	0.59	
0.13	5.84	0.86	0.62	
0.135	5.84	0.86	0.64	
0.14	5.84	0.86	0.67	
0.145	5.84	0.86	0.69	
0.15	5.84	0.86	0.72	

0.155	5.84	0.86	0.74	
0.16	5.84	0.86	0.77	
0.165	5.84	0.86	0.79	
0.17	5.84	0.86	0.81	
0.175	5.84	0.86	0.84	
0.18	5.84	0.86		0.87
0.185	5.84	0.86		0.89
0.19	5.84	0.86		0.92
0.195	5.84	0.86		0.94
0.2	5.84	0.86		0.97
0.205	5.84	0.86		0.99
0.21	5.84	0.86		1.02
0.215	5.84	0.86		1.04
0.22	5.84	0.86		1.06
0.225	5.84	0.86		1.09
0.23	5.84	0.86		1.11
0.235	5.84	0.86		1.14
0.24	5.84	0.86		1.16
0.245	5.84	0.86		1.19
0.25	5.84	0.86		1.21
0.255	5.84	0.86		1.24
0.26	5.84	0.86		1.26
0.265	5.84	0.86		1.29
0.27	5.84	0.86		1.31
0.275	5.84	0.86		1.34
0.28	5.84	0.86		1.36
0.285	5.84	0.86		1.39
0.29	5.84	0.86		1.41
0.295	5.84	0.86		1.44
0.3	5.84	0.86		1.46
0.305	5.84	0.86		1.49
0.31	5.84	0.86		1.51
0.315	5.84	0.86		1.54
0.32	5.84	0.86		1.56
0.325	5.84	0.86		1.59
0.33	5.84	0.86		1.61
0.335	5.84	0.86		1.64
0.34	5.84	0.86		1.67
0.345	5.84	0.86		1.69
0.35	5.84	0.86		1.72
0.355	5.84	0.86		1.74
0.36	5.84	0.86		1.77
0.365	5.84	0.86		1.79
0.37	5.84	0.86		1.82
0.375	5.84	0.86		1.84
0.38	5.84	0.86		1.87

0.385	5.84	0.86		1.89
0.39	5.84	0.86		1.92
0.395	5.84	0.86		1.95
0.4	5.84	0.86		1.97
0.405	5.84	0.86		2.00
0.41	5.84	0.86		2.02
0.415	5.84	0.86		2.05
0.42	5.84	0.86		2.07
0.425	5.84	0.86		2.10
0.43	5.84	0.86		2.13
0.435	5.84	0.86		2.15
0.44	5.84	0.86		2.18
0.445	5.84	0.86		2.20
0.45	5.84	0.86		2.23
0.455	5.84	0.86		2.25
0.46	5.84	0.86		2.28
0.465	5.84	0.86		2.31
0.47	5.84	0.86		2.33
0.475	5.84	0.86		2.36
0.48	5.84	0.86		2.38
0.485	5.84	0.86		2.41
0.49	5.84	0.86		2.44
0.495	5.84	0.86		2.46
0.5	5.84	0.86		2.49

Appendix H – Theoretical CASCC Collection Rate

The theoretical collection rate for the CASCC is calculated below.

LWC	Theoretical CASCC Collection Rate $Cr = (n_1)(n_2)Q(LWC)$ Hoffmann et al., (1989)	$Q = 24.5$ m^3/min Demoz et al., (1996)	$n_2 = \{1-(1-d_c/x)^r\}$ Friedlander (1977)	$n_1 = 262*LWC^5-389*LWC^4+219*LWC^3-58.2*LWC^2+7.4*LWC+0.59$ for $0.025 \leq LWC \leq 0.175$ Hoffmann et al., (1989)	$n_1 = 0.098*LWC + 0.94$ for $0.175 < LWC \leq 0.5$ Hoffmann et al., (1989)
g/m^3	ml/min	Q	n_2	n_1	
0.025	0.39	24.5	0.86	0.74	
0.03	0.49	24.5	0.86	0.77	
0.035	0.58	24.5	0.86	0.79	
0.04	0.68	24.5	0.86	0.81	
0.045	0.78	24.5	0.86	0.82	
0.05	0.89	24.5	0.86	0.84	
0.055	0.99	24.5	0.86	0.85	
0.06	1.10	24.5	0.86	0.87	
0.065	1.21	24.5	0.86	0.88	
0.07	1.32	24.5	0.86	0.89	
0.075	1.42	24.5	0.86	0.90	
0.08	1.53	24.5	0.86	0.91	
0.085	1.64	24.5	0.86	0.91	
0.09	1.75	24.5	0.86	0.92	
0.095	1.86	24.5	0.86	0.93	
0.1	1.97	24.5	0.86	0.93	
0.105	2.08	24.5	0.86	0.93	
0.11	2.18	24.5	0.86	0.94	
0.115	2.29	24.5	0.86	0.94	
0.12	2.40	24.5	0.86	0.94	
0.125	2.50	24.5	0.86	0.95	
0.13	2.61	24.5	0.86	0.95	
0.135	2.71	24.5	0.86	0.95	
0.14	2.82	24.5	0.86	0.95	
0.145	2.92	24.5	0.86	0.95	
0.15	3.02	24.5	0.86	0.95	
0.155	3.12	24.5	0.86	0.95	

0.16	3.23	24.5	0.86	0.95	
0.165	3.33	24.5	0.86	0.95	
0.17	3.43	24.5	0.86	0.95	
0.175	3.53	24.5	0.86	0.95	
0.18	3.65	24.5	0.86		0.96
0.185	3.75	24.5	0.86		0.96
0.19	3.85	24.5	0.86		0.96
0.195	3.96	24.5	0.86		0.96
0.2	4.06	24.5	0.86		0.96
0.205	4.16	24.5	0.86		0.96
0.21	4.27	24.5	0.86		0.96
0.215	4.37	24.5	0.86		0.96
0.22	4.47	24.5	0.86		0.96
0.225	4.58	24.5	0.86		0.96
0.23	4.68	24.5	0.86		0.96
0.235	4.79	24.5	0.86		0.96
0.24	4.89	24.5	0.86		0.96
0.245	5.00	24.5	0.86		0.96
0.25	5.10	24.5	0.86		0.96
0.255	5.20	24.5	0.86		0.96
0.26	5.31	24.5	0.86		0.97
0.265	5.41	24.5	0.86		0.97
0.27	5.52	24.5	0.86		0.97
0.275	5.62	24.5	0.86		0.97
0.28	5.73	24.5	0.86		0.97
0.285	5.83	24.5	0.86		0.97
0.29	5.94	24.5	0.86		0.97
0.295	6.05	24.5	0.86		0.97
0.3	6.15	24.5	0.86		0.97
0.305	6.26	24.5	0.86		0.97
0.31	6.36	24.5	0.86		0.97
0.315	6.47	24.5	0.86		0.97
0.32	6.57	24.5	0.86		0.97
0.325	6.68	24.5	0.86		0.97
0.33	6.79	24.5	0.86		0.97
0.335	6.89	24.5	0.86		0.97
0.34	7.00	24.5	0.86		0.97
0.345	7.11	24.5	0.86		0.97
0.35	7.21	24.5	0.86		0.97
0.355	7.32	24.5	0.86		0.97
0.36	7.43	24.5	0.86		0.98
0.365	7.53	24.5	0.86		0.98
0.37	7.64	24.5	0.86		0.98
0.375	7.75	24.5	0.86		0.98
0.38	7.85	24.5	0.86		0.98
0.385	7.96	24.5	0.86		0.98

0.39	8.07	24.5	0.86		0.98
0.395	8.18	24.5	0.86		0.98
0.4	8.28	24.5	0.86		0.98
0.405	8.39	24.5	0.86		0.98
0.41	8.50	24.5	0.86		0.98
0.415	8.61	24.5	0.86		0.98
0.42	8.72	24.5	0.86		0.98
0.425	8.82	24.5	0.86		0.98
0.43	8.93	24.5	0.86		0.98
0.435	9.04	24.5	0.86		0.98
0.44	9.15	24.5	0.86		0.98
0.445	9.26	24.5	0.86		0.98
0.45	9.37	24.5	0.86		0.98
0.455	9.47	24.5	0.86		0.98
0.46	9.58	24.5	0.86		0.99
0.465	9.69	24.5	0.86		0.99
0.47	9.80	24.5	0.86		0.99
0.475	9.91	24.5	0.86		0.99
0.48	10.02	24.5	0.86		0.99
0.485	10.13	24.5	0.86		0.99
0.49	10.24	24.5	0.86		0.99
0.495	10.35	24.5	0.86		0.99
0.5	10.46	24.5	0.86		0.99

Adjusted Theoretical CASCC Collection Rate

The following collection rates were calculated based on the lower power supply voltage. To roughly compensate for the difference in actual voltage (10.65 volts) from the accepted voltage (13.3 volts) we multiplied Q by (10.65)/(13.3) [(actual)/(accepted)] and used this as our new Q.

LWC	Adjusted Theoretical CASCC Collection Rate Cr = $(n_1)(n_2)Q(LWC)$ Hoffmann et al., (1989)	Adjusted Q = 19.6 m^3/min based on Demoz et al., (1996)	$n_2 = \{1-(1-d_c/x)^r\}$ Friedlander (1977)	$n_1 = 262*LWC^5-389*LWC^4+219*LWC^3-58.2*LWC^2+7.4*LWC+0.59$ for $0.025 \leq LWC \leq 0.175$ Hoffmann et al., (1989)	n1 = 0.098*LWC + 0.94 for 0.175< LWC < 0.5 Hoffmann et al., (1989)
g/m^3	ml/min	Q	n_2	n_1	
0.025	0.31	19.6	0.86	0.74	
0.03	0.39	19.6	0.86	0.77	
0.035	0.47	19.6	0.86	0.79	
0.04	0.55	19.6	0.86	0.81	
0.045	0.63	19.6	0.86	0.82	
0.05	0.71	19.6	0.86	0.84	
0.055	0.79	19.6	0.86	0.85	
0.06	0.88	19.6	0.86	0.87	
0.065	0.97	19.6	0.86	0.88	
0.07	1.05	19.6	0.86	0.89	
0.075	1.14	19.6	0.86	0.90	
0.08	1.23	19.6	0.86	0.91	
0.085	1.31	19.6	0.86	0.91	
0.09	1.40	19.6	0.86	0.92	
0.095	1.49	19.6	0.86	0.93	
0.1	1.57	19.6	0.86	0.93	
0.105	1.66	19.6	0.86	0.93	
0.11	1.75	19.6	0.86	0.94	
0.115	1.83	19.6	0.86	0.94	
0.12	1.92	19.6	0.86	0.94	
0.125	2.00	19.6	0.86	0.95	
0.13	2.09	19.6	0.86	0.95	
0.135	2.17	19.6	0.86	0.95	
0.14	2.25	19.6	0.86	0.95	

0.145	2.34	19.6	0.86	0.95	
0.15	2.42	19.6	0.86	0.95	
0.155	2.50	19.6	0.86	0.95	
0.16	2.58	19.6	0.86	0.95	
0.165	2.66	19.6	0.86	0.95	
0.17	2.74	19.6	0.86	0.95	
0.175	2.83	19.6	0.86	0.95	
0.18	2.92	19.6	0.86		0.96
0.185	3.00	19.6	0.86		0.96
0.19	3.08	19.6	0.86		0.96
0.195	3.16	19.6	0.86		0.96
0.2	3.25	19.6	0.86		0.96
0.205	3.33	19.6	0.86		0.96
0.21	3.41	19.6	0.86		0.96
0.215	3.50	19.6	0.86		0.96
0.22	3.58	19.6	0.86		0.96
0.225	3.66	19.6	0.86		0.96
0.23	3.75	19.6	0.86		0.96
0.235	3.83	19.6	0.86		0.96
0.24	3.91	19.6	0.86		0.96
0.245	4.00	19.6	0.86		0.96
0.25	4.08	19.6	0.86		0.96
0.255	4.16	19.6	0.86		0.96
0.26	4.25	19.6	0.86		0.97
0.265	4.33	19.6	0.86		0.97
0.27	4.42	19.6	0.86		0.97
0.275	4.50	19.6	0.86		0.97
0.28	4.58	19.6	0.86		0.97
0.285	4.67	19.6	0.86		0.97
0.29	4.75	19.6	0.86		0.97
0.295	4.84	19.6	0.86		0.97
0.3	4.92	19.6	0.86		0.97
0.305	5.01	19.6	0.86		0.97
0.31	5.09	19.6	0.86		0.97
0.315	5.17	19.6	0.86		0.97
0.32	5.26	19.6	0.86		0.97
0.325	5.34	19.6	0.86		0.97
0.33	5.43	19.6	0.86		0.97
0.335	5.51	19.6	0.86		0.97
0.34	5.60	19.6	0.86		0.97
0.345	5.68	19.6	0.86		0.97
0.35	5.77	19.6	0.86		0.97
0.355	5.86	19.6	0.86		0.97
0.36	5.94	19.6	0.86		0.98
0.365	6.03	19.6	0.86		0.98
0.37	6.11	19.6	0.86		0.98

0.375	6.20	19.6	0.86		0.98
0.38	6.28	19.6	0.86		0.98
0.385	6.37	19.6	0.86		0.98
0.39	6.45	19.6	0.86		0.98
0.395	6.54	19.6	0.86		0.98
0.4	6.63	19.6	0.86		0.98
0.405	6.71	19.6	0.86		0.98
0.41	6.80	19.6	0.86		0.98
0.415	6.89	19.6	0.86		0.98
0.42	6.97	19.6	0.86		0.98
0.425	7.06	19.6	0.86		0.98
0.43	7.15	19.6	0.86		0.98
0.435	7.23	19.6	0.86		0.98
0.44	7.32	19.6	0.86		0.98
0.445	7.41	19.6	0.86		0.98
0.45	7.49	19.6	0.86		0.98
0.455	7.58	19.6	0.86		0.98
0.46	7.67	19.6	0.86		0.99
0.465	7.75	19.6	0.86		0.99
0.47	7.84	19.6	0.86		0.99
0.475	7.93	19.6	0.86		0.99
0.48	8.02	19.6	0.86		0.99
0.485	8.10	19.6	0.86		0.99
0.49	8.19	19.6	0.86		0.99
0.495	8.28	19.6	0.86		0.99
0.5	8.37	19.6	0.86		0.99

Theoretical sf-CASCC Collection Rates

LWC	Theoretical sf-CASCC Collection Rate $Cr = (n_1)(n_2)Q(LWC)$ Hoffmann et al., (1989)	$Q = 19\ m^3/min$ Demoz et al., (1996)	Combined stages $n_2 = \{1-(1-d_c/x)^r\}$ Friedlander (1977)	Combined stages $n_1 = 262*LWC^5-389*LWC^4+219*LWC^3-58.2*LWC^2+7.4*LWC+0.59$ for $0.025 \leq LWC \leq 0.175$ Hoffmann et al., (1989)	$n1 = 0.098*LWC + 0.94$ for $0.175 < LWC < 0.5$ Hoffmann et al., (1989)
g/m^3	ml/min	Q	n_2	n_1	
0.025	0.31	19	0.89	0.74	
0.03	0.39	19	0.89	0.77	
0.035	0.46	19	0.89	0.79	
0.04	0.54	19	0.89	0.81	
0.045	0.62	19	0.89	0.82	
0.05	0.71	19	0.89	0.84	
0.055	0.79	19	0.89	0.85	
0.06	0.87	19	0.89	0.87	
0.065	0.96	19	0.89	0.88	
0.07	1.05	19	0.89	0.89	
0.075	1.13	19	0.89	0.90	
0.08	1.22	19	0.89	0.91	
0.085	1.31	19	0.89	0.91	
0.09	1.39	19	0.89	0.92	
0.095	1.48	19	0.89	0.93	
0.1	1.57	19	0.89	0.93	
0.105	1.65	19	0.89	0.93	
0.11	1.74	19	0.89	0.94	
0.115	1.82	19	0.89	0.94	
0.12	1.91	19	0.89	0.94	
0.125	1.99	19	0.89	0.95	
0.13	2.07	19	0.89	0.95	
0.135	2.16	19	0.89	0.95	
0.14	2.24	19	0.89	0.95	
0.145	2.32	19	0.89	0.95	
0.15	2.40	19	0.89	0.95	
0.155	2.48	19	0.89	0.95	
0.16	2.57	19	0.89	0.95	
0.165	2.65	19	0.89	0.95	
0.17	2.73	19	0.89	0.95	
0.175	2.81	19	0.89	0.95	
0.18	2.90	19	0.89		0.96
0.185	2.98	19	0.89		0.96
0.19	3.06	19	0.89		0.96

0.195	3.14	19	0.89		0.96
0.2	3.23	19	0.89		0.96
0.205	3.31	19	0.89		0.96
0.21	3.39	19	0.89		0.96
0.215	3.47	19	0.89		0.96
0.22	3.56	19	0.89		0.96
0.225	3.64	19	0.89		0.96
0.23	3.72	19	0.89		0.96
0.235	3.81	19	0.89		0.96
0.24	3.89	19	0.89		0.96
0.245	3.97	19	0.89		0.96
0.25	4.05	19	0.89		0.96
0.255	4.14	19	0.89		0.96
0.26	4.22	19	0.89		0.97
0.265	4.30	19	0.89		0.97
0.27	4.39	19	0.89		0.97
0.275	4.47	19	0.89		0.97
0.28	4.55	19	0.89		0.97
0.285	4.64	19	0.89		0.97
0.29	4.72	19	0.89		0.97
0.295	4.81	19	0.89		0.97
0.3	4.89	19	0.89		0.97
0.305	4.97	19	0.89		0.97
0.31	5.06	19	0.89		0.97
0.315	5.14	19	0.89		0.97
0.32	5.23	19	0.89		0.97
0.325	5.31	19	0.89		0.97
0.33	5.40	19	0.89		0.97
0.335	5.48	19	0.89		0.97
0.34	5.56	19	0.89		0.97
0.345	5.65	19	0.89		0.97
0.35	5.73	19	0.89		0.97
0.355	5.82	19	0.89		0.97
0.36	5.90	19	0.89		0.98
0.365	5.99	19	0.89		0.98
0.37	6.07	19	0.89		0.98
0.375	6.16	19	0.89		0.98
0.38	6.24	19	0.89		0.98
0.385	6.33	19	0.89		0.98
0.39	6.42	19	0.89		0.98
0.395	6.50	19	0.89		0.98
0.4	6.59	19	0.89		0.98
0.405	6.67	19	0.89		0.98
0.41	6.76	19	0.89		0.98
0.415	6.84	19	0.89		0.98
0.42	6.93	19	0.89		0.98

0.425	7.02	19	0.89		0.98
0.43	7.10	19	0.89		0.98
0.435	7.19	19	0.89		0.98
0.44	7.27	19	0.89		0.98
0.445	7.36	19	0.89		0.98
0.45	7.45	19	0.89		0.98
0.455	7.53	19	0.89		0.98
0.46	7.62	19	0.89		0.99
0.465	7.71	19	0.89		0.99
0.47	7.79	19	0.89		0.99
0.475	7.88	19	0.89		0.99
0.48	7.97	19	0.89		0.99
0.485	8.05	19	0.89		0.99
0.49	8.14	19	0.89		0.99
0.495	8.23	19	0.89		0.99
0.5	8.32	19	0.89		0.99

Adjusted Theoretical sf-CASCC Collection Rate

The following collection rates were calculated based on the lower power supply voltage. To roughly compensate for the difference in actual voltage (11.12 volts) from the accepted voltage (13.3 volts) we multiplied Q by (11.12)/(13.3) [(actual)/(accepted)] and used this as our new Q.

LWC	Theoretical adjusted sf-CASCC Collection Rate Cr = $(n_1)(n_2)Q(LWC)$ Hoffmann et al., (1989)	Adjusted Q Q = 15.9 m^3/min	Combined stages $n_2 = \{1-(1-d_c/x)^r\}$	$n_1 = 262*LWC^5-389*LWC^4+219*LWC^3-58.2*LWC^2+7.4*LWC+0.59$ for $0.025 \leq LWC \leq 0.175$Hoffmann et al., (1989)	n1 = 0.098*LWC + 0.94 for 0.175< LWC < 0.5 Hoffmann et al., (1989)
g/m^3	ml/min	Q	n_2	n_1	
0.025	0.26	15.9	0.89	0.74	
0.03	0.32	15.9	0.89	0.77	
0.035	0.39	15.9	0.89	0.79	
0.04	0.45	15.9	0.89	0.81	
0.045	0.52	15.9	0.89	0.82	
0.05	0.59	15.9	0.89	0.84	
0.055	0.66	15.9	0.89	0.85	
0.06	0.73	15.9	0.89	0.87	
0.065	0.80	15.9	0.89	0.88	
0.07	0.88	15.9	0.89	0.89	
0.075	0.95	15.9	0.89	0.90	
0.08	1.02	15.9	0.89	0.91	
0.085	1.09	15.9	0.89	0.91	
0.09	1.17	15.9	0.89	0.92	
0.095	1.24	15.9	0.89	0.93	
0.1	1.31	15.9	0.89	0.93	
0.105	1.38	15.9	0.89	0.93	
0.11	1.45	15.9	0.89	0.94	
0.115	1.52	15.9	0.89	0.94	
0.12	1.59	15.9	0.89	0.94	
0.125	1.66	15.9	0.89	0.95	
0.13	1.73	15.9	0.89	0.95	
0.135	1.80	15.9	0.89	0.95	
0.14	1.87	15.9	0.89	0.95	
0.145	1.94	15.9	0.89	0.95	
0.15	2.01	15.9	0.89	0.95	

0.155	2.08	15.9	0.89	0.95	
0.16	2.15	15.9	0.89	0.95	
0.165	2.21	15.9	0.89	0.95	
0.17	2.28	15.9	0.89	0.95	
0.175	2.35	15.9	0.89	0.95	
0.18	2.43	15.9	0.89		0.96
0.185	2.49	15.9	0.89		0.96
0.19	2.56	15.9	0.89		0.96
0.195	2.63	15.9	0.89		0.96
0.2	2.70	15.9	0.89		0.96
0.205	2.77	15.9	0.89		0.96
0.21	2.84	15.9	0.89		0.96
0.215	2.91	15.9	0.89		0.96
0.22	2.98	15.9	0.89		0.96
0.225	3.05	15.9	0.89		0.96
0.23	3.12	15.9	0.89		0.96
0.235	3.18	15.9	0.89		0.96
0.24	3.25	15.9	0.89		0.96
0.245	3.32	15.9	0.89		0.96
0.25	3.39	15.9	0.89		0.96
0.255	3.46	15.9	0.89		0.96
0.26	3.53	15.9	0.89		0.97
0.265	3.60	15.9	0.89		0.97
0.27	3.67	15.9	0.89		0.97
0.275	3.74	15.9	0.89		0.97
0.28	3.81	15.9	0.89		0.97
0.285	3.88	15.9	0.89		0.97
0.29	3.95	15.9	0.89		0.97
0.295	4.02	15.9	0.89		0.97
0.3	4.09	15.9	0.89		0.97
0.305	4.16	15.9	0.89		0.97
0.31	4.23	15.9	0.89		0.97
0.315	4.30	15.9	0.89		0.97
0.32	4.37	15.9	0.89		0.97
0.325	4.44	15.9	0.89		0.97
0.33	4.52	15.9	0.89		0.97
0.335	4.59	15.9	0.89		0.97
0.34	4.66	15.9	0.89		0.97
0.345	4.73	15.9	0.89		0.97
0.35	4.80	15.9	0.89		0.97
0.355	4.87	15.9	0.89		0.97
0.36	4.94	15.9	0.89		0.98
0.365	5.01	15.9	0.89		0.98
0.37	5.08	15.9	0.89		0.98
0.375	5.15	15.9	0.89		0.98
0.38	5.23	15.9	0.89		0.98

0.385	5.30	15.9	0.89		0.98
0.39	5.37	15.9	0.89		0.98
0.395	5.44	15.9	0.89		0.98
0.4	5.51	15.9	0.89		0.98
0.405	5.58	15.9	0.89		0.98
0.41	5.65	15.9	0.89		0.98
0.415	5.73	15.9	0.89		0.98
0.42	5.80	15.9	0.89		0.98
0.425	5.87	15.9	0.89		0.98
0.43	5.94	15.9	0.89		0.98
0.435	6.01	15.9	0.89		0.98
0.44	6.09	15.9	0.89		0.98
0.445	6.16	15.9	0.89		0.98
0.45	6.23	15.9	0.89		0.98
0.455	6.30	15.9	0.89		0.98
0.46	6.38	15.9	0.89		0.99
0.465	6.45	15.9	0.89		0.99
0.47	6.52	15.9	0.89		0.99
0.475	6.59	15.9	0.89		0.99
0.48	6.67	15.9	0.89		0.99
0.485	6.74	15.9	0.89		0.99
0.49	6.81	15.9	0.89		0.99
0.495	6.89	15.9	0.89		0.99
0.5	6.96	15.9	0.89		0.99

Appendix I – Theoretical vs. Actual and Adjusted CASCC and sf-CASCC Collection Rates

Table I.1 is a breakout of the data from the January 31, 2001 event where we sampled using the CASCC. The theoretical rates (see Appendix H) are calculated and compared to the actual and adjusted collection rates.

Sample Time	Sample Volume of CASCC	Actual sf-CASCC Collection Rate	PVM Mean LWC	Theoretical from PVM	Theoretical "adjusted" from PVM	CSU OFD MEAN LWC	Theoretical from CSU OFD	Theoretical "adjusted" from CSU OFD
Start Time	grams	$ml*min^{-1}$	$ml*m^{-3}$	$ml*min^{-1}$	$ml*min^{-1}$	$ml*m^{-3}$	$ml*min^{-1}$	$ml*min^{-1}$
5:25-7:00 AM	220.1	2.30	278	4.5	3.8	377	2.3	5.2
7:00-8:00 AM	96.6	1.60	155	2.5	2.1	241	3.9	3.3
8:00-9:00 AM	90.7	0.90	67	1	0.9	51	0.4	0.6
		Actual CASCC Collection Rate						
5:25-7:00 AM	236	2.50	278	5.7	4.6	377	7.8	6.2
7:00-8:00 AM	94.3	1.57	155	3.1	2.5	241	4.9	3.9

Table I.1 Comparison of theoretical, actual and adjusted collection rates.

The CSU OFD and PVM theoretical and adjusted collection rates are graphed against each other and the actual collection rates in Figures I.1 and I.2.

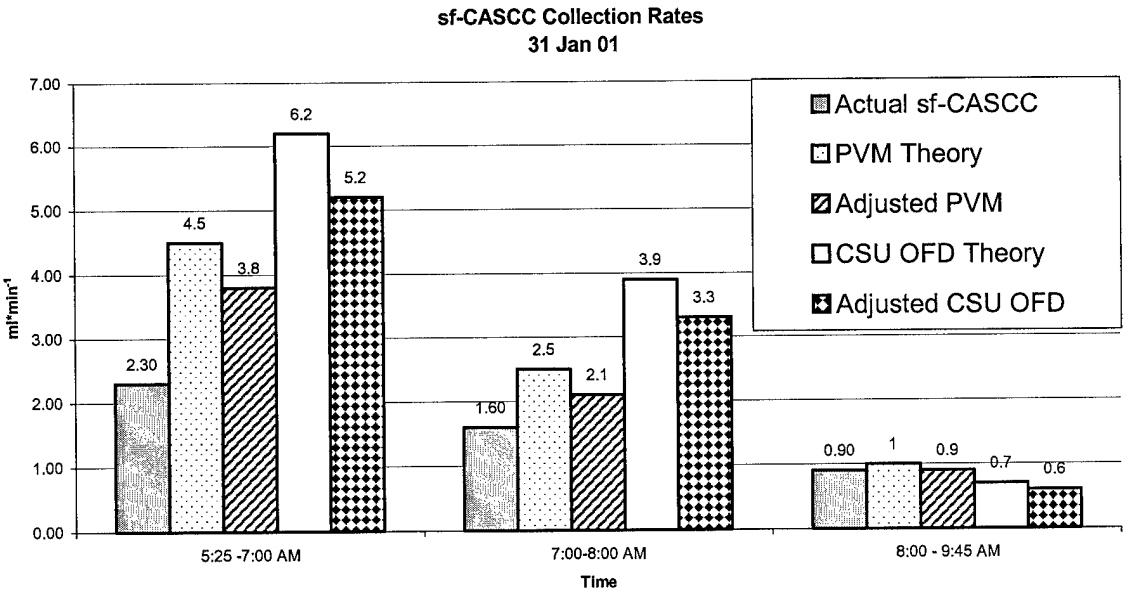

Figure I.1 Theoretical, actual and adjusted sf-CASCC collection rates for January 31, 2001 event.

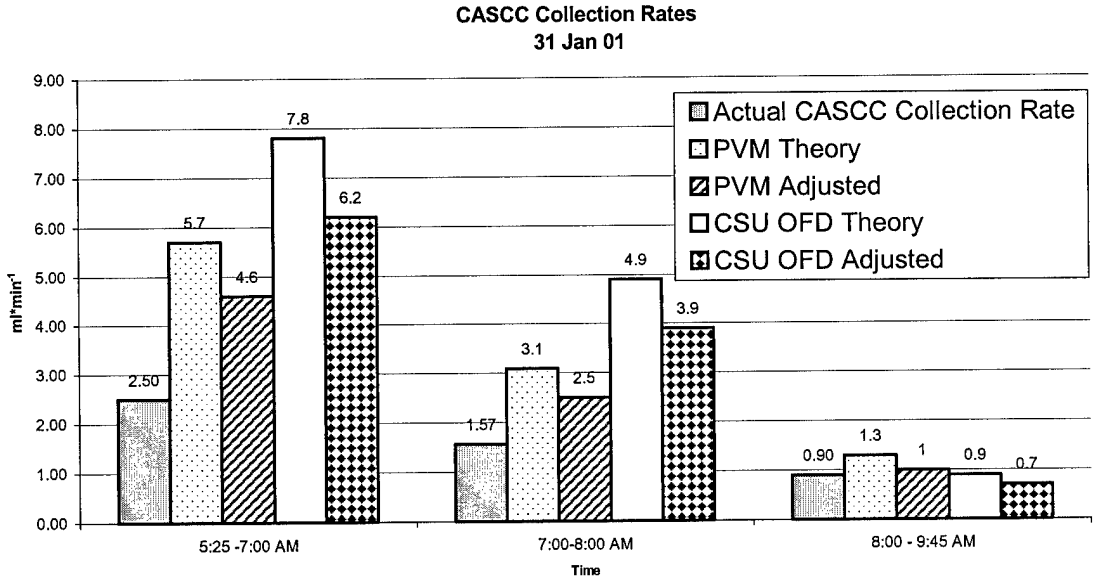

Figure I.2 Theoretical, actual and adjusted CASCC collection rates for January 31, 2001 event.

The PVM and CSU OFD theoretical rates are higher than the actual collection rates during all sample times, except the last (08:00 – 09:45). This was when the fog was dissipating.

Figure I.3 shows a scatter plot of OFD-predicted and PVM predicted vs. observed sf-CASCC collection rates Both sensors have positively correlated R^2 values.

Figure I.4 shows a scatter plot of OFD-predicted and PVM predicted vs. observed CASCC collection rates. Both sensors have positively correlated R^2 values

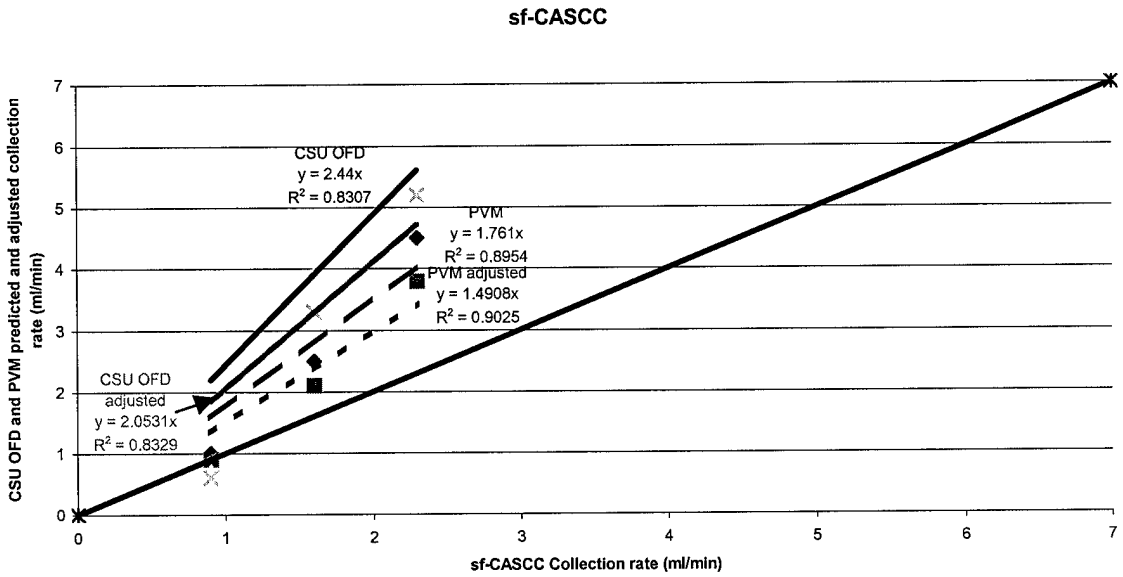

Figure I.3 Scatter plot of predicted, actual and adjusted sf-CASCC collection rates for January 31, 2001 event.

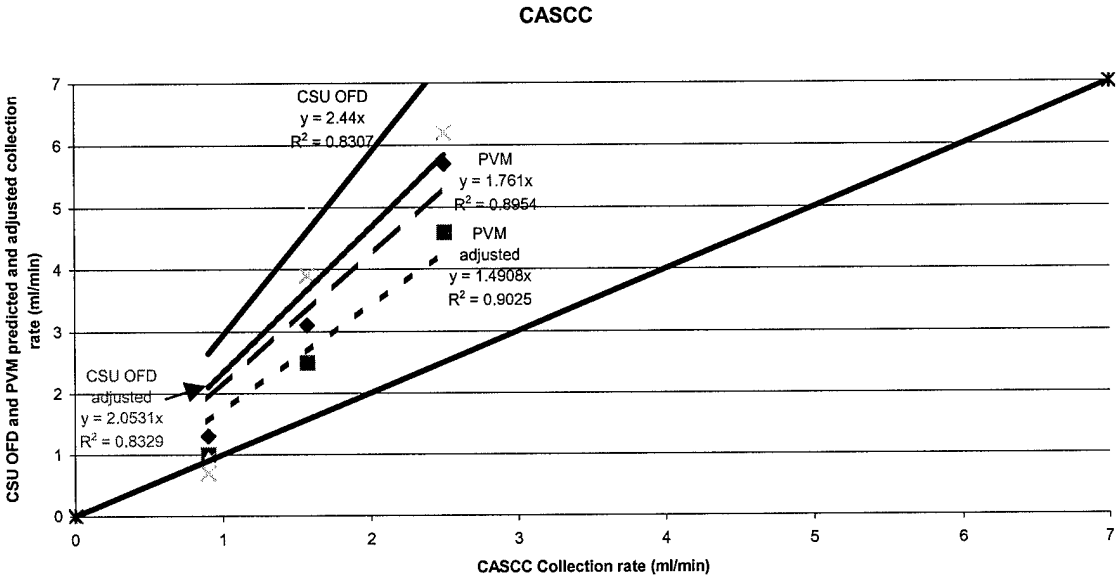

Figure I.4 Scatter plot of predicted, actual and adjusted CASCC collection rates for January 31, 2001 event.

This finding suggests that the CSU OFD and the PVM probably did overestimate the LWC during this event, although it is possible that the CASCC and sf-CASCC did not efficiently sample the very large fog drops that appeared to comprise an important fraction of the LWC. It is also possible that the reduced voltage attributed to the under collection of both the CASCC and the sf-CASCC. We can see that a rough correction, based strictly on the reduced voltage, has brought the measurements closer to the one to one value we hoped to obtain.